

**KERNFORSCHUNGSZENTRUM
KARLSRUHE**

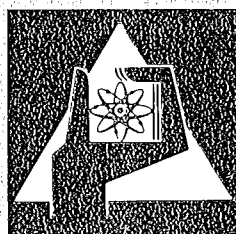
September 1975

KFK 2194

Institut für Experimentelle Kernphysik

**Superconducting Niobium Accelerator Structures
for a Proton Linear Accelerator from 200 to 600 Mev**

W. Bauer, K. Mittag



**GESELLSCHAFT
FÜR
KERNFORSCHUNG M.B.H.**

KARLSRUHE

Als Manuskript vervielfältigt

Für diesen Bericht behalten wir uns alle Rechte vor

GESELLSCHAFT FÜR KERNFORSCHUNG M. B. H.
KARLSRUHE

KERNFORSCHUNGSZENTRUM KARLSRUHE

KFK 2194

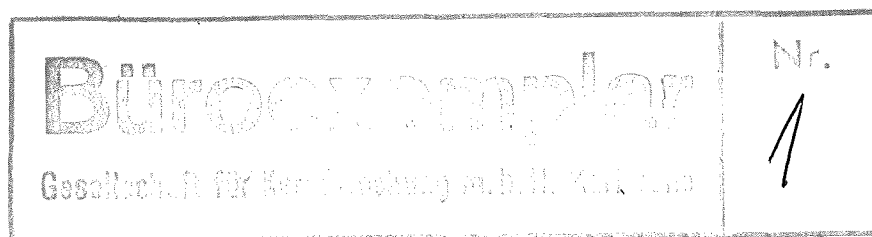
Institut für Experimentelle Kernphysik

SUPERCONDUCTING NIOBIUM ACCELERATOR

STRUCTURES FOR A PROTON LINEAR

ACCELERATOR FROM 200 TO 600 MeV

W. Bauer, K. Mittag



Gesellschaft für Kernforschung mbH, Karlsruhe

Abstract

Design criteria for superconducting linear accelerator structures are reviewed, and various structures known in the literature are discussed with respect to their applicability in a 200 - 600 MeV proton linac. Using the "LALA"-Program several iris loaded structures are calculated and a reasonable preliminary set of parameters for a proton linac is worked out.

Supraleitende Niob-Beschleunigungsstrukturen für einen Protonen-Linearbeschleuniger im Energiebereich von 200 - 600 MeV

Kriterien für den Entwurf von Strukturen für einen supraleitenden Linearbeschleuniger werden zusammengestellt. Verschiedene in der Literatur bekannte Strukturen werden im Hinblick auf ihre Anwendbarkeit für einen 200 - 600 MeV-Protonen-Linac diskutiert. Mit Hilfe des Programms "LALA" werden mehrere Varianten der Iris-Struktur berechnet; ein verwirklichter erscheinender Parametersatz für einen Protonen-Linac wird angegeben.

Table of contents

p.

	Abstract	
I.	INTRODUCTION	1
II.	DESIGN CRITERIA	2
1.	Shunt impedance, accelerating field and power consumption	2
2.	Peak fields	3
3.	Surface preparation	5
4.	Frequency and geometrical dimensions	6
a)	acceptance in longitudinal phase space	
b)	acceptance in transverse phase space	
c)	diameter of structure	
d)	effects depending on small rf bandwidth of structure	
5.	Tolerances and structure length	8
6.	Using a fixed structure geometry to accelerate protons over a large energy range	10
7.	Manufacture	11
III.	KNOWN ACCELERATOR STRUCTURES AND THEIR COMPATIBILITY WITH OUR DESIGN CRITERIA	12
1.	Structures operating in a TM_{010}^- like mode of a right circular cylinder	
A)	Alvarez type structures	
B)	Iris type structures	
a)	Coupling through the beam hole	
b)	Coupling through slots in the discs	
c)	Other coupling devices	
2.	Structures with drift tubes and current carrying supports	13
3.	Structures operating in a TM_{020}^- like mode	14
4.	Structure operating in a TM_{110}^- like mode of a rectangular resonator	14
IV.	IRIS AND SLOTTED IRIS STRUCTURES	15
1.	Geometry optimization	15
2.	Structure length	16
3.	Coupling slots and tolerances	16
a)	Slotted iris structure	
b)	Iris structure	
4.	Manufacturing and surface preparation	19
V.	CONCLUSIONS	22
	Appendix: Summary of recent results in rf superconductivity	23
	References	

Superconducting Niobium Accelerator Structures for a Proton Linear Accelerator from 200 to 600 MeV

I. INTRODUCTION

A π -meson factory for medical applications can be composed of a 200 MeV cyclotron for protons followed by a superconducting linear accelerator delivering protons of 600 MeV. This article discusses the properties of accelerator structures for such a linac. The energy range between 200 and 600 MeV is characterized by a proton velocity varying only slowly between $\beta = v/c = 0.57$ and 0.8. Many studies have been made on structures for this energy range¹, especially before the construction of the normal conducting π -meson factory at Los Alamos. However, new design criteria have to be applied, when technology involving superconducting niobium is used. Structures designed according to these criteria differ considerably from those of normal conducting machines. For superconducting electron linear accelerators a summary of important points can be found in references 2 and 3. In the following paper we compiled the present knowledge about superconducting proton accelerator structures under this aspect.

The main design goal of the structure is the acceleration of a proton beam of typically 100 μ A average current, emitted by a 50 MHz cyclotron at an energy of 200 MeV, to an end energy of 600 MeV⁴. Among the numerous possible sets of parameters characterizing the linac structure one set has to be chosen which minimizes the costs of construction and operation of the integral linac system, as the structure parameters affect other components of the linac, such as the rf- and the cryogenic system.

A survey of all factors influencing the design is given in the following section. Section III contains a discussion of different accelerator structures known in the literature. In Section IV some computations leading to a reasonable set of structure parameters are summarized.

II. DESIGN CRITERIA

1. Shunt impedance, accelerating field strength, and power consumption

The shunt impedance Z relates the rf power loss P_s in a structure of a length ℓ to the accelerating field amplitude,

$$E_0 \text{ by } Z = E_0^2 T^2 \ell / P_s = E^2 \ell / P_s^1, \quad E = E_0 T.$$

The transit time-factor T takes into account that due to the finite time which the design particle needs to cross the accelerating gap its energy gain is less than E_0/ℓ . In Section IV numerical results of this shunt impedance Z as a function of geometry are given. In all practical cases the real particles may have a transit time factor T_{eff} different from that of the design particle and the accelerating field amplitude is reduced by $\cos\phi$ necessary for phase stability, so that the effective shunt impedance Z_{eff} becomes

$$Z_{\text{eff}} = Z \left(\frac{T_{\text{eff}}}{T} \cos\phi \right)^2 = \frac{E_{\text{eff}}^2 \cdot \ell}{P_s} ; \quad E_{\text{eff}} = E_0 T_{\text{eff}} \cos\phi .$$

In a superconducting structure the shunt impedance is not a critical design parameter for the following reason:

The losses are reduced by the improvement factor IF (IF = Q (superconducting structure) / Q (Cu-structure, 300 K)) compared to a normal conducting structure. The status of the rf superconducting technology is such that IF may vary between 10^4 and 10^6 depending on surface preparation technique and type of cavity (see appendix). Therefore, in optimizing the structure geometry with respect to Z it is by far more important to insure the possibility of a good surface preparation than to gain a few percent in value of Z (300 K).

The following rough estimates shall give an idea of the order of magnitude of the variables involved. We ask which field strength E minimizes the power installation for the cryogenic refrigerators? The total power loss P at helium temperature is the sum of rf losses in the structures P_s and of the insulation losses of the cryostats P_c . To begin with, we assume that P_s equals P_c

$$P_s = \frac{E_{\text{eff}} \Delta W}{Z_{\text{eff}}(\text{Cu}, 300\text{K}) \text{IF}} = P_c = \frac{P_c}{\ell} \frac{\Delta W}{E_{\text{eff}}} ,$$

ΔW being the total energy gain of (600-200) MeV = 400 MeV.

Typically we have $Z_{\text{eff}}(\text{Cu}, 300\text{K}) \approx 20 \text{ M}\Omega/\text{m}$, $IF = 10^5$, $P_c/\ell = 3 \text{ W/m}$, therefore $E_{\text{eff}} = \sqrt{P_c Z_{\text{eff}}(\text{Cu}, 300\text{K})IF/\ell} \approx 2.5 \text{ MV/m}$, $P \approx 1000 \text{ W}$.

Doubling the field gradient to 5 MV/m results in $P = 1250 \text{ W}$, which means that for only 13% increase of installed power we achieve a reduction of the length dependent costs such as structures, rf components, buildings by a factor of 2. This in turn clearly favors the higher value of E_{eff} from a standpoint of minimizing construction costs. A detailed study of costs^{4,5} results in an even higher optimal value for E_{eff} as long as costs of operating the accelerator are of no concern. For this case $P_s > P_c$, and the cost of operating the accelerator as well as of power installation decreases with increasing Z_{eff} .

In this connection a cost analysis also has to show whether the decrease in P_s - that is decrease in rf surface resistance - by lowering the operating temperature from 4.2 K to 1.85 K overcompensates the higher cost of a 1.85 K refrigerator compared to a 4.2 K one.

2. Peak fields

The peak electric (E_p) and magnetic (H_p) rf fields attainable in a superconducting structure are limited by various effects.⁶ Depending on geometry and frequency electron multipacting sets barriers ranging from very low fields (which generally can be overcome) to high fields up to 10 MV/m. For simple two point multipacting problems should become less severe if the geometry of the structure is so that pure homogeneous electric fields are avoided by avoiding parallel surfaces. In GHz-accelerator structures regions of homogeneous electric field do not occur to any appreciable amount because the radially varying electric field is accompanied by a radially varying magnetic field. This causes electron trajectories to be quite complicated, in general only calculable with computer programs,⁷ so that the feedback to structure design is not simple either. Most probably a design optimal with respect to multipacting would incorporate some geometry asymmetries, which in turn would increase manufacturing costs. In any case it should be avoided that multipactor levels are just at operating fields, and only the "real thing" will prove that multipacting problems can be overcome.

Multipacting or field emitted electrons also can couple power into other modes by an effect similar to the Reflex-Klystron or to beam breakup⁸. The probability of this occurring is the larger the more cells there are in the structure. However, by placing the rf input probe just one cell next to the symmetry plane of the structure, most of these modes can be loaded down to the same order of magnitude as the accelerator mode itself. Thereby the starting current for breakdown due to multipactor electrons can be increased.

The higher the field values are the more a mixture between multipacting and field emission takes place. The field emitted electrons gain energy, thereby loading down the Q-value of the structure. Further, high energy electrons cause radiation damage, lowering the Q_0 -value permanently.^{6,9,11} To keep electron emission low, the surface preparation of the structure has to insure a low micro-roughness, (e.g. by electropolishing), and a clean surface (e.g. by UHV firing). The state of the metal-oxide interface at the surface seems to play an essential role in electron emission, a thin and homogeneous oxid layer being preferable.^{6,10}

In order to keep electron problems low, an important goal in structure design should be to minimize the ratio E_p/E_{eff} , although generally this will have a detrimental effect on the shunt impedance. The status of technology (see appendix) is such that at operating field level the peak electric field savely should not be much higher than 10 MV/m in complex accelerator systems. In most practical cases the critical magnetic field of niobium will not be limiting because it is sufficiently high ($H_c = 190$ mT at $T = 0$). Limiting can be a thermal breakdown by rf losses in high magnetic field. Therefore, the wall thickness has to be chosen such that even at bad surface spots (e.g. $IF = 10^4$) the temperature gradients across the wall and across the niobium-helium interface (Kapitza resistance) will be small enough not to cause thermal run-away. At present, peak magnetic fields of 200 Oe can be considered as a conservative design. Fields up to 400 Oe are possible if the occurence of bad surface spots can be avoided.

3. Surface preparation

At present surface preparation is the crucial point in superconducting accelerator technique. Even for simple cavity geometries no standard surface treatment is agreed upon, although some kind of chemical treatment in combination with UHV-firing seems to be essential (see appendix).

At the best the inner surface of the structure should be electropolished¹² after manufacturing, followed by UHV-firing at 1800°C. Electropolishing requires good accessibility to the interior of the structure, firing is only possible with a rigid structure design or if weak structure elements can easily be supported during firing.

In some cases electropolishing after manufacturing would only be possible at the expense of either demountable flanges or large beam holes. Mountable flanges would imply to have rf currents flowing across some kind of joint, leading to intolerably increased rf losses in the joint at least with present technology. Large beam holes imply a reduction in shunt impedance together with an increase of peak fields for a given accelerating field, and therefore are possible only to a very limited extent. In these cases a compromise could be to electropolish structure components before final welding, and to either oxipolish¹³ or chemically polish at low temperature¹⁴ - that is at a very small etching rate - afterwards. Care has to be taken in designing the access to the interior of the structure so that thoroughly rinsing is easily possible after chemical treatments. Using a concept with small beam holes and no flanges of course means to take the risk of not being able to remove bad surface spots after manufacturing.

The aim of any surface preparation is to obtain an extremely smooth and clean surface. It is essential that this surface state does not deteriorate by contaminants such as dust, oil, etc. afterwards. This has to be insured when handling, storing or setting up the structure into the cryostat. Also during accelerator operation devices such as electrostatic filters and cold traps should hinder the structure to be a perfect pump for the beam vacuum.

4. Frequency and geometrical dimensions

The choice of frequency depends on numerous considerations, which complicates a decision considerably. Among them there are:

a) Acceptance in longitudinal phase space

Let n be the ratio of the linac frequency to the cyclotron frequency (≈ 50 MHz). Then the proton bunches of a given duration in time occupy a factor n larger phase space at the linac frequency than at 50 MHz¹⁵. Consequently, chopping, prebunching and stability of rf phase are the more complicated the larger n is. As shown in ref.16 $n \approx 15$ seems to be an upper limit if one tries to avoid losing particles at 200 MeV. This restricts to operating frequency to values around 700 MHz.

b) Acceptance in transverse phase space

The transverse acceptance η of the linac has to be safely larger than the emittance of the cyclotron (e.g. $\eta = \pi x x' = 1.57$ cm mrad at 200 MeV for the cyclotron at SIN).¹⁷ η depends mainly on the maximum beam diameter $2r_{\max}$ tolerated, on the length of the accelerator sections ℓ (corresponding to distance between focussing quadrupoles), on the frequency f , on the phase ϕ at which the "design particle" is accelerated, on the accelerating field gradient E_{eff} , on particle velocity $\beta = v/c$, and on particle energy $\gamma = W/mc^2$. To obtain the order of magnitude of the acceptance of a single defocussing accelerator section the following formula can be used:¹⁸

$$\eta = \pi x x' = \frac{\pi r_{\max}^2 \Omega}{2 \cosh \Omega \ell \sinh \Omega \ell} \quad \text{with } \Omega = \sqrt{\frac{e E_{\text{eff}}}{m c^2} \frac{\pi f \sin |\phi|}{\beta^3 \gamma^3}}$$

Deriving this expression it has been assumed that the beam is focussed to the entrance of the structure, having constant velocity inside, and no coupling between longitudinal and radial motion takes place. The results of this simplified formula have been confirmed by more detailed computer calculations¹⁹. It follows that the emittance of the cyclotron sets an upper limit to the structure length, and a lower limit to the beam hole diameter $2a$ inside the structure. But on the other hand, to minimize peak fields and to get high shunt impedance $2a$ has to be as small as possible, which in turn generally complicates the surface preparation. The upper limit

for η ($\eta = \pi r_{\max}^2 / 2\ell$) is obtained, if $\Omega\ell$ is in the order of 0.5 or less, which means that the defocussing effect of the accelerating field can be neglected. For proton energies above 200 MeV and for the design particle this is generally the case, and than the frequency dependence of η is weak. Whether particles differing in phase from the design particle (as proposed in 6.) also are accepted, can only be decided by detailed computer analysis of particle motion. From these considerations a beam aperture radius of about $a = 2$ cm seems reasonable at all frequencies.

c) Diameter of structure

For many types of structures their diameter D scales inversely proportional to the frequency. Surface preparation techniques favor small D (and length ℓ !), as especially chemically processing gets the more complicated the larger D (and ℓ !) is, diameter much above 30 cm being extremely difficult to handle. Also as D (and ℓ) gets larger the area of inner surface increases and thereby also the probability of "bad spots".^{20,21} Naturally, fabrication cost for both structures and cryostats will be more favorable at higher frequencies. These arguments together with the trend of attained rf fields and Q -values (see appendix) clearly favor short sections at high (\geq S-band) frequencies.

d) Effects depending on small rf bandwidth of structure

The bandwidth of the superconducting structure for high beam currents I is determined by the beam loaded Q -value $Q_b = (E_{\text{eff}}/I) \times (Q_o/Z_{\text{eff}})$,²² which for $I = 100 \mu\text{A}$ turns out to be typically in the order of 10^7 . At this point an additional argument for a high shunt impedance can be found: By a high Z_{eff} Q_b is decreased, simplifying the frequency regulating system.

Therefore, the frequency should be stabilized to the order of 10^8 , and the structure design has to be rigid to insure this. During accelerator operation mechanical vibrations of structure components should be kept sufficiently small. Besides from external sources such vibrations can be induced by changes in He-pressure and by radiation pressure.

A slow tuner - either based on the plunger principle or on deforming the walls of the structure - has to be installed to make up for manufacturing errors leading to frequency errors in the order of 10^{-4} .

It also should be mentioned that a type of structure whose frequency can be calculated with an accuracy of 10^{-4} by a computer program greatly simplifies the structure design, as labor intensive and time consuming modelling can be avoided.

5. Tolerances and structure length

The correlation between fabricating tolerances and field flatness in the structure has been studied extensively,^{1,2,3-25} resulting in the proposition of various types of "compensated structures" or multi-periodic structures. The basic result of these studies is that for given tolerances, for a given number N of cells in a structure, and for a given electromagnetic coupling κ between adjacent cells of the structure,* $\pi/2$ -mode operation is superior to π -mode for large N; deviations of fields in single cells from the design field (flatness) and the phase shift along the structure due to the power flow are smaller in $\pi/2$ - than in π -mode. Computer studies of beam dynamics indicate²⁶ that a flatness of 0.1 does not seriously degrade the longitudinal dynamics, provided that the average field in the structures is close enough to the design value. Then taking this value of flatness, taking the deviation of single cell frequencies from design frequency due to machining errors, and taking the value of κ determined by structure geometry, the maximum value of N allowed can be calculated for each mode of operation (in general, problems related to phase shift along the structure are not severe in superconducting accelerators²⁷). This, in turn, determines for a given frequency an upper limit for the length of the structure. One also has to make sure that the mode separation in the passband of the operating mode is large enough not to cause problems in the rf feedback system. A mode separation of about 100 kHz seems acceptable for a superconducting accelerator.

Designers of normal conducting accelerators want to have N as large as allowable by power flow considerations. The reason is that the

* $\kappa = \frac{f_{\pi}^2 - f_0^2}{f_{\pi}^2 + f_0^2}$, f_{π} and f_0 being the π -mode and zero-mode frequencies, respectively.

cost for rf power installations is a major part of the total cost of construction, and a few number of high power klystrons are cheaper than a large number of low power ones, total installed power assumed to be the same. Therefore $\pi/2$ -mode like structures are preferred in this case.

For a superconducting accelerator the cost of manufacturing the structures is much larger than that for the rf amplifiers. As mass production is much cheaper than producing many different components, a superconducting accelerator should be composed of as many identical structure modules as possible, each module having a length not exceeding about 1 m because of surface preparation techniques. For an electron accelerator this can easily be realized using a multiperiodic structure, divided into identical modules of short length.²⁸ For a proton accelerator identical long multiperiodic structures are not feasible (see 6.).

Another argument for employing short identical sections is the failure rate in producing superconducting structures of both high Q_0 - and E_{eff} -values. This failure rate - although due to lack of good statistics not known - certainly is higher than for copper technology.

A further point favoring short identical sections is the problem of good low-loss rf-joints. Using In-joints has been demonstrated to be feasible only if careful pre-tuning of single cells at room temperature is applied. This pre-tuning is quite labor intensive and therefore expensive; also if chemically etching at room temperature has to be one means of pre-tuning, this might result in a deteriorated structure performance.

Next there is the problem of beam break-up, which is awesome to prevent in long structures, because many deflecting rf modes can be excited by the beam in the structure.²⁹ The starting current I_s for beam break-up in TM_{010} - like modes for 200 MeV protons in structures of 1 m length at a frequency f of 1 GHz is in the order of 150 μA , if a shunt impedance Z_{eff} of the excited mode of $10^{12} \Omega/\text{m}$ is assumed. For the same parameters beam break-up in deflecting HEM_{11} - like modes would occur at about 300 μA . As I_s scales inversely proportional to the product $\ell^2 Z_{\text{eff}} f$, structures of length below 1 m probably can be used without employing methods to prevent beam break-up. On the contrary structures much longer than 1 m certainly would show beam

break-up at the design current of 100 μ A if no precautions would be taken.

All of these arguments favor short identical structures for a superconducting proton linac, and these can be uniform periodic and operating in π - or 0-mode if κ is sufficiently high. Then, of course, there is no question, that the structures should be operated in a standing wave mode.

6. Using a fixed structure geometry to accelerate protons over a large energy range

The manufacturing costs of the structure depend to a large extent on the question over how large an energy range structure units of fixed geometry can be used. To obtain optimal energy gain the velocity of the travelling wave (β_w) which accelerates the protons should be identical to their velocity β . This leads to the synchronous condition $L = \beta\lambda/2$ for π -mode operation (L = cell length, λ = free space wave length). Changing L results in the necessity to change other dimensions of the cell too, e.g. the diameter because the eigenfrequency of the cell has to remain constant. If instead we use a structure composed of N identical cells to accelerate protons with e.g. $\beta < \beta_w$ we can make up for this mismatch of velocities by letting the particle bunches enter the first structure cell too early with respect to optimum timing (phasing). When passing the structure the field wave will overtake the particles. The resulting energy gain ΔW - or the transit-time factor T - will be less than in the ideal case. This reduction in T results in a larger total length of the accelerator. A cost analysis has to show which decrease in T can be tolerated to minimize the total costs.

Mathematically T can be calculated as:

$$T = \frac{\Delta W}{\Delta V}; \quad \Delta V = N \int_0^L E(z) dz;$$

$$\Delta W = \int_0^{NL} E(z) \cos(2\pi f t(z) + \phi) dz; \quad t(z) = \int_0^z \frac{dz}{\beta(z)c}$$

$$\beta(z) = \sqrt{1 - \frac{1}{\frac{W_1 + \Delta W(z)}{1 + \frac{1}{mc^2}}}}$$

with: $E(z)$ = electric field along the beam axis z , ϕ = injection phase
 f = frequency, c = velocity of light, W_1 = kinetic energy at injection, mc^2 = proton rest energy.

If $E(z)$ is known a computer evaluates T by an iteration method, giving also the injection phase which maximizes T for given W_i and f . (For results in special cases see IV)

Let us assume we want to cover the velocity range from β_a to β_f with one type of structure having N cells and designed for the velocity β_s , tolerating a certain decrease ΔT in T for β_a and β_f . ΔT will depend mainly on the differences in phase shift $\Delta\phi$ measured over the structure length NL between particles with β_a (or β_f) and β_s :

$$\Delta\phi_{a,f} \approx 2\pi \frac{fNL}{c} \left(\frac{1}{\beta_{a,f}} - \frac{1}{\beta_s} \right)$$

Due to synchronous condition: $L = \beta_s \lambda / 2$.

$$\text{Therefore } \Delta\phi_{a,f} \approx \pi N \beta_s \left(\frac{1}{\beta_{a,f}} - \frac{1}{\beta_s} \right).$$

It follows that if we want to cover the same range $\beta_f - \beta_a$ with structures of different frequencies N has to be a constant, or the total length of structure allowed scales as $1/f$. This estimate has been proven to be valid by detailed computer calculations (see IV).

7. Manufacture

A major requirement in structure design is the possibility of applying cheap mass production techniques such as hydroforming, coining, punching or argon arc welding.³⁰ Turning or milling to high tolerances should be avoided, the number of electron beam welds minimized. Until now most niobium test resonators have been built according to the best manufacturing techniques available, but generally these are the most expensive ones. Research still has to decide which steps in manufacturing, which requirements really are essential to deliver a high Q -value, high field performance of a superconducting niobium structure.

III. KNOWN ACCELERATOR STRUCTURES AND THEIR COMPATIBILITY WITH
OUR DESIGN CRITERIA

1. Structures operating in a TM_{010} -like mode of a right circular
cylinder

A.) ALVAREZ type structures

Normal conducting Alvarez structures operating between 100 and 200 MHz are in wide use to accelerate protons to the 100 MeV range.^{3 1-3 3} Superconducting Alvarez structures have been proposed at 700 MHz for low energy protons around 10 MeV at Karlsruhe.^{1 8} A lower frequency is not feasible because the structure diameter would exceed 30 cm. At 700 MHz for proton energies above the 100 MeV range the length of the drift tubes gets comparable to the distance between drift tube and outer diameter of the tank. This means that the longer the drift tubes the more electric field lines will end on the outer cylindrical surface of the drift tube, leading to very high E_p/E_{eff} and H_p/E_{eff} ratios at the drift tube. Also the shunt impedance decreases rapidly due to the higher losses on the drift tube. These arguments of course also hold for the compensated Alvarez structures employing post couplers or several stems.^{3 4}

B.) IRIS type structures

Many iris type structures have been invented,^{3 4} which differ from one another in the device by which the rf coupling between adjacent structure cells is achieved.

a) Coupling through the beam hole

This structure is in wide use for electron accelerators, both normal^{3 5} and superconducting ones^{3 6}. For proton accelerators the beam hole diameter $2a$ has to be sufficiently small to insure good E_p/E_{eff} , H_p/E_{eff} and Z_{eff} values (see IV for details). But then the cell to cell coupling is so small that tolerance requirements would be very tough.

b) Coupling through slots in the discs

If the beam hole is sufficiently small the electric field coupling from cell to cell through the beam hole can be overcompensated by

magnetic field coupling through slots in the discs, leading to the family of slotted iris structures^{34,37,38}. The magnetic field at the slot is enhanced by a factor of 2 (for a circular hole) or higher (depending on slot geometry) compared to the unperturbed case. Good cooling of the slot therefore is essential to keep it superconducting. As milling and electron beam welding of a complicated slot geometry is very expensive, the only geometry which can be manufactured with reasonable costs is a circular hole (see IV for details).

c) Other coupling devices

The side - coupled structure has been installed successfully in the normal conducting proton linac at Los Alamos³⁹. A superconducting version of this structure would have serious drawbacks both for resonant or non-resonant coupling: e.g. complicated shapes of electron beam welds at the side coupled cavity, necessity of In-joint because of accessibility during chemical processing.

Other structures³⁴, like loop-coupled, centipede or cloverleaf structure all have too complicated geometry for superconducting niobium technology. The same holds for the relative of the side-coupled structure proposed by Andreev et al.⁴⁰ in which coupling is achieved with annular coupling cavities.

2. Structures with drift tubes and current carrying supports

In this class of structures there are the interdigital line^{34,41} the H-type structure³⁴, the spiral resonator⁴² and the split ring structure^{34,43}. All of these have in common a rapid drop in shunt impedance Z_{eff} as relative particle velocity β increases³⁴. For example, in the case of the interdigital line this is due to the fact that the cell length $\beta\lambda/2$ (λ = free space wave length) gets larger than the structure diameter of between 0.1λ and 0.2λ , and the capacitance between adjacent drift tubes gets shunted by a capacitance between drift tube and outer wall, leading also to high E_p/E_{eff} values.

The decrease in Z_{eff} with increasing β is less pronounced in the compensated cross-bar structure³⁴. Its diameter is relatively small (about 20 cm at 700 MHz). Unfavourable is the relative complicated geometry, the necessity of modelling to find optimum parameters, and rather high H_p/E_{eff} values due to the current carrying stems.

The uncompensated symmetrical cross-bar structure³⁴ is a relative of the slotted-iris in which the support of the inner part of the disc has been reduced to two stems. These stems now have to carry the total current which flows across the discs of the iris structure. Therefore the cross-bar has higher H_p/E_{eff} values than the slotted iris structure, and of course much higher bandwidth. If it would be sufficient to cool the drift-tubes of the symmetrical cross-bar structure only by thermal conduction, its mechanical complexity is comparable to that of the slotted iris.

3. Structure operating in a TM_{020} -like mode

A compensated structure operating in a TM_{020} -like mode^{34,40} has a diameter of about 62 cm at a operating frequency of 700 MHz. Therefore, using superconducting niobium technology would be possible only for frequencies larger than about 1.4 GHz. As the inner disc of this structure would have to be cooled with liquid helium many welds would be necessary in the construction. The welds at the stems connecting the inner and the outer discs could be done only by argon arc technique. Therefore a superconducting version of this structure seems to be not promising, although its rf properties are.

4. Structure operating in a TM_{110} -like mode of a rectangular resonator

A structure of this type, called muffin tin structure, has been developed at Cornell⁴⁴. Its main advantage is that it is composed of two halves, which are flanged together in a plane through the beam axis. No currents are flowing across this joint, if upside down asymmetries are zero. The inner surface of the structure is easy to access for surface preparation, especially if bad surface spots have been discovered. Good performance of a S-band muffin tin structure - manufactured by milling or deep drawing, electron beam welding, and cold surface preparation techniques only - are reported⁴⁴. The structures main parameters are: $f = 3$ GHz, mode = π , $Z_{eff}(Cu, 300K) = 45$ M Ω /m, $E_p/E_{eff} = 2.6$, $H_p/E_{eff} = 44$ Oe/(MV/m), bandwidth = 4.7%, beam and coupling aperture width = 2.5 cm. The properties of this structure are so promising that studies at Karlsruhe have begun for its application in a proton linac.

IV. IRIS AND SLOTTED IRIS ACCELERATOR STRUCTURES

1. Geometry optimization

The LALA-program⁴⁵ has been used to study for rotational symmetric iris structures the influence of variations in geometry on the shunt impedance Z and on the ratios of peak to accelerating field (E_p/E , H_p/E , $E = E_0 T$; multiply H_p/E by the field enhancement factor of 2 for the slotted iris structure with circular coupling slots!). Parameter are the frequencies of 700 MHz, 1.3 GHz and 3 GHz. (700 MHz being acceptable from the phase acceptance point of view, 3 GHz preferred by rf superconductivity arguments, see Section II, 4.) The structure diameter was chosen to yield these frequencies with an error of less than 5%. The cell length L was varied to cover at least the energy range from $E_{kin} = 200$ to 600 MeV. The radius of the beam hole, a , was taken between .5 and 2 cm.

The geometrically most simple iris structure has parallel discs; results are shown in Figs. 1,2,7, and 10 for fixed disc thickness $2d$. (The main geometrical dimensions of the iris cell can be taken from its quarter cross section in connection with the table depicted in the figures.) E_p/E can be minimized by choosing an elliptical instead of a circular cross section at the edge of the beam hole - the ratio of major to minor axis being 2:1 (Fig. 2b) - without affecting Z and H_p/E very much. A minimum of E_p/E as a function of disc thickness⁴⁶ can be found in Figs. 3,8 and 11, whereas shunt impedance and H_p/E decrease with increasing d . Due to the relatively small iris diameters considered the values for E_p/E are already approaching the theoretical minimum which can easily be computed to be $\pi/2$. A reentrant shape of the disc at the beam hole increases the transit time factor, and therefore can improve Z and H_p/E without affecting E_p/E too much (Figs. 4,5,9). Z can be enhanced further by rounding the edge between disc and cylinder wall (Figs. 3,5). However a significant improvement of Z can only be obtained by a Ω -shaped cell, as in the Los Alamos side-coupled structure⁴⁷, giving rise to extremely complicated geometry at the coupling slots in the discs.

If rinsing of the structure after chemical treatment is of major concern the cell can be shaped with tapered discs as in ref.28, Fig.6 resulting in only minor changes of Z , E_p/E and H_p/E compared to the parallel disc case, but again the geometry of the coupling slots in the discs is not simple.

2. Structure length

As shown in section II.5 we are considering only a uniform periodic structure operating in π -mode with a module length not exceeding 1 m. The question which energy range can be covered by a sequence of such identical structures is discussed in Figs. 12,13 and 14, which are based on the formulas of II.6. As a plausible assumption let us tolerate at the most a reduction of 10% in transit time factor compared to the case of synchronism between particles and accelerating wave. Then a structure composed of only three or less full cells would cover the energy range from 200 to 600 MeV. Two types of structures having six cells each is another alternative. The first structure designed for $\beta = 0.594$ ($E_{kin} \approx 230$ MeV) would be used from $\beta = 0.564$ ($E_{kin} \approx 200$ MeV) to $\beta = 0.678$ ($E_{kin} \approx 330$ MeV). The second designed for $\beta = 0.715$ (400 MeV) covers the range $\beta \approx 0.678$ to $\beta \approx 0.782$ (600 MeV). The injection phase of the particles relative to the rf wave which maximizes the transit time factor would be about -32° for the lower energies and $+55^\circ$ for the higher ones.

To insure a large enough acceptance in longitudinal phase space a phase shift of -30° has to be added to these values. However, these rough estimates will have to be supported by detailed calculations of the acceptance. At an operating frequency of 700 MHz the length of these two structures would be 0.77 m and 0.92 m, at a higher frequency the length would be reduced by the frequency ratio.

3. Coupling slots and tolerances

a) Slotted Iris structure

The rf coupling between the fields of adjacent cells can be achieved by circular slots evenly distributed in the discs (slotted iris structure). Once manufacturing tolerances and flatness requirements are specified, the coupling coefficient κ necessary can be calculated from the theory of perturbed lumped circuits^{2,3} leaving the number N of cells in the structure (two half end cells are counted as one cell) and the operating mode as parameters. The results of such a calculation are summarized in Table I. κ in turn determines the number n of coupling slots and their radius ρ , which are also given in Table I for a 700 MHz slotted iris of $\beta = 0.8$ (600 MeV). The values of ρ have been extrapolated from measurements on a 720 MHz

slotted iris structure designed for $\beta = 0.2^{18}$, using for scaling the relation

$$\kappa = (f_{\pi}^2 - f_0^2) / (f_{\pi}^2 + f_0^2) \sim (n\rho^3 \cdot 10^{-3,2} d/\rho) / \beta,^{18}$$

(f_{π} , f_0 = frequencies of π - and 0-mode, $2d$ = disc thickness).

This scaling law holds as long as the longitudinal electric field of the structure does not start to compensate the magnetic field coupling. LALA-calculations show that this happens for values of ρ exceeding 30 mm. Therefore, slots with ρ larger than 30 mm should not be used, and a "?" is added to these values in Table I.

Slater's perturbation method³⁵ has been applied to determine experimentally the field enhancement factor at a circular coupling slot. The result was a factor of two¹⁸. Due to additional losses in the coupling slots, the Q-value decreases for increasing κ . From model measurements⁴⁸ it can be concluded that for κ in the order of 0.01 these additional losses will not exceed the order of 10%. From the table one concludes that a π -mode structure with 6 cells, 4 coupling slots in discs of 10 mm thickness is the most promising choice. Due to the fact that κ_{te} is $\sim N^2$ in π -mode, but only $\sim N$ in $\pi/2$ -mode, there is no advantage of the $\pi/2$ -mode at this low number N of cells in the structure.

Table I: Coupling coefficients and slot diameters

mode	N	κ_{sce} (%)	κ_{te} (%)	n = 4	n = 4	n = 8
				ρ (mm) for 2d = 10 mm	ρ (mm) for 2d = 20 mm	ρ (mm) for 2d = 20 mm
π	2	0.25	0.1	17	23	21
π	3	0.39	0.3	20	27	24
$\pi/2$	6	0.40	0.6	23	31?	27
π	6	0.92	1.1	27	35?	31?
$\pi/2$	12	0.60	1.0	26	34?	30
π	8	1.4	2.1	31?	39?	34?
$\pi/2$	16	0.65	1.4	28	36?	32?
π	N	$N \cdot 0.24$	$N^2 \cdot 0.033$			
$\pi/2$	2N	0.76	$N \cdot 0.19$			

N = number of cells in the structure (two half end cells are counted as one full cell).

κ_{sce} = coupling coefficient necessary to achieve flatness of 0.1 for a single cell error in frequency of $\pm 2 \cdot 10^{-4}$ (corresponding to a manufacturing tolerance of ± 0.06 mm for a cell diameter of 300 mm, $f = 700$ MHz).

κ_{te} = coupling coefficient necessary to hold flatness better than 0.1, if the tuning range of a single tuner unit is $\Delta f/f = \pm 10^{-4}$; the tuner can be located either at the center cell or symmetrically at the end cells which are "half" cells.

ρ = radius of circular coupling slots in discs of 700 MHz iris for $\beta = 0.8$ (600 MeV), which would yield a coupling of κ_{te} , 2d = disc thickness

n = number of slots

2d = disc thickness at the slot

b) Iris structure

In Table II the coupling coefficients κ_i are given for some iris structures using beam hole coupling only

Table II: Coupling coefficient using beam hole coupling only

Frequency (GHz)	beam hole diameter 2a (mm)	disc thickness 2d (mm)	κ_i (%)
0.7	80	10	1.2
0.7	40	10	0.1
0.7	40	16	0.02*
0.7	40	20	0.009*
1.3	40	10	0.63
3	20	10	0.5

κ_i = coupling coefficient of an iris structure of $\beta = 0.8$ (600 MeV) f_π and f_o were calculated by means of LALA; values marked by * are extrapolated using the scaling law $\kappa_i \sim a^3 10^{-4.2 d/a_1}$.

The first set of parameters in Table II leads to excessively high E_p/E_{eff} and low Z_{eff} values (see Section IV.1). Because of tolerance requirements (see Table I) the other sets at 700 MHz are only reasonable if $N \leq 2$, and the ones at 1.3 and 3 GHz if $N \leq 4$. For the sets marked by * the mode separation at the π -mode ($\Delta f/f \approx \kappa \sin^2(\pi/2N)$ for half end cells, and $\Delta f/f \approx \kappa \sin(3\pi/2(N+1)) \cdot \sin(\pi/2(N+1))$ for full end cells) gets critical (≤ 100 kHz) even for $N = 2$.

4. Manufacturing and surface preparation

The discs of the slotted iris and iris structures can be hydroformed from sheet material and welded together at the beam hole. For the slotted iris circular holes would have to be machined into the discs, into which premachined tubes would be welded. In order to keep a constant shape of the discs and a constant diameter of the cylinders

for all energies the slot diameter may be adjusted to give a constant frequency. The outer cylinder of each cell is rolled from sheet material and welded to form a tube. Then discs and tubes are electro-polished separately, without any finishing machining after hydro-forming and rolling. Further, the outer cylinder is welded on each side to the discs, forming a structure which is not demountable. All welds are intended to be argon arc welds. A UHV firing process would both stress release and clean the structure. Field measurements in connection with an on line computer would aid in pretuning the individual cells and the total structure by deforming the cylinder walls of the cells. Finally, chemically polishing at -20°C for a short time or oxipolishing would clean the structure before mounting into the cryostat.

This procedure differs considerably from those applied up to now in rf superconductivity. Research still has to prove, whether these relaxed requirements during manufacture and for surface preparation are leading to the desired values in costs, tolerances, fields, and Q-values.

V. CONCLUSIONS

From the previous discussions these structures seem to us most promising to be used in a superconducting proton linear accelerator for the energy range 200 to 600 MeV: the muffin tin (III.4), the iris (III.1 Ba), and the slotted iris structure (III.1 Bb) (Fig.15,16).

As work on the muffin tin structure is not yet conclusive, we only give possible parameter sets for the iris and slotted iris structure. The arguments which led to these sets are by no means compulsory, so that a certain amount of intuition was involved. As these arguments are distributed over the previous sections, they are repeated shortly in the following paragraph:

Phase acceptance problems at the injection from a 50 MHz-cyclotron fixed the operating frequency at 700 MHz, although it is assumed that rf properties would improve at higher frequencies. Manufacturing and cost considerations as well as surface treatment feasibility require as many as possible identical structure units with the most simple shape and not exceeding a length of 1 m and a diameter of 30 cm. Results of transit-time-factor calculations allowed for two types of six cell units or one type of two cell units covering the energy range from 200-600 MeV. Tolerance and tuning requirements and the

mode separation needed for the frequency feedback system demand a slotted iris for the 6-cell case and allow coupling through the beam hole alone for the two-cell units.

We realize that among the various possible structures discussed the ones proposed have no outstanding superior properties. Among their major drawbacks are: large diameter and heavy weight; interior not easy accessible to remove bad surface spots; electropolishing after manufacture only possible with umbrella like folding cathode; uncertainty about achievable peak fields (especially in H_p for the slotted iris), improvement factor, and multipactor problems has to be cleared in experiments on prototypes before a final proposal can be written. The extrapolated value for the mode separation (70 kHz) in the iris is very low and has to be looked at carefully. On the other hand these properties are promising: low ratio of E_p/E , and low H_p/E ratio for iris; mass production techniques applicable; large acceptance in transverse phase space; acceptance acceptable in longitudinal phase space. To conclude we give in Table III the two sets of parameters for the iris and slotted iris structures according to the considerations outlined above (see also Fig.15).

Table III:

	iris structure	slotted iris structure
frequency		700 MHz
inner diameter		about 330 mm
diameter of beam hole		40 mm
disc thickness in region of electric field near the beam hole	16 mm	- 20 mm
rounding of corner between disc and beam hole	ellipse, ratio of major to minor axis = 2=1	
disc thickness in region of magnetic field	16 mm	- 10 mm
number of circular magnetic coupling slots	0	- 4
diameter of coupling slot	0	- about 60 mm
longitudinal acceptance	$\geq (\pm 2.3 \text{ MeV}) \times (\pm 25^\circ)$	(ref. 19)
transverse acceptance $\pi_{xx'}$, when focussing is done at distances of 4mm	4 cm mrad	(ref. 17,18)
mode of operation	π , uniform periodic	
number of cells per structure	2	- 6
accuracy of single cell pre-tuning after manufacturing	$\pm 10^{-4}$	- $\pm 10^{-4}$
number of slow tuners	one at each end cell	

Table III, continued

	iris structure	slotted iris structure	
tuning range of slow tuner	$\pm 2 \cdot 10^{-4}$	-	$\pm 10^{-4}$
cell to cell coupling coefficient	0.0002	-	0.01
flatness		≤ 0.1	
mode separation near π -mode	70 kHz	-	475 kHz
	iris structure	slotted iris structure	
	200 to 600 MeV	200 to 330 MeV	330 to 600 MeV
length of one cell	0.128 m	0.128 m	0.153 m
electric length of structure	0.257 m	0.770 m	0.918 m
ratio of effective accelerating field to accelerating field calculated by LALA	0.89	0.78	0.78
$= E_{\text{eff}}/E = T_{\text{eff}} \cos 30^\circ / T$			
E_p/E_{eff}	2.22	2.58	2.53
H_p/E_{eff}	3.85 mT/(MV/m)	8.5 mT/(MV/m)	8.3 mT/(MV/m)
$Z_{\text{eff}} = E_{\text{eff}}^2 \ell / P_s$ (Cu, 300K)	17.7 M Ω /m	14.9 M Ω /m	16.9 M Ω /m
unloaded Q-value (Cu, 300K)	$2.68 \cdot 10^4$	$2.73 \cdot 10^4$	$3.03 \cdot 10^4$

at an accelerating field of $E_{\text{eff}} = F$ MV/m and a beam current of 100 μ A we get:

beam loaded Q-value for matched rf-input	$7.57 \cdot 10^6 F$	$9.16 \cdot 10^6 F$	$8.95 \cdot 10^6 F$
beam loaded band-width for matched rf-input	93 Hz/F	76 Hz/F	78 Hz/F
E_p	2.22 F MV/m	2.58 F MV/m	2.53 F MV/m
H_p	3.85 F mT	8.5 F mT	8.3 F mT
P_s/ℓ at 1.8 K for an improvement factor of 10^5	$0.57 F^2$ W/m	$0.67 F^2$ W/m	$0.59 F^2$ W/m
P_s/ℓ at 4.2 K for the theoretical improvement of $4.7 \cdot 10^4$	$1.20 F^2$ W/m	$1.43 F^2$ W/m	$1.26 F^2$ W/m
electric length of accelerator	400 m/F	130 m/F + 270 m/F = 400 m/F	
number of structures	1556/F	169/F + 294/F = 463/F	
total number of cells	3112/F	1014/F + 1764/F = 2778/F	
total rf power required for beam acceleration	40 kW	13 kW + 27 kW = 40 kW	
rf power for each structure required for beam acceleration	25.7 F W	77.0 F W	91.8 F W
total refrigerator power at 1.8K for an improvement factor of 10^5	226 F W	87 F W + 160 F W = 247 F W	
total refr. power at 4.2K for the theoretical improvement factor of $4.7 \cdot 10^4$	481 F W	186 F W + 340 F W = 526 F W	

Appendix

Summary of recent results in rf superconductivity

Investigations on superconducting accelerating structures have been carried through so far in Stanford (HEPL), Urbana, Argonne, Brookhaven, Cornell, Cal.Tech, Geneva (CERN), Japan, England (RHEL) and Karlsruhe⁵⁰. The various results depend on the superconductor used (e.g. lead, niobium) and on the type of cavity, especially the field configuration (mode), the frequency and many design details like rf coupling or joints.

All groups working in this field use niobium as superconductor, except the group at Rutherford Lab⁵¹ and Cal-Tech.⁵² who measured lead plated copper cavities. Lead, however, shows restricted Q-values compared to the numbers achieved with niobium. This is tolerable only for a short piece of cavity as used, e.g. in a particle separator, whereas for a long accelerator one has to aim at the highest possible Q-values.

Without trying to be complete Table IV summarizes some recent results which we feel to be interesting in the context of the preceding report. For each type of cavity the measured peak magnetic fields H_p , peak electric fields E_p and accelerating field E are given, together with the Q-value and improvement-factor IF at these fields. The treatment preceding each measurement is also given.

Inspecting the table one may conclude the following tendencies:

- a) In general at higher frequencies one achieves better results than at lower frequencies. This tendency can be observed most clearly in the results by HEPL (1,2 and 3) where S-band accelerating structures achieved twice the accelerating field of L-band-structures. As it is now generally accepted⁶ that electrons play a major role in causing the rf breakdown, further investigations are necessary to deminish the detrimental effect of electrons whenever one plans to operate accelerator structures at low frequencies. (The helix seems to be an exception from this rule due to its completely different shape compared with iris type structures).
- b) Short test cavities usually give better results than multiple cell cavities (see for instance 4,5 or 11,12). This is probably mainly

due to the technical problems of surface treatment that become more involved the larger the cavities are, and to the increasing probability of intrinsic bad spots on the cavity walls with increasing surface area.

- c) Although there are different surface treatment procedures used, each of them resulting in reasonable values, there is only the Cornell-measurement (4,5) known where a niobium accelerating structure has achieved good values with chemical methods alone. In all other cases an UHV-heat treatment in connection with some kind of polishing was necessary.

The fabrication of the cavities is different and cannot be compiled in detail here, but it may be stated, that in most cases the cavity parts are machined from either solid material or from pre-fabricated (deep-drawn, rolled) pieces. All parts are connected by electron beam welding. This clearly is a very expensive method, but searching for cheaper designs (e.g. deep-drawing, hydroforming without machining afterwards, other welding methods) may result in poorer surfaces. So one has to clear whether present or future surface treatment procedures can overcome this additional difficulties.

The table shows that both an improvement factor of the order or 10^5 and an accelerating field of about 5 MV/m (aimed at for 700 MHz in the preceding report) have been achieved so far only at 3 GHz (and almost in the quite different single helix structure No.8). Although the results mentioned at 700 MHz (6,7) have to be considered as preliminary because there was no UHV heat treatment possible till now, it can clearly be seen, that continuing work has to be done to achieve values which make a large accelerator project attractive.

Table IV:

Recent results of superconducting accelerating and deflecting cavities

No.	Type of cavity	β	Treatment	Frequ. (GHz)	Low field		High field		H_p (mT)	E_p MV/m	E MV/m	Lab
					Q $\times 10^9$	IF $\times 10^5$	Q $\times 10^9$	IF $\times 10^5$				
1	Iris accelerator, 7 cells	1	d,m,ebw,cp,a,h 1800 $^\circ$,10 $^{-6}$	2.85	16	12	4.5	3.4	35.6	23	6.4	HEPL ¹⁴
2	Iris accelerator, 7 cells	1	d,m,ebw,ep,o,h 1800 $^\circ$,10 $^{-6}$	2.85	19	14	3.1	2.3	35.5	23	6.4	HEPL ¹⁴
3	Iris accelerator,55 cells	1	d,m,ebw,cp,a,h 1700 $^\circ$,10 $^{-6}$	1.3	5.4	2.7	6.9	3.5	16.2	10.8	3.0	HEPL ²⁸
4	rectangular open structure 1 cell	1	m,ep,cp,a	2.8	≥ 20	≥ 11	3	1.7	60	25	13.5	Cornell ⁵²
5	rectangular open structure 11 cells	1	m,ep,cp,a	2.8	~ 2	1.1	1	.6	20	≥ 10	4.5	Cornell ⁵²
6	Iris accelerator, 2 cells	.2	m,ep,ebw,op,cp, h -1200 $^\circ$ -10 $^{-5}$ t	.72	3	3.8	1	1.1	21	9.2	3	Karlsruhe ¹⁸
7	Alvarez accelerator, 2 cells	.1	m,ep,ebw,op,cp, h -1200 $^\circ$ -10 $^{-5}$ t	.72	15	7.5	2	1	24	16	2.2	Karlsruhe ¹⁸
8	Helix accelerator 1 $\lambda/2$ -helix	.1	d,m,ep,ebw,op, h -1100 $^\circ$ -10 $^{-7}$, ep	.108	1.5	5	0.7	2.5	105	29	4.0	Karlsruhe ⁵³
9	Helix accelerator 2.5 $\lambda/2$ helices	.1	d,m,ep,ebw,op, h -1100 $^\circ$ -10 $^{-7}$.090	1	1.6	0.1	0.16	50	16	1.4	Karlsruhe ⁵⁴
10	Iris deflector, 6 cells	1	m,ebw, cp,a,h 1800 $^\circ$,10 $^{-8}$	8.7	4.5	5	.56	.6	74	25	6.9	BNL ⁵⁵
11	Iris deflector, 4 cells	1	m,ebw,ep,o, h 1800 $^\circ$,10 $^{-8}$	2.85	4.6	4.6	2.4	2.4	85	30	5.5	Karlsruhe ⁵⁶
12	Iris deflector,20 cells	1	m,ebw,ep,o,h 1800 $^\circ$, 10 $^{-8}$	2.85	2.5	2.5	1.6	1.6	40	14	2.6	Karlsruhe ⁵⁷
13	Iris deflector,10 cells	1	lead, electropolated on copper	1.3	$\geq .21$.1	0.08	0.034	36.4	9.2	2.5	RHEL ⁵⁰

Legend: d: deep drawn o: oxypolished
 m: machined ep: electropolished
 ebw: electron beam welded h: heat treated at
 cp: chemical polished ... $^\circ$ C and ...torr
 a: anodized

References

- ¹P.M. Lapostolle, A.L. Septier, Linear Accelerators, (North Holland Publ.Co 1970)
- ²I.N. Weaver, T.I. Smith, P.B. Wilson, IEEE Trans. NS-14, No.3 (1967) 345
- ³W.B. Hermannsfeld, R.H. Helm, R.R. Cochran, Proc.1970 Proton Linear Accelerator Conf.Batavia (1970) 265
- ⁴A. Citron, M. Kuntze, W. Bauer, F. Graf, W. Jüngst, H. Kluge, W. Lehmann, K. Mittag, D. Schulze, K. Zieher. "Konzeptstudie für einen Supraleitenden Protonenlinac", KFK-Ext. 3/75-3
(Kernforschungszentrum Karlsruhe, 1974)
- ⁵M. Kuntze. IEKP, Internal Report (Kernforschungszentrum Karlsruhe, 1975) (unpublished)
- ⁶see for instance: P. Kneisel, O. Stoltz, and J. Halbritter. J.Appl.Phys. 45 (1974) 2302
- ⁷J.Ben Zvi, J.F. Crawford, J.P. Turneure. IEEE Trans. NS-20 No.3 (1973) 54
- ⁸C. Lyneis, Y. Kojima, J.P. Turneure, N.T.Viet, Proc.1973 Particle Accelerator Conference, San Francisco, IEEE Trans.Nucl.Sci. NS-20 (1973) 101
- ⁹W. Bauer, A. Citron, G. Dammertz, M. Grundner, L. Husson, H.Lengeler, E. Rathgeber. IEEE Trans. NS-22, No.3 (1975)
- ¹⁰C.M. Lyneis, P. Kneisel, O. Stoltz, J. Halbritter. IEEE Trans. MAG-11 (1975)
- ¹¹P. Kneisel, O. Stoltz, J. Halbritter. J.Appl.Phys. 45 (1974) 2296
- ¹²H. Diepers, O. Schmidt, H. Martens, F.S. Sun. Phys.Lett. 37A (1971) 139
- ¹³H. Martens, H. Diepers, B. Hillenbrand. Phys.Lett. 44A, 1973 p.213
- ¹⁴P. Kneisel, C. Lyneis, J.P. Turneure. IEEE Trans. NS-22, No.3 (1975)
- ¹⁵E. Sauter. (IEKP, Kernforschungszentrum Karlsruhe) (1972) (unpublished)
- ¹⁶K. Zieher; to be published
- ¹⁷SIN-Newsletter, Schweizerisches Institut für Nuclearforschung, August 1974
- ¹⁸K. Mittag; to be published
- ¹⁹W. Jüngst, private communication
- ²⁰J.P. Turneure; 1972 Appl.Superconductivity Conf.Annapolis (IEEE, 1972) 621
- ²¹P.B. Wilson; Proc.Proton Linear Acc.Conf. Los Alamos (1972) 82
- ²²see, for instance, ref.1, p.1118
- ²³T.I. Smith; HEPL Internal Report 437 (Stanford, 1966)
- ²⁴W. Jüngst;KFK-Ext. 3/69-16, (Kernforschungszentrum Karlsruhe, 1969)
- ²⁵W. Bauer, Internal Report BNL 17767, AADD 73-3 (Brookhaven 1973)

- ²⁶G.R. Swain, R.A. Jameson, R. Kandarian, D.J. Liska, E.R. Martin, J.M. Potter; Proc.1972 Proton Linear Acc.Conf., Los Alamos, 242
- ²⁷M.A. Allen, P.B. Wilson. Proc.1972 Proton Linear Accelerator Conf. Los Alamos (1972) 279
- ²⁸J.P. Turneure, H.A. Schwettman, H.D.Schwarz, M.S.Mc Ashan; Appl.Phys.Lett.25 (1974) 247
- ²⁹K. Mittag, H.A. Schwettman, H.D.Schwarz; IEEE Trans.Nucl.Sci.NS-20 (1973) 86
- ³⁰R.R. Cochran; Internal Report SLAC-TN-72-2(SLAC 1972)
- ³¹C.S. Taylor in ref.1, p. 879
- ³²A. Carne in ref.1, p. 587
- ³³M.S. Livingston; Los Alamos report LA-5000, VC 23, 28, 834 (Los Alamos 1972)
- ³⁴G. Dome in ref.1, p. 637
- ³⁵G.A. Loew, R.B. Neal in ref.1, p.39
- ³⁶M.S. McAshan, K. Mittag, H.A. Schwettman, L.R. Suelzle, J.P.Turneure Appl.Phys.Letters 22 (1973)605
- ³⁷S. Giordano; Linear Acc.Conf. 1964 MURA Report No.714 (1964) 60
- ³⁸Studie über einen supraleitenden Protonen-Linearbeschleuniger im GeV-Bereich, KFK-IEKP-1967 (unpublished)
- ³⁹E.A. Knapp in ref.1, p.601
- ⁴⁰V.G. Andreev, V.M. Belugin, V.G. Kulman, E.A. Mirochnik, B.M. Pirozhenko; Proc.1972 Prot.Lin.Acc.Conf., Los Alamos (1972) 114
- ⁴¹M. Bres, A. Chabert, F. Foret, D.T. Trau, G. Voisin; Part.Acc. 2 (1972) 17
- ⁴²G.J. Dick, K.W. Shepard; Appl.Phys.Lett.24 (1974) 40
- ⁴³K.W. Shepard, J.E. Mercerau, G.J. Dick; IEEE Trans.NS-22, No.3 (1975)
- ⁴⁴J. Kirchgessner, H. Padamsee, H.L. Philips, D. Rice, R. Sundelin, M. Tigner, E.v.Borstel; IEEE Trans.NS-22, No.3 (1975)
- ⁴⁵H.C. Hoyt, D.D. Simmons, W.R. Rich; Rev.Sc.Instr.37 (1966) 755
- ⁴⁶V. Vaghin; thesis (CERN report 71-4, 1971)
- ⁴⁷E.A. Knapp, B.C. Knapp, J.M. Potter; Rev.Sc.Instr.39 (1968) 979
- ⁴⁸H. Eschelbacher, H. Schopper; Proc.Lin.Acc.Conf.,Los Alamos (1966) 502
- ⁴⁹For a survey see the latest Accelerator- and Applied superconductivity-Conferences, and as a general introduction:
H. Hahn in Externer Bericht, Kernforschungszentrum Karlsruhe
KFK-Ext. 3/72-11 (1972) G1
- ⁵⁰A. Carne, R.G. Bendall, J.R.J. Bennett, B.G. Brady, J.A. Hirst, J.v. Smith, Proc.IX.Int.Conf.High Energy Acc, Stanford (1974) 154
- ⁵¹K.W. Shepard, J.E. Mercereau, G.J. Dick, IEEE Trans.NS-22,No.3(1975)
- ⁵²R.M. Sundelin, J. Kirchgessner, H. Padamsee, H.L. Philips, D. Rice, M. Tigner, E.v.Borstel, Proc.IX.Int.Conf.High Energy Acc.,Stanford (1974) 128
- ⁵³B. Piosczyk, G. Hochschild, J.E. Vetter; IEEE Trans.NS-22, No.3(1975)
- ⁵⁴M. Kuntze, IEKP,Kernforschungszentrum Karlsruhe, Internal Report (1975) and to be published

- ⁵⁵J.R. Aggus, W. Bauer, S. Giordano, H. Hahn, H.J. Halama,
Appl.Phys.Lett. 24 (1974) 144
- ⁵⁶W. Bauer, A. Citron, G. Dammertz, M. Grundner, L. Husson,
H. Lengeler, E. Rathgeber, IEEE Trans. NS-22, No.3 (1975)
- ⁵⁷W. Bauer, A. Citron, G. Dammertz, M. Grundner, L. Husson,
H. Lengeler, E. Rathgeber, Proc. IX.Int.Conf. High Energy
Acc., Stanford (1974) 133

Acknowledgement

The assistance of M. Rutz in programming and drafting is very much appreciated.

fig. 1a

700 MHz-iris with parallel discs

	d_1	d	d_2	a	a_1	R_1	R	rounding of the iris
—x—	0	0.5	1.0	1.0	1.5	15.5	16.0	circular
—•—	"	"	"	1.5	2.0	"	"	
—+—	"	"	"	2.0	2.5	"	"	
—*—	"	"	"	3.0	3.5	"	"	
—o—	"	"	"	4.0	4.5	"	"	
—⊗—	0.25	"	"	1.0	1.5	15.9	16.4	elliptic
—⊙—	"	"	"	1.5	2.0	"	"	
—⊕—	"	"	"	2.0	2.5	"	"	
—⊗—	"	"	"	3.0	3.5	"	"	
—⊙—	"	"	"	3.0	3.5	"	"	

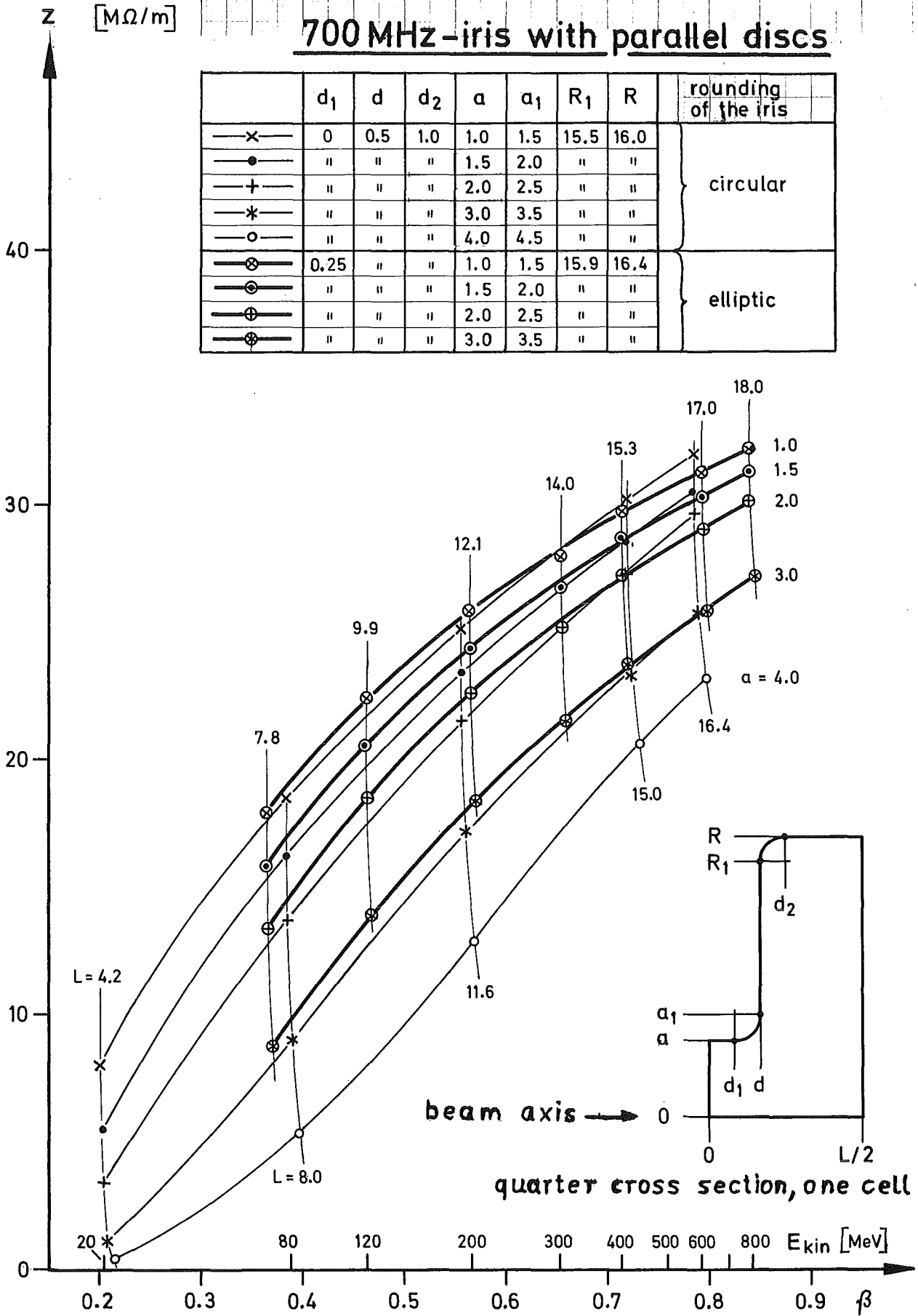


fig. 1b

700MHz-iris with parallel discs

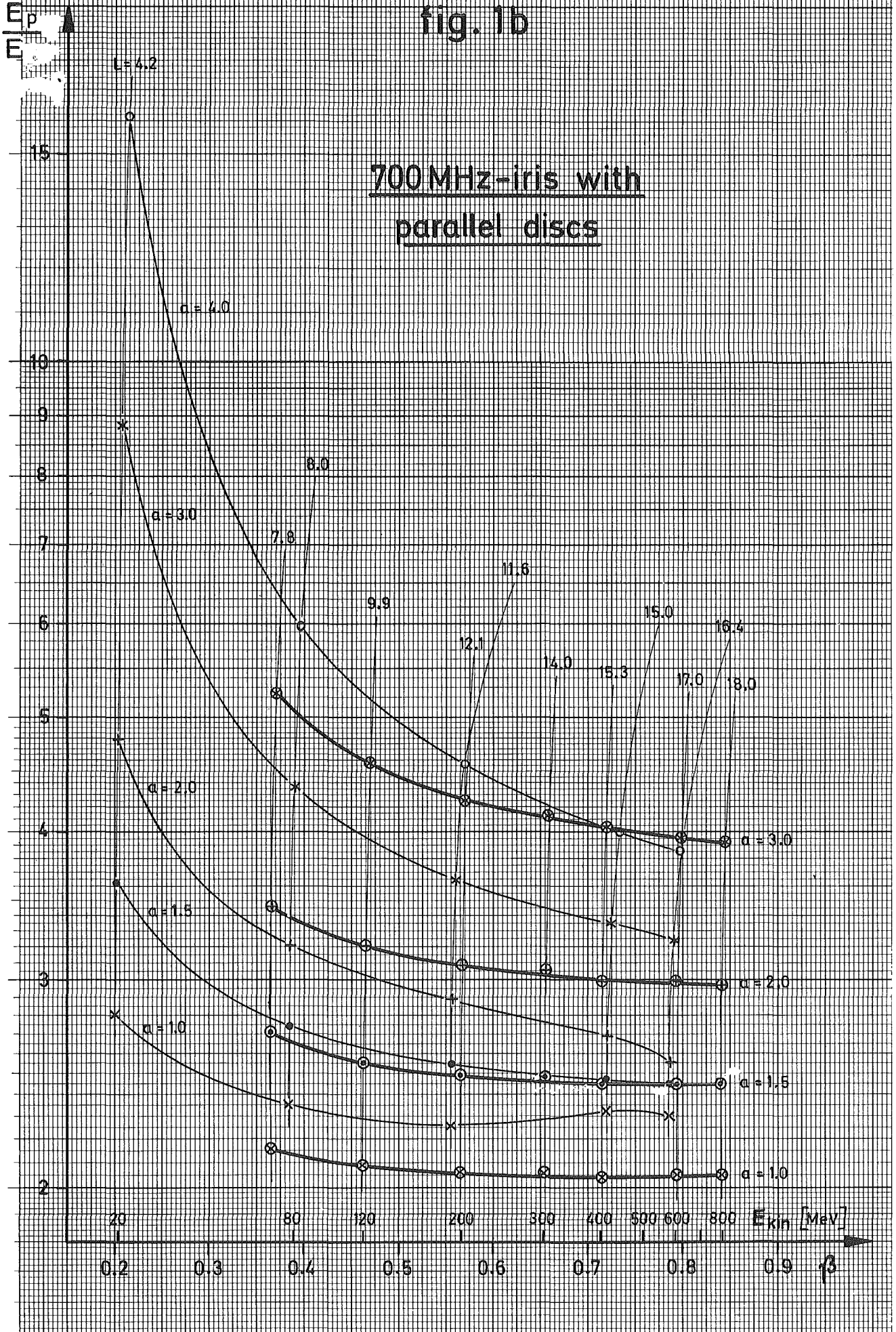


fig. 1c

700 MHz - iris with parallel discs

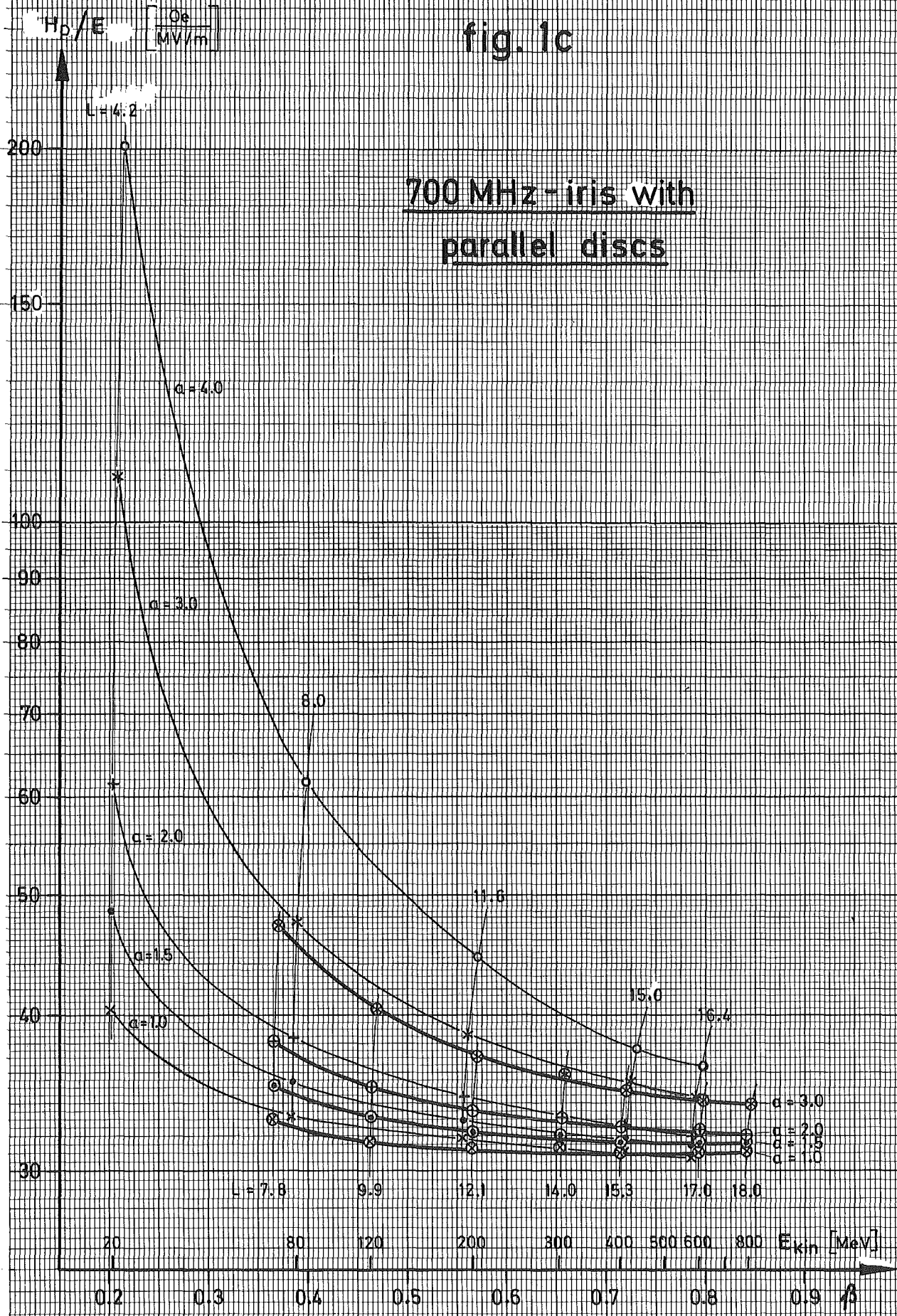


fig. 2a

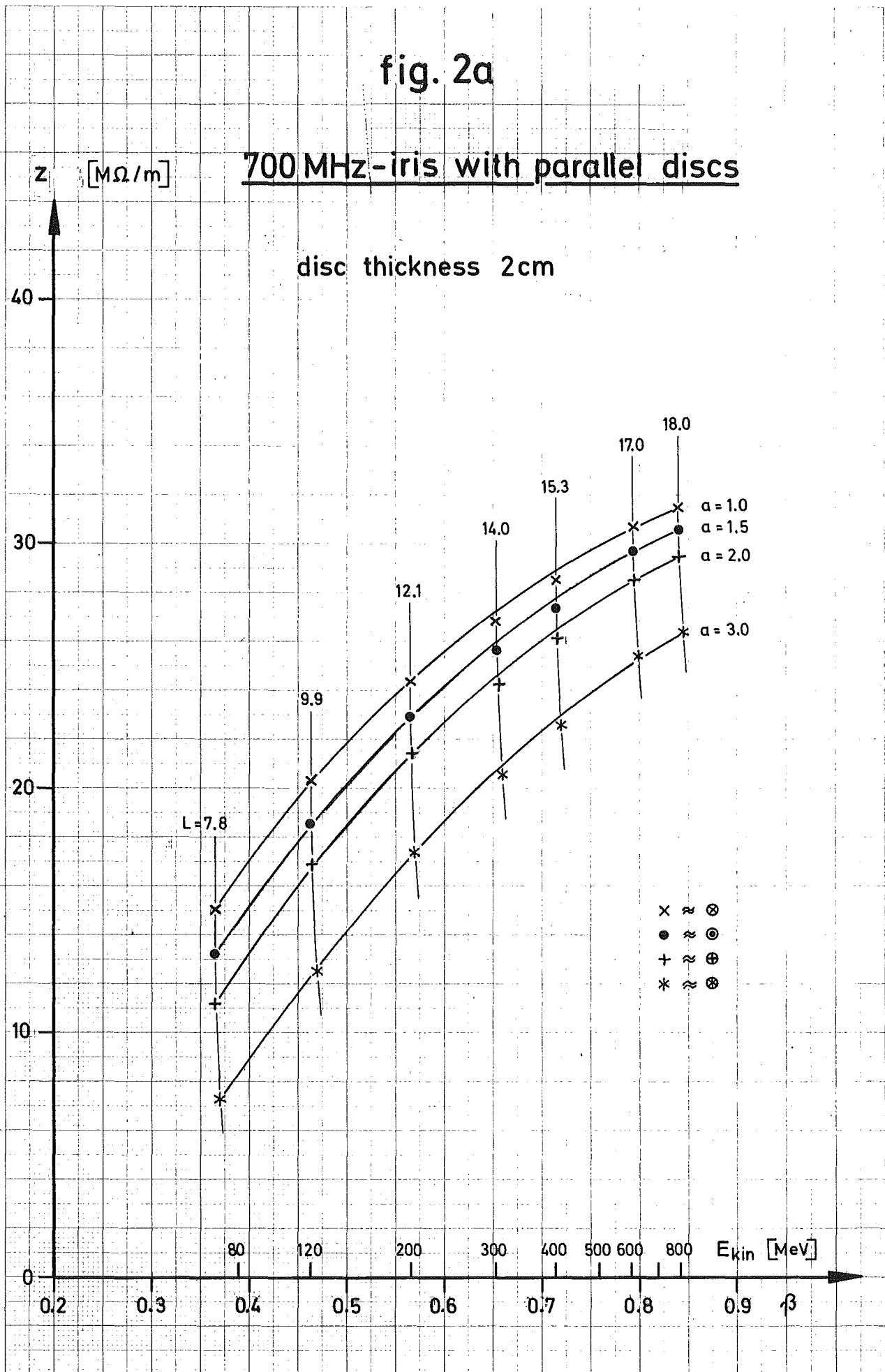
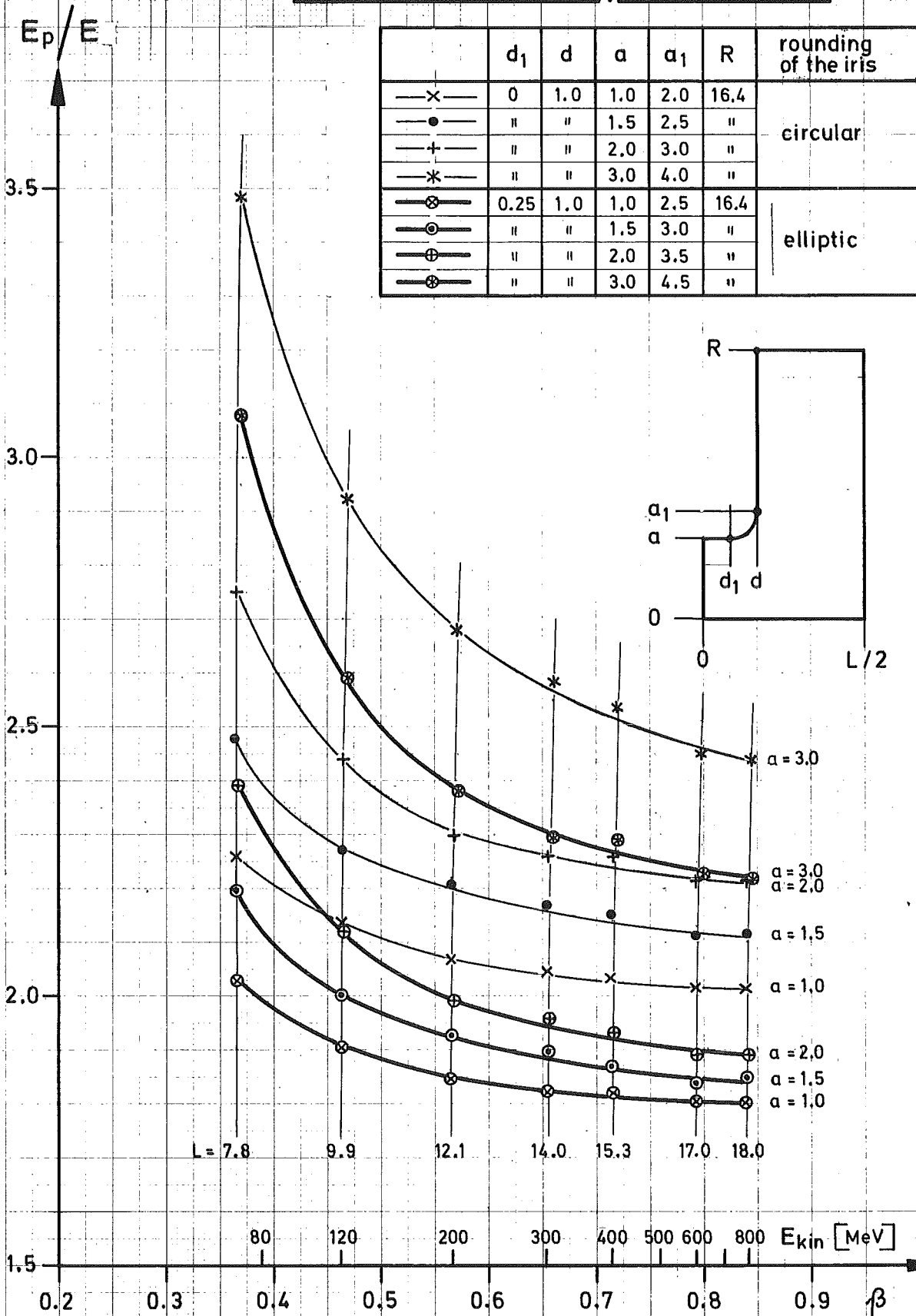


fig. 2b

700 MHz-iris with parallel discs



	d_1	d	a	a_1	R	rounding of the iris
—x—	0	1.0	1.0	2.0	16.4	circular
—●—	"	"	1.5	2.5	"	
—+—	"	"	2.0	3.0	"	
—*—	"	"	3.0	4.0	"	
—⊗—	0.25	1.0	1.0	2.5	16.4	elliptic
—○—	"	"	1.5	3.0	"	
—⊕—	"	"	2.0	3.5	"	
—⊗—	"	"	3.0	4.5	"	

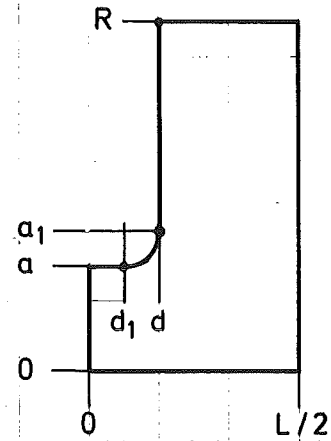


fig. 2c

700 MHz - iris with parallel discs

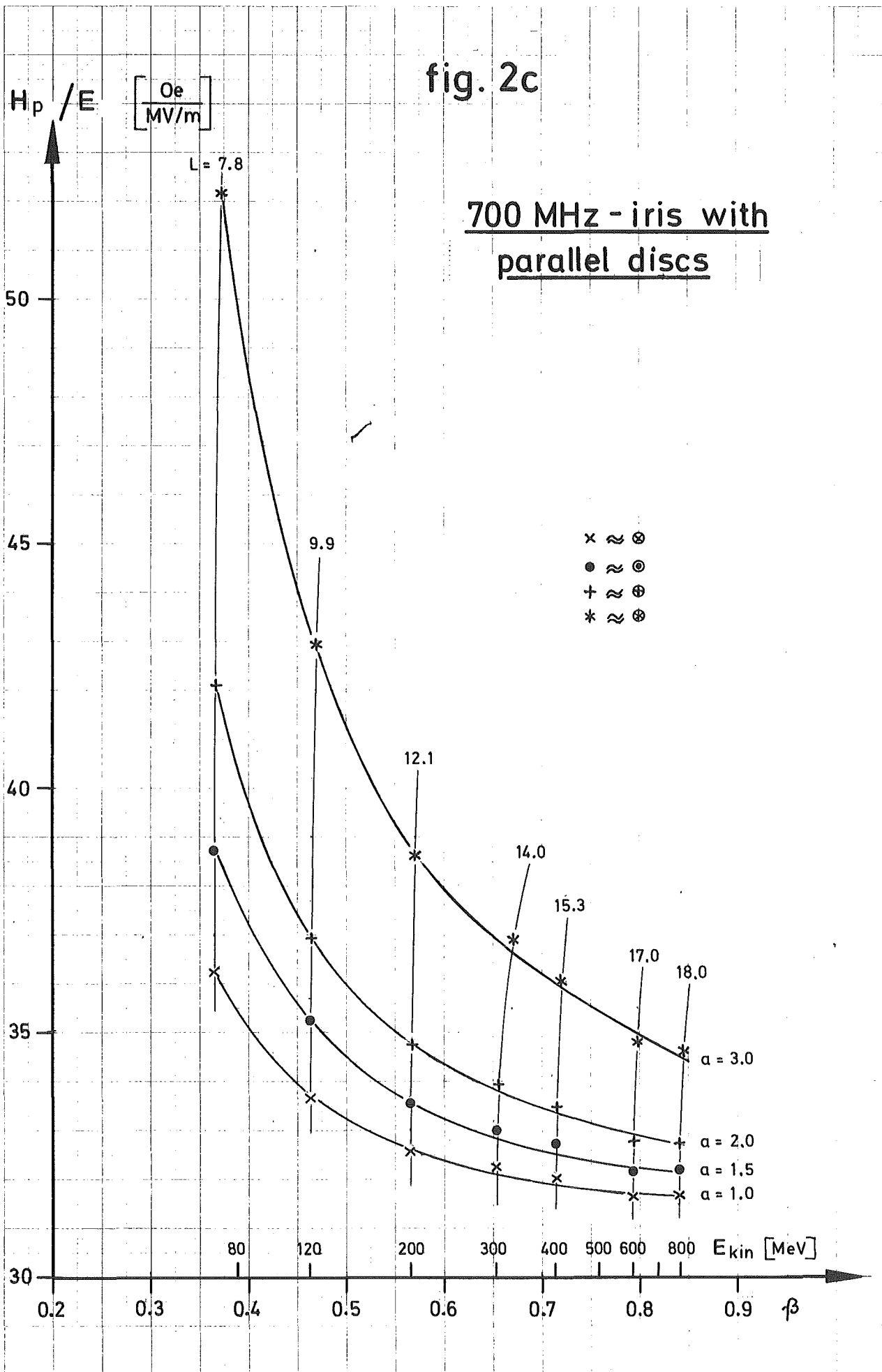


fig. 3a

700 MHz-iris with parallel discs

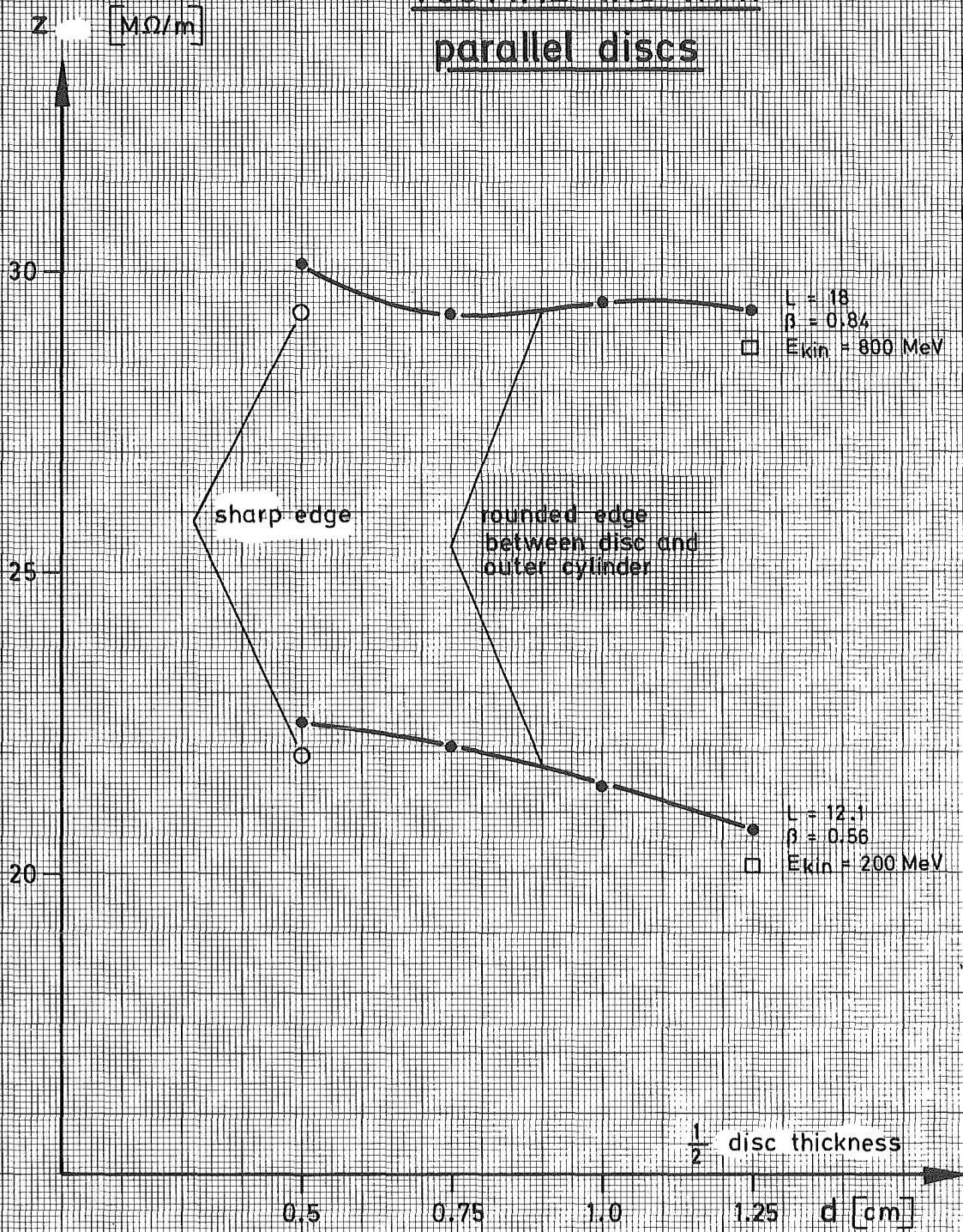


fig. 3b

700 MHz-iris with parallel discs

E_p/E

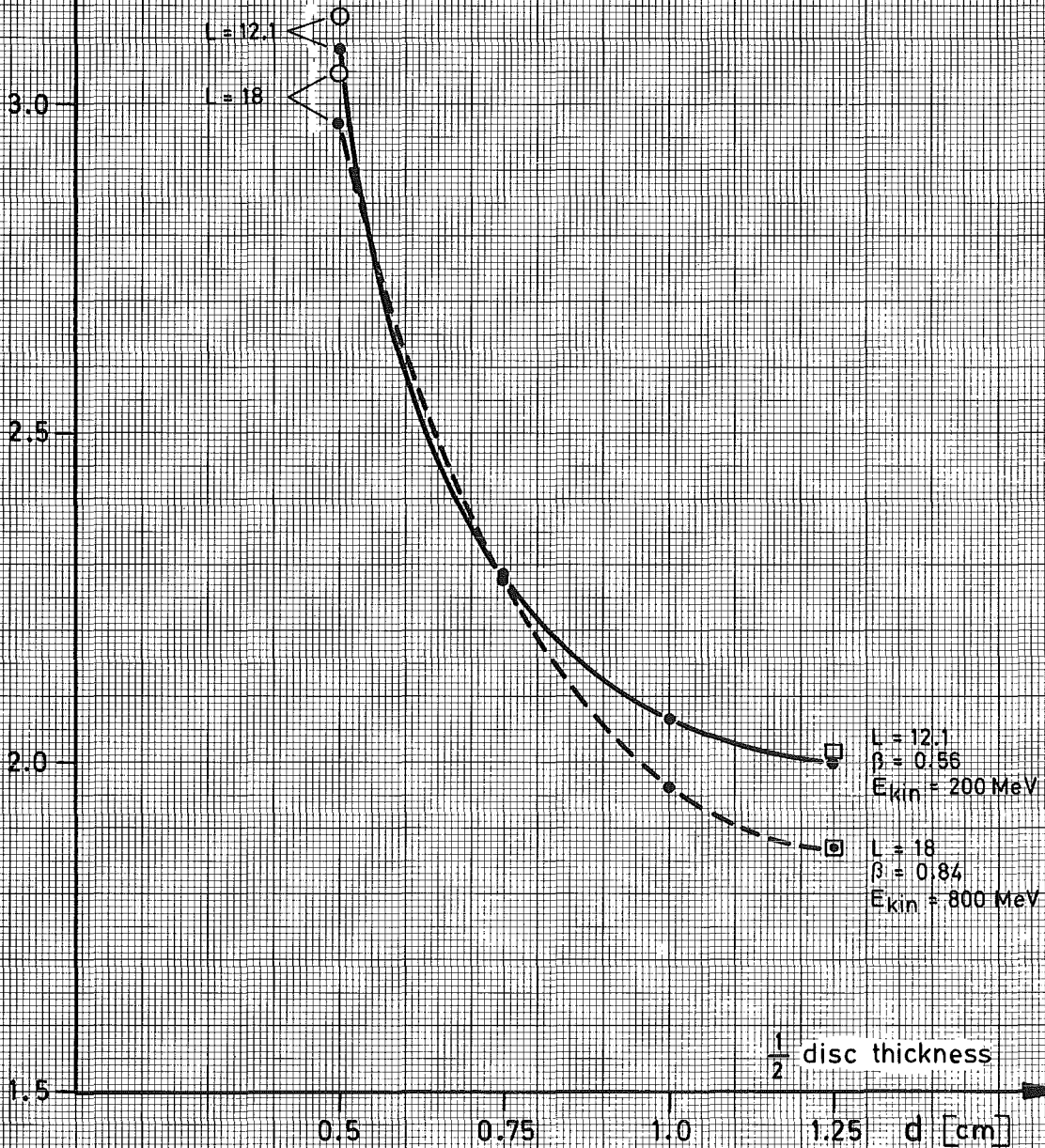
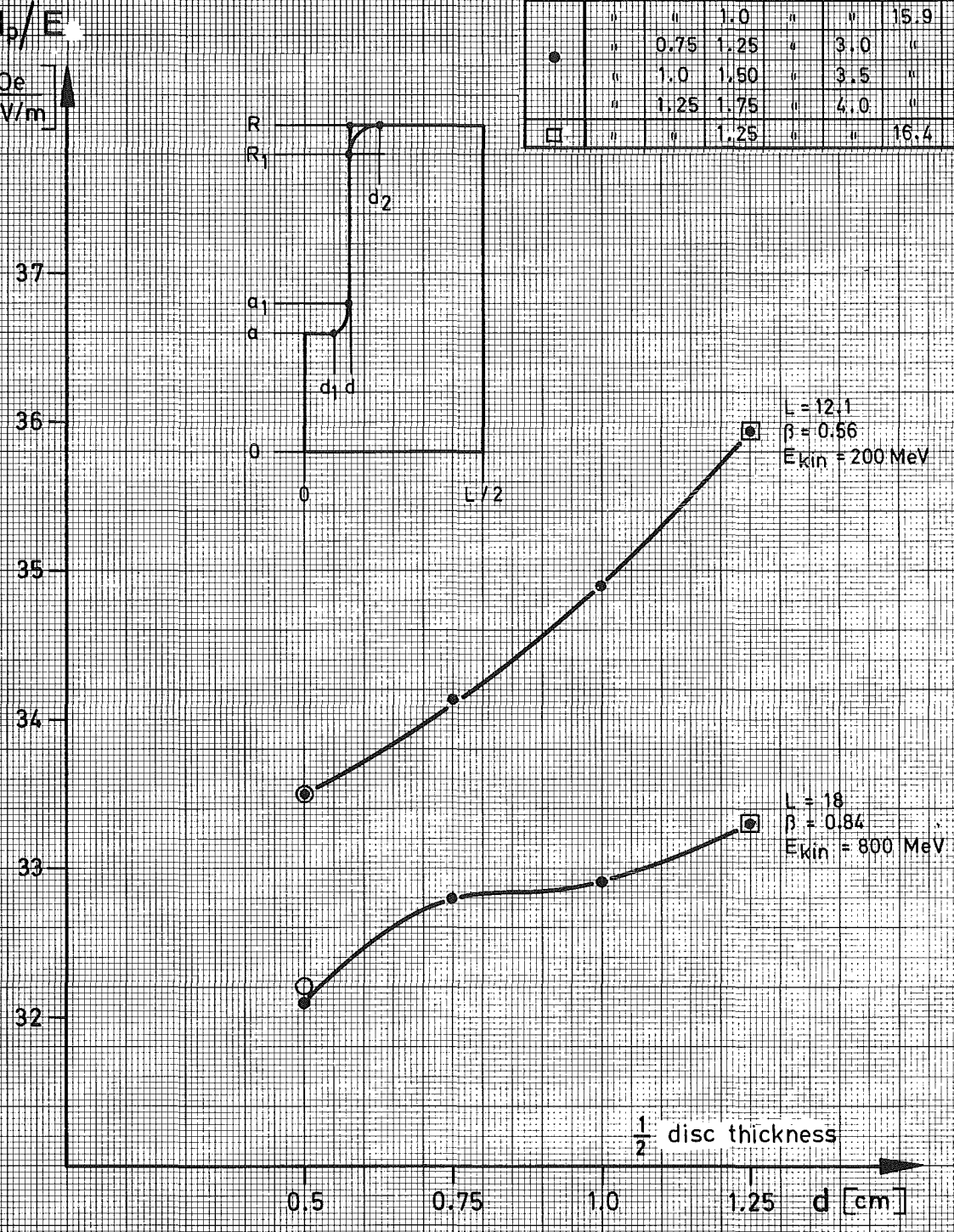
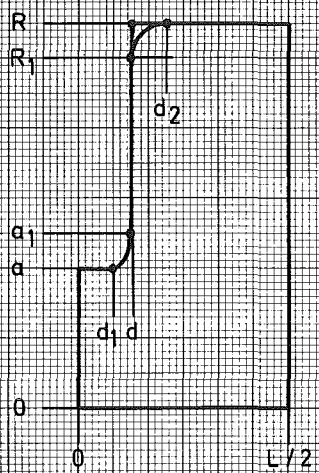


fig. 3c

700 MHz - iris with parallel discs

	d_1	d	d_2	a	a_1	R_1	R
○	0.25	0.5	0.5	2.0	2.5	16.4	16.4
●	"	"	1.0	"	"	15.9	"
	"	0.75	1.25	"	3.0	"	"
	"	1.0	1.50	"	3.5	"	"
	"	1.25	1.75	"	4.0	"	"
□	"	"	1.25	"	"	16.4	"

H_p/E
 $\frac{Oe}{MV/m}$



700 MHz - reentrant iris fig. 4a

	d_1	d	d_2	d_3	d_4	a	a_1	a_2	a_3	R_1	R
x	0.75	1.0	0.75	0.5	1.0	1.0	1.5	4.5	7.5	14.5	15.0
•	"	"	"	"	"	1.5	2.0	5.0	8.0	"	"
+	"	"	"	"	"	2.0	2.5	5.5	8.5	"	"
*	"	"	"	"	"	3.0	3.5	6.5	9.5	"	"
o	"	"	"	"	"	4.0	4.5	7.5	10.5	"	"

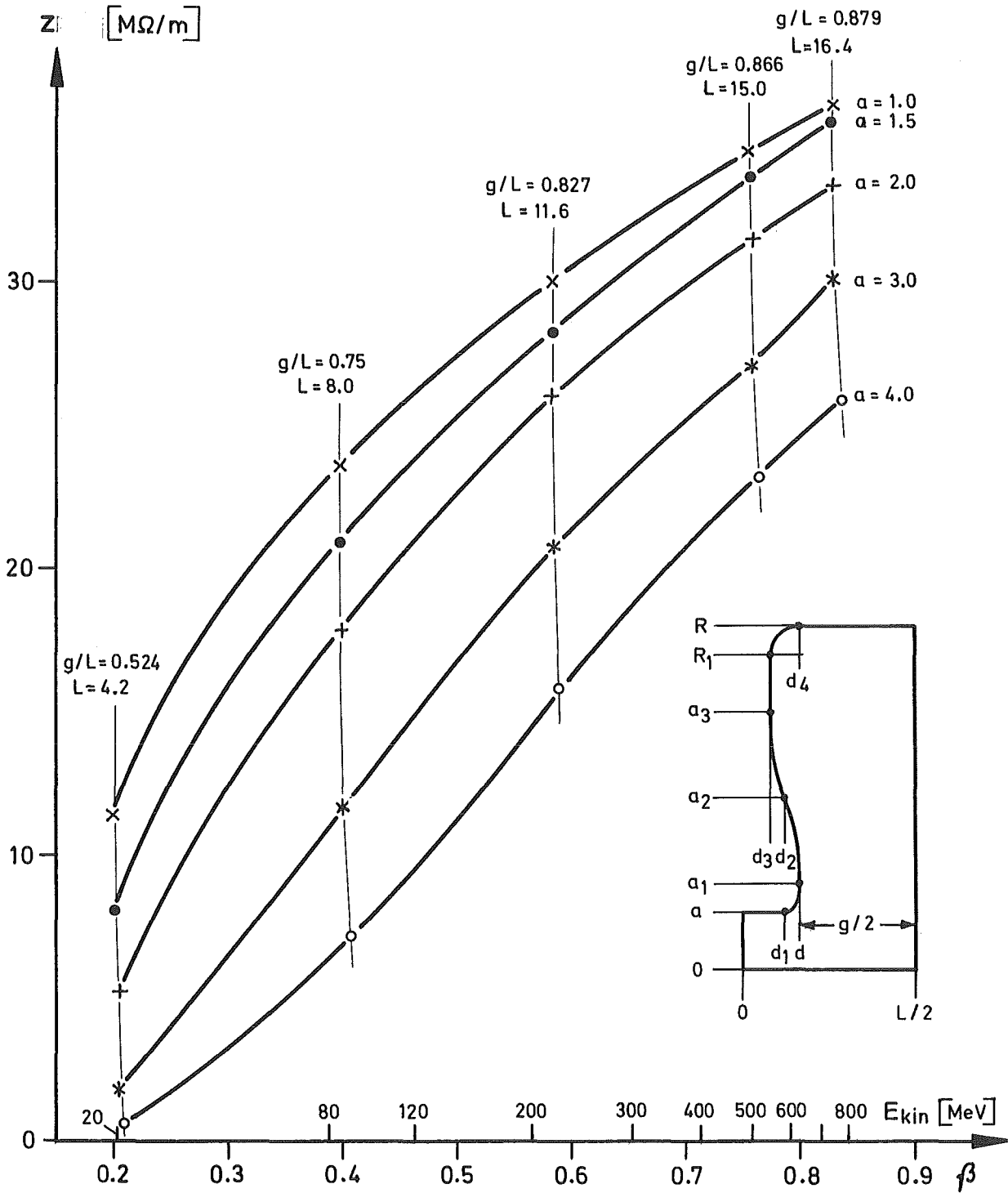


fig. 4b

E_p/E_{kin} [MeV]

700 MHz - reentrant iris

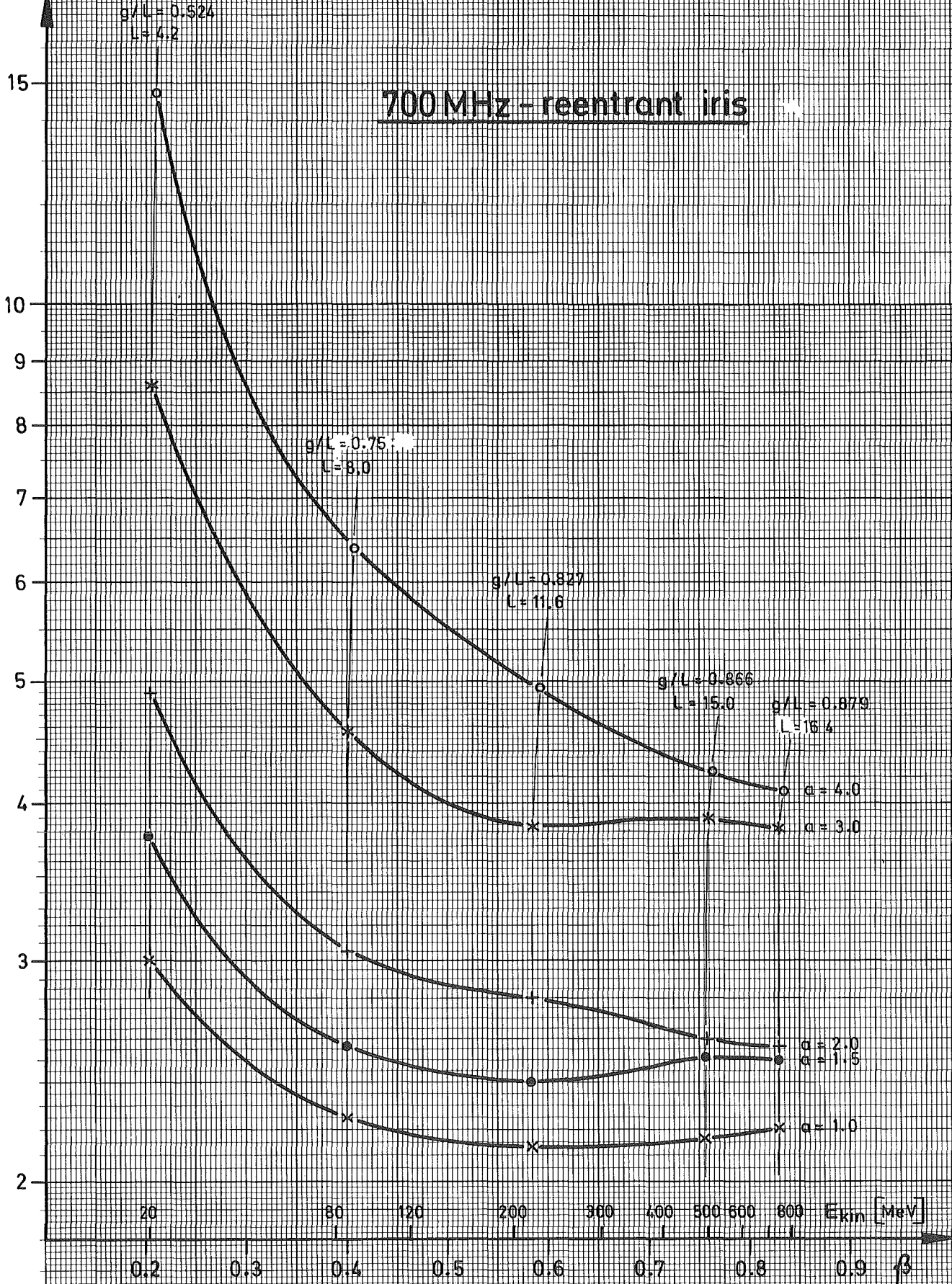


fig. 4c

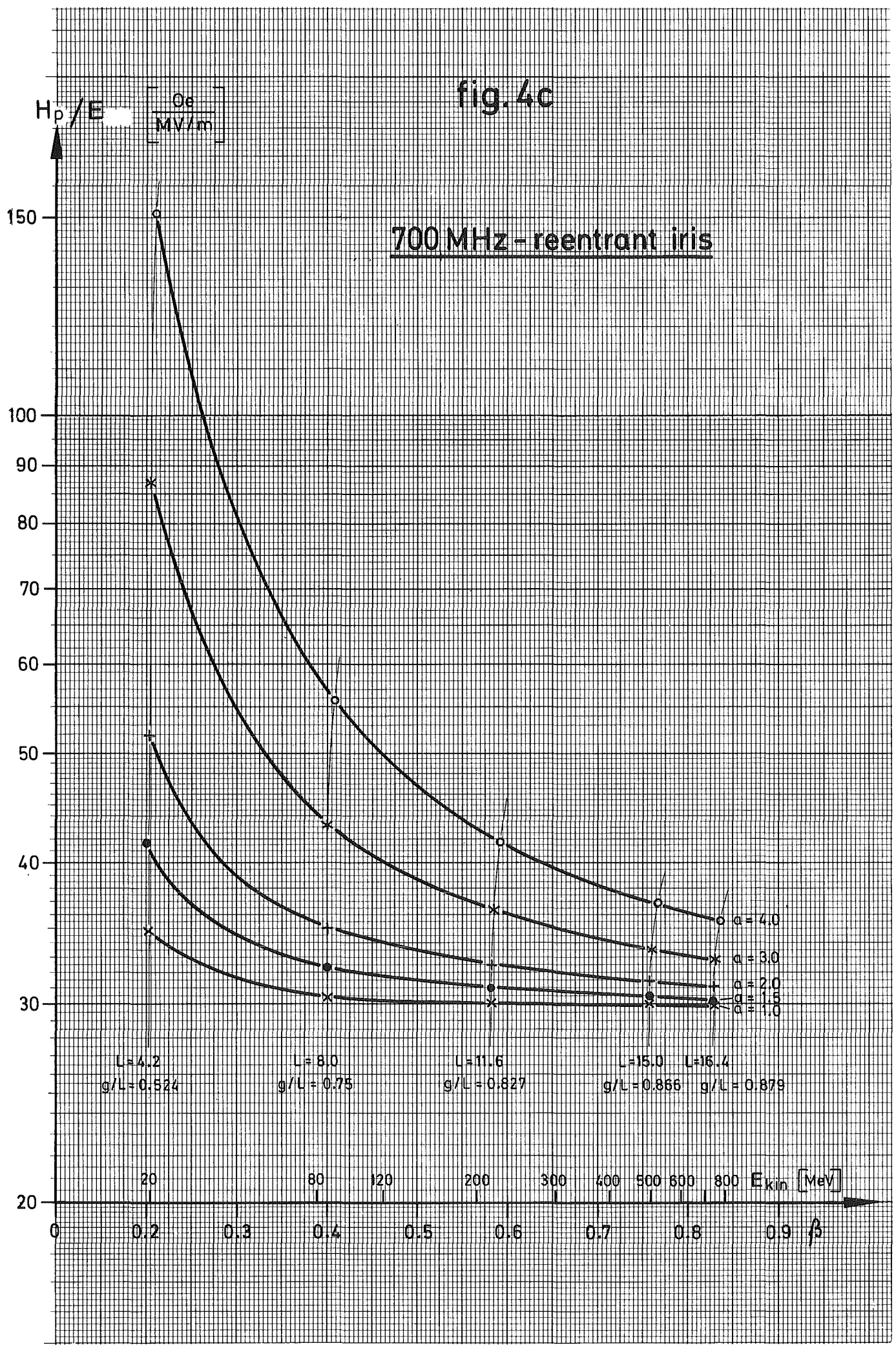


fig. 5a

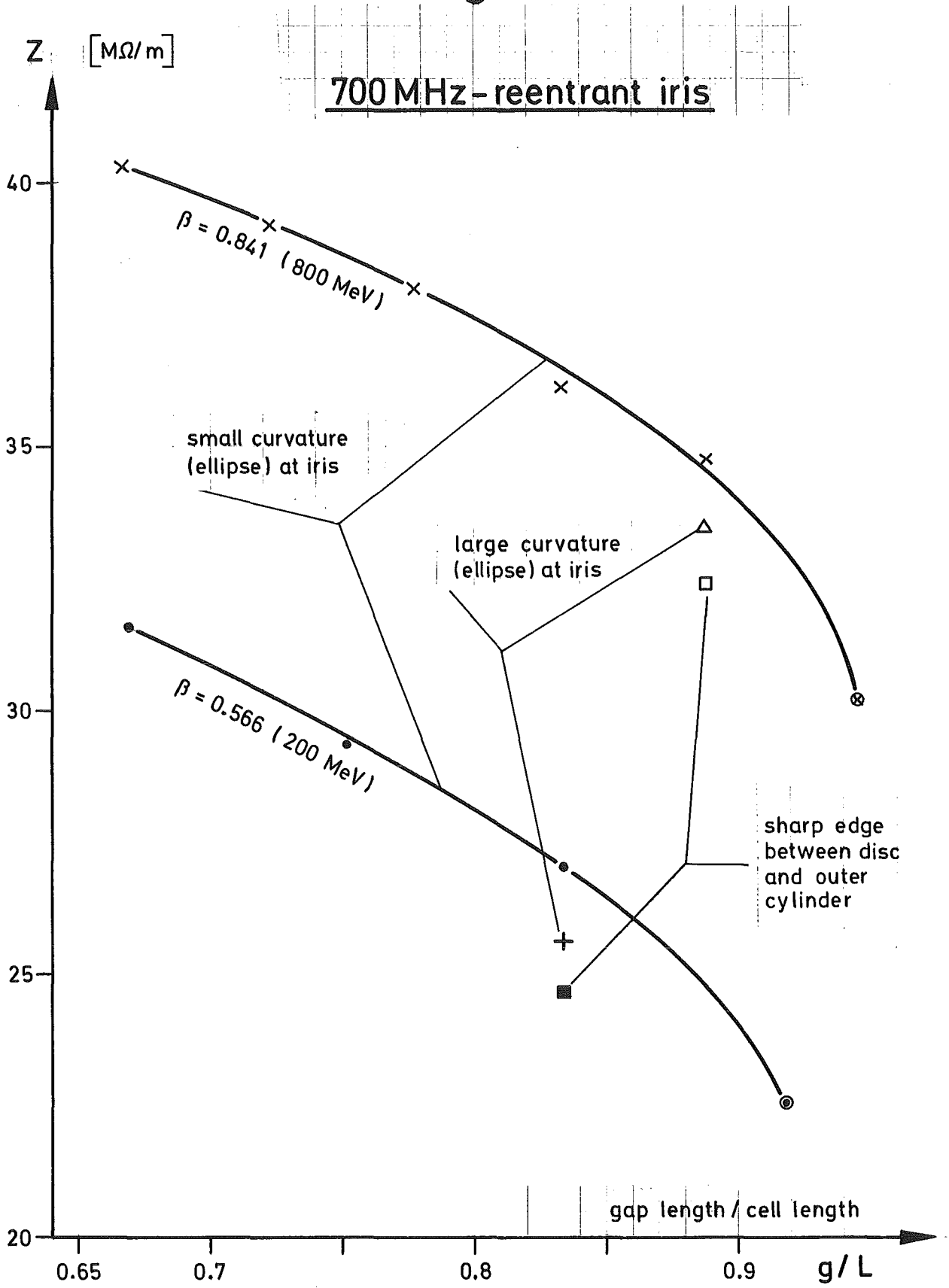
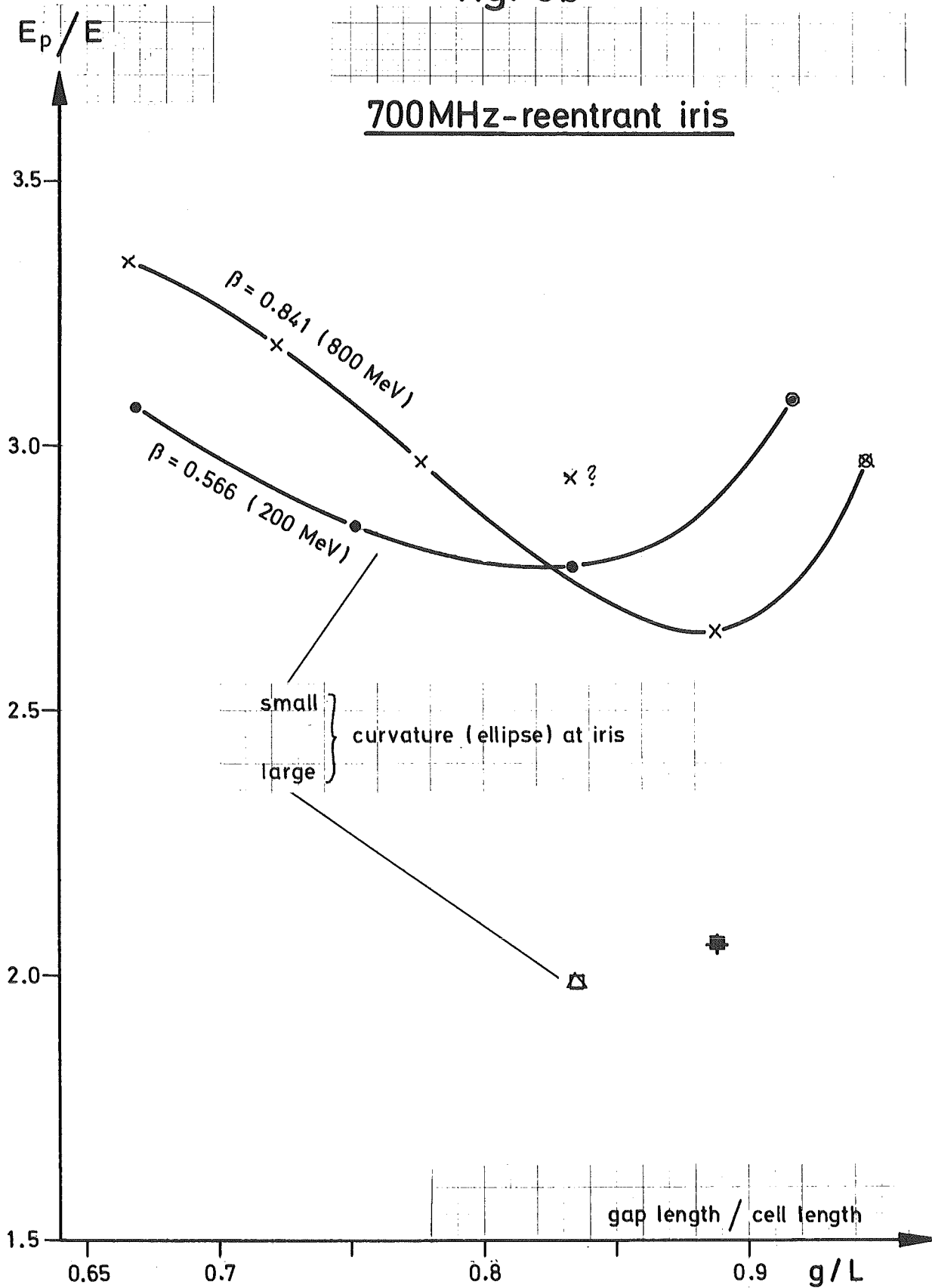


fig. 5b



700 MHz - reentrant iris

fig. 5c

	d_1	d	d_2	d_3	d_4	a	a_1	a_2	a_3	R_1	R	$L/2$
⊙	0.25	0.5	0.5	0.5	1.0	2.0	2.5	-	-	15.9	16.4	6.05
•	0.75	1.0	0.75	"	1.5	"	"	5.0	7.5	14.5	15.5	"
	1.25	1.5	1.0	"	"	"	"	"	"	"	"	"
	1.75	2.0	1.25	"	"	"	"	"	"	"	"	"
+	0.25	1.0	0.75	"	"	"	3.5	5.5	"	"	"	"
■	"	"	"	"	0.5	"	"	"	"	15.5	"	"
⊗	"	0.5	0.5	"	1.0	"	2.5	-	-	15.9	16.4	9.0
x	0.75	1.0	0.75	"	1.5	"	"	5.0	7.5	14.5	15.5	"
	1.25	1.5	1.0	"	"	"	"	"	"	"	"	"
	1.75	2.0	1.25	"	"	"	"	"	"	"	"	"
	2.25	2.5	1.5	"	"	"	"	"	"	"	"	"
	2.75	3.0	1.75	"	"	"	"	"	"	"	"	"
△	0.25	1.0	0.75	"	"	"	3.5	5.5	"	"	"	"
□	"	"	"	"	0.5	"	"	"	"	15.5	"	"

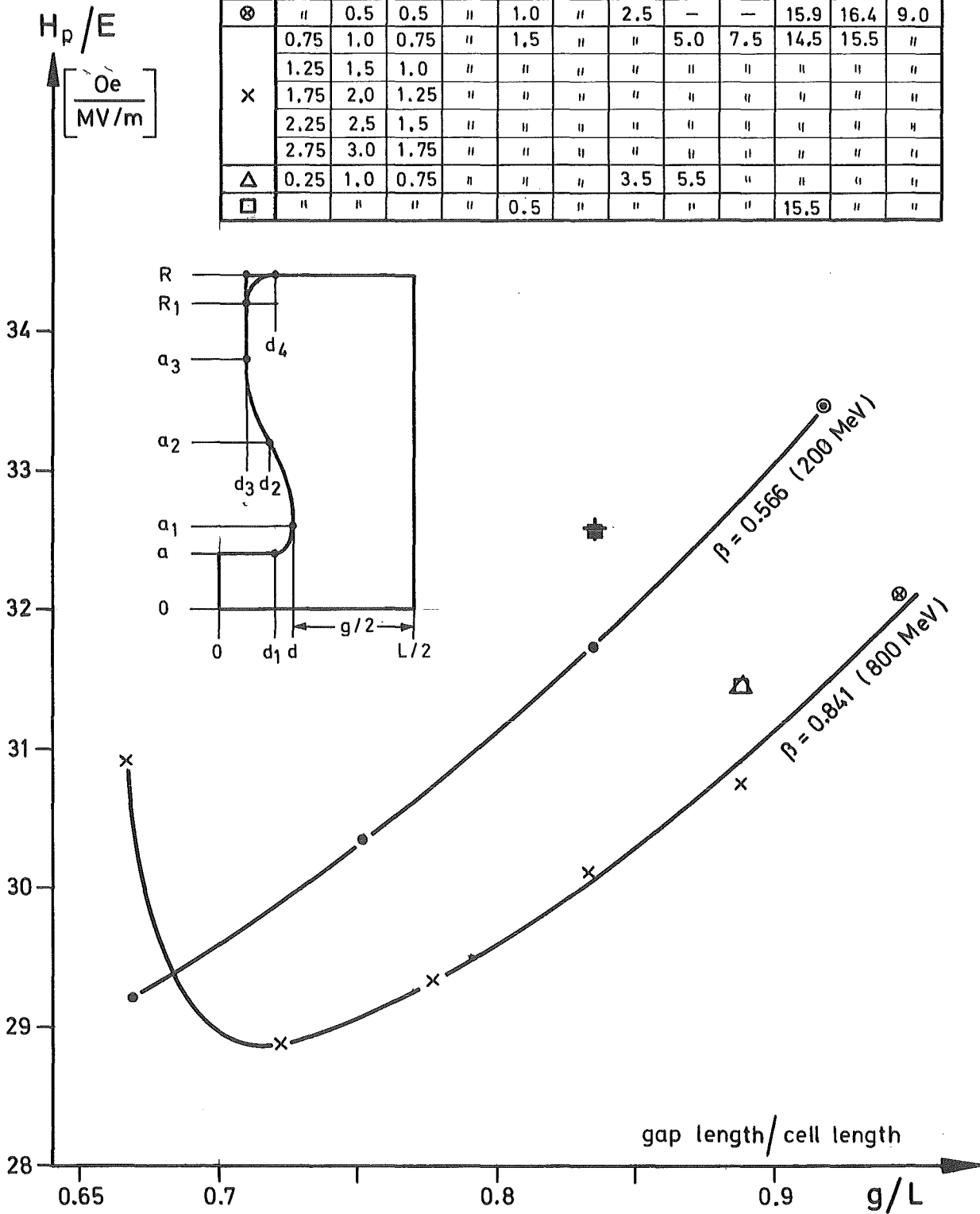


fig. 6a

700 MHz iris with tapered discs

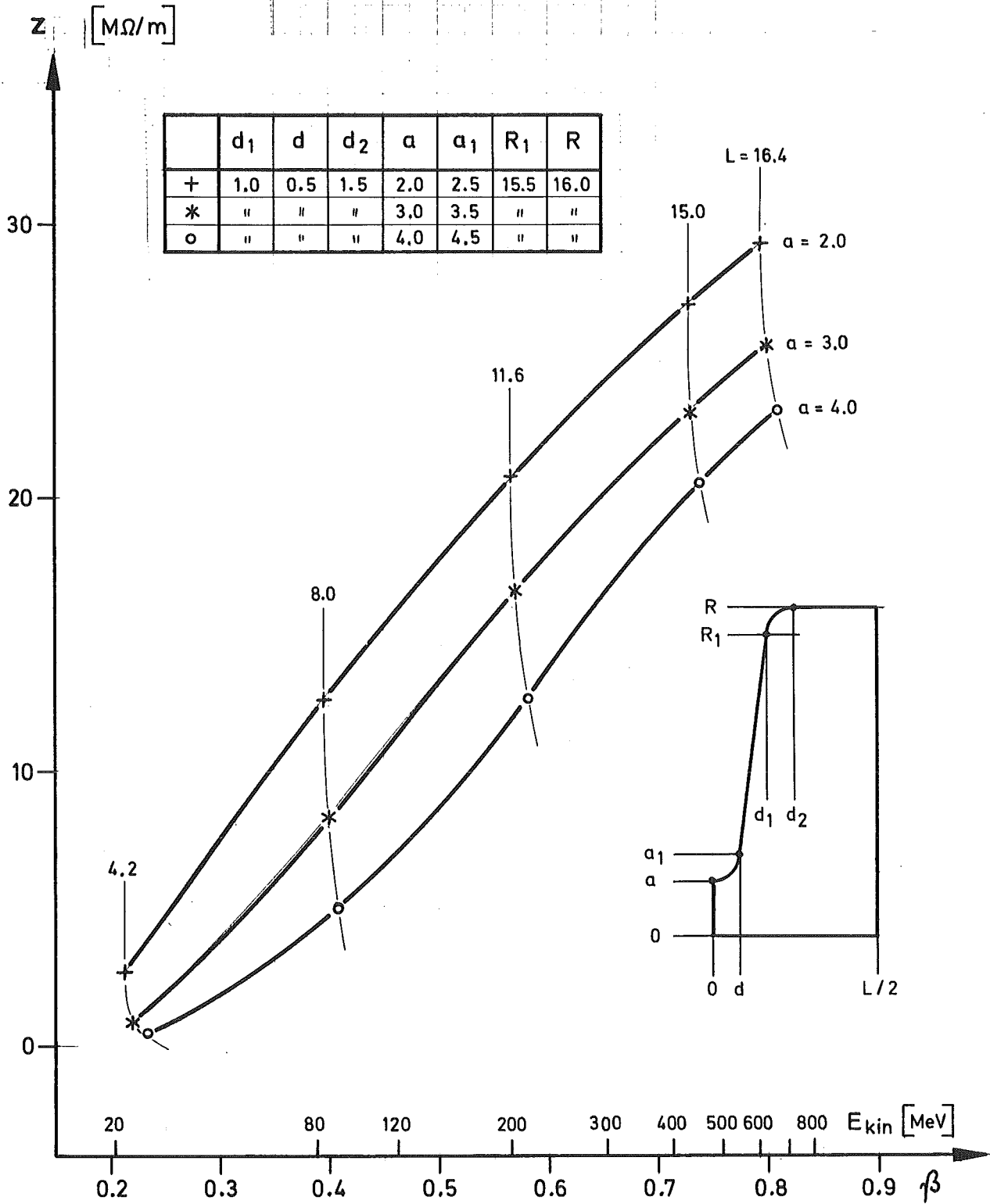


fig. 6b

700 MHz - iris with tapered discs

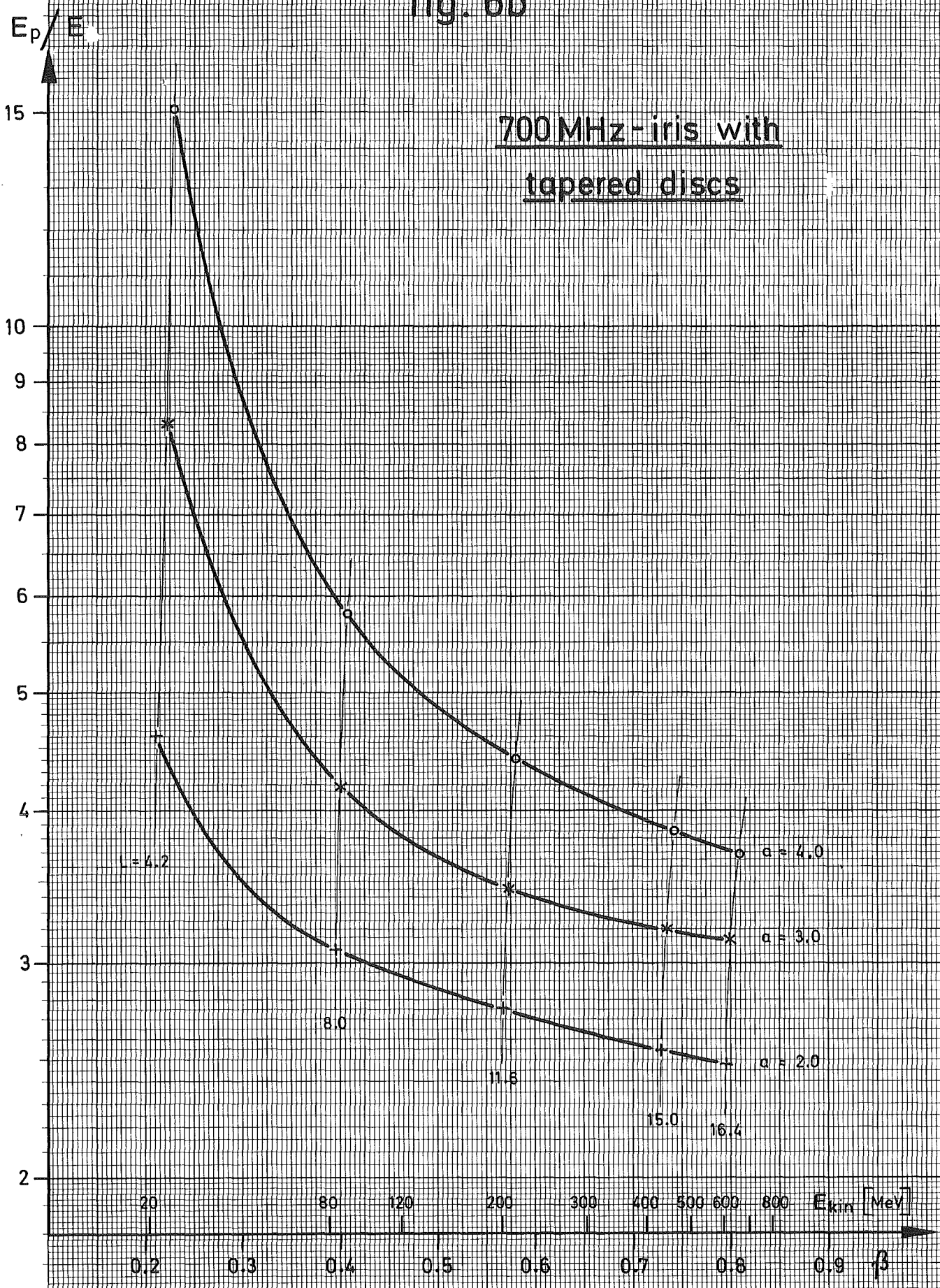


fig. 6c

700 MHz-iris with tapered discs

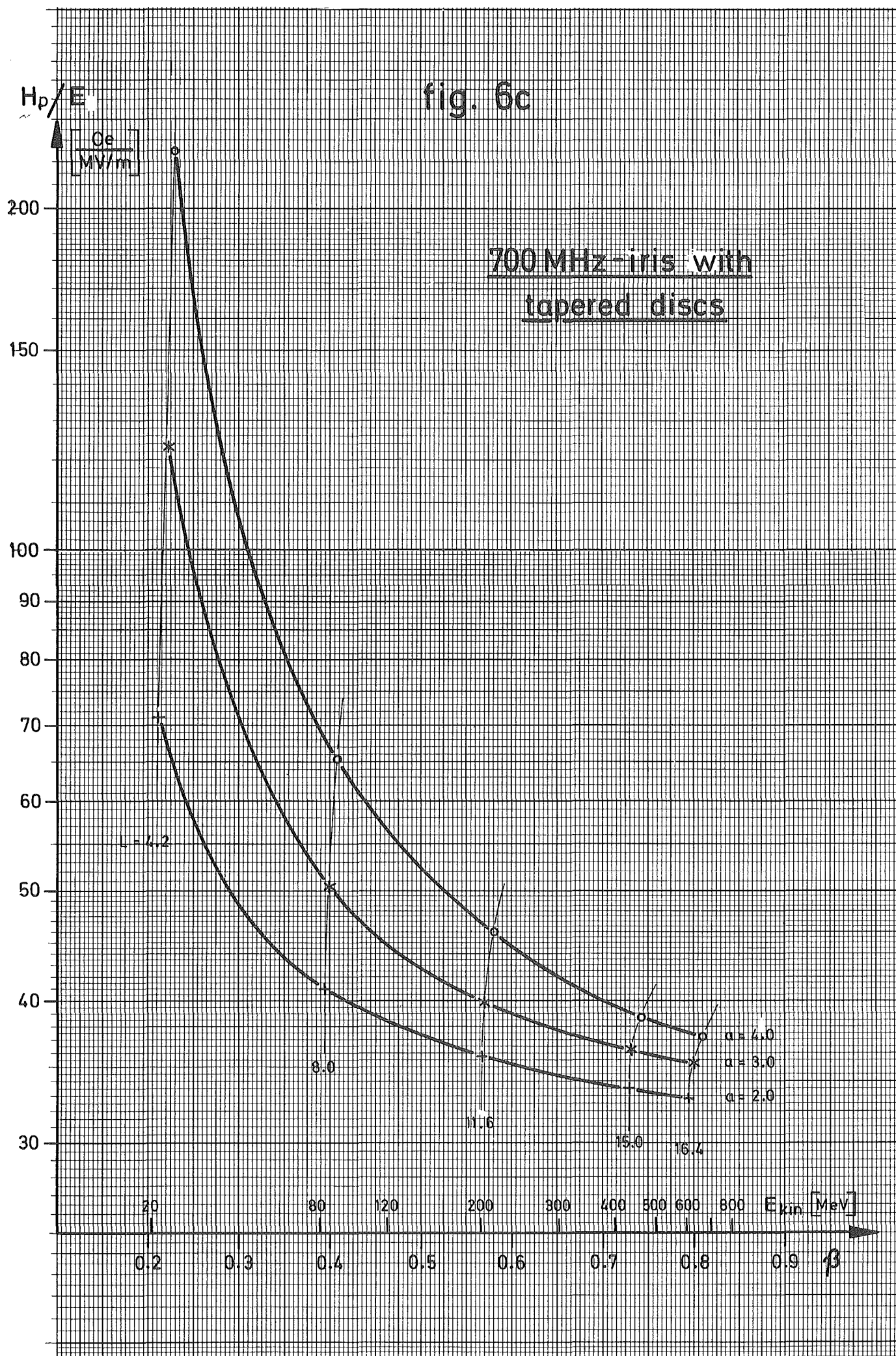


fig. 7a

1.3 GHz-iris

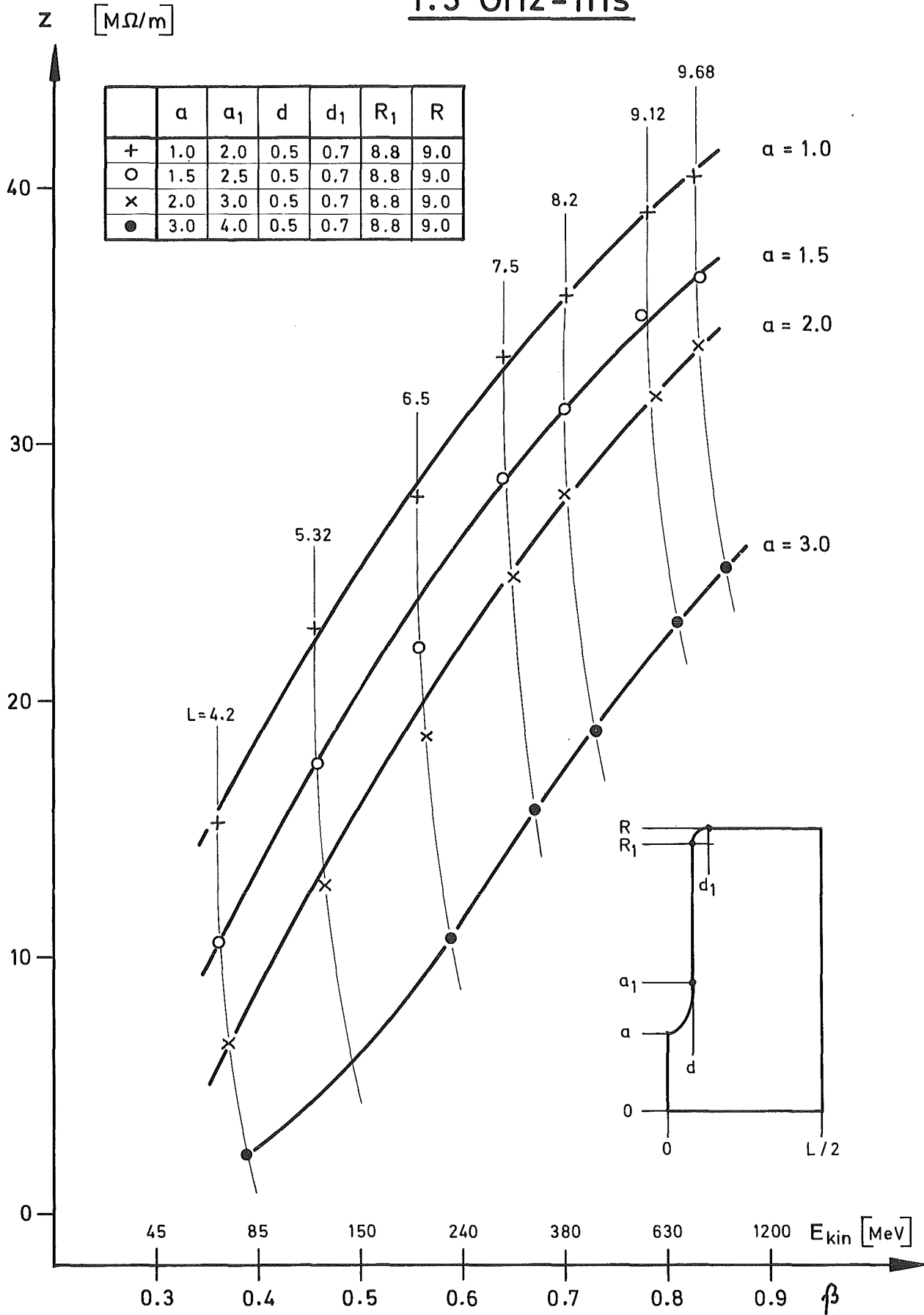


fig. 7b

1.3 GHz - iris

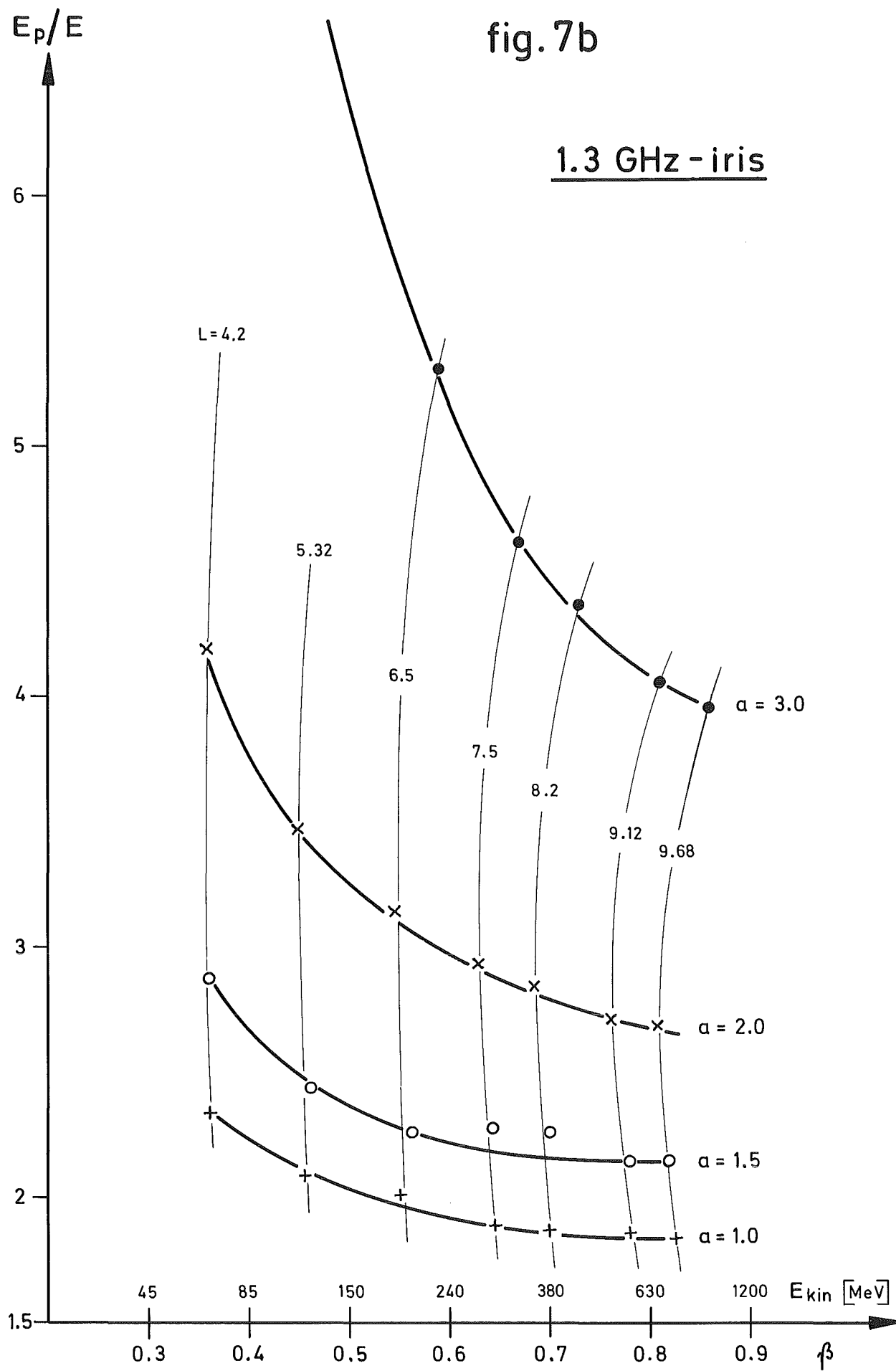


fig. 7c

1.3 GHz - iris

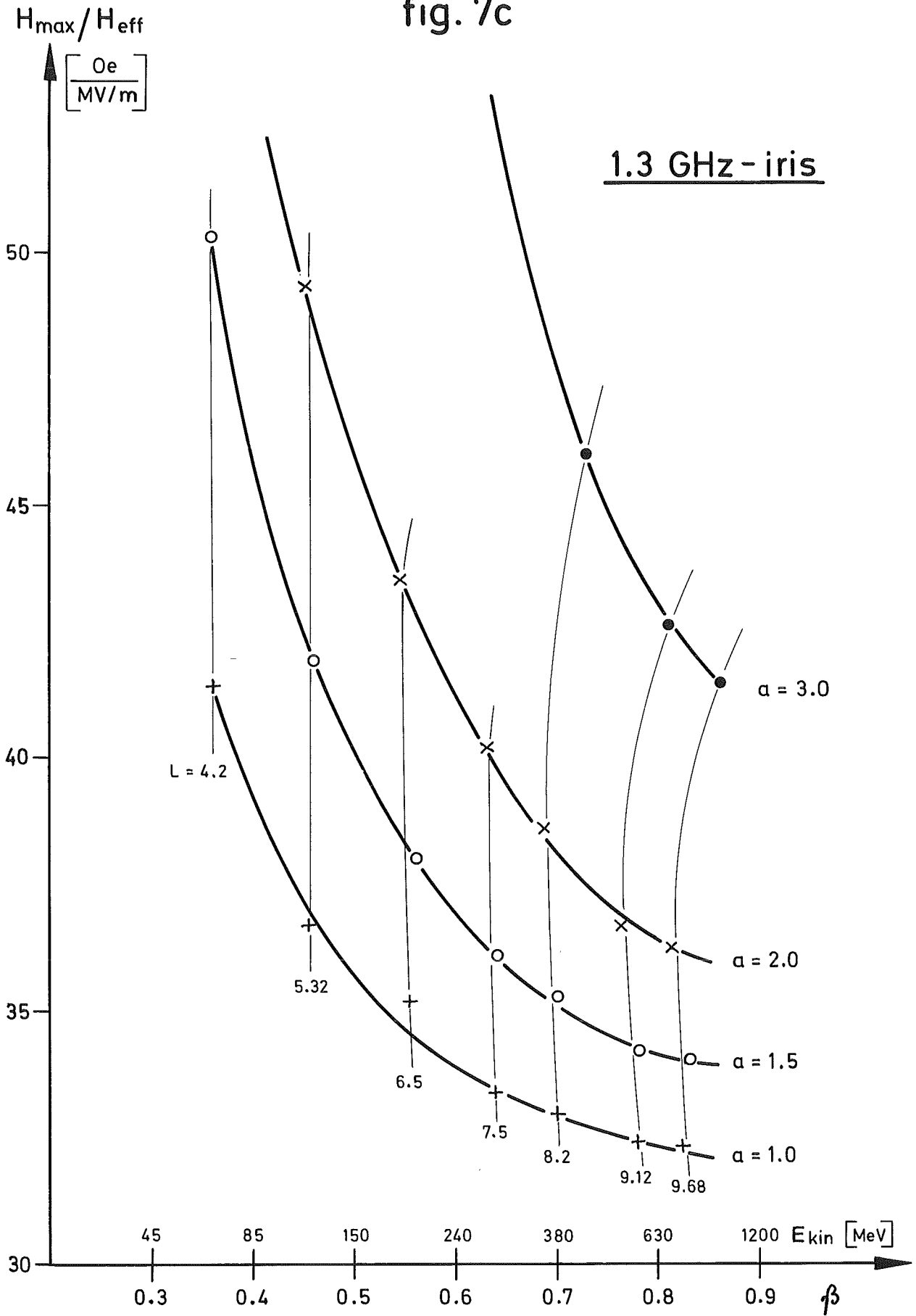


fig. 8a

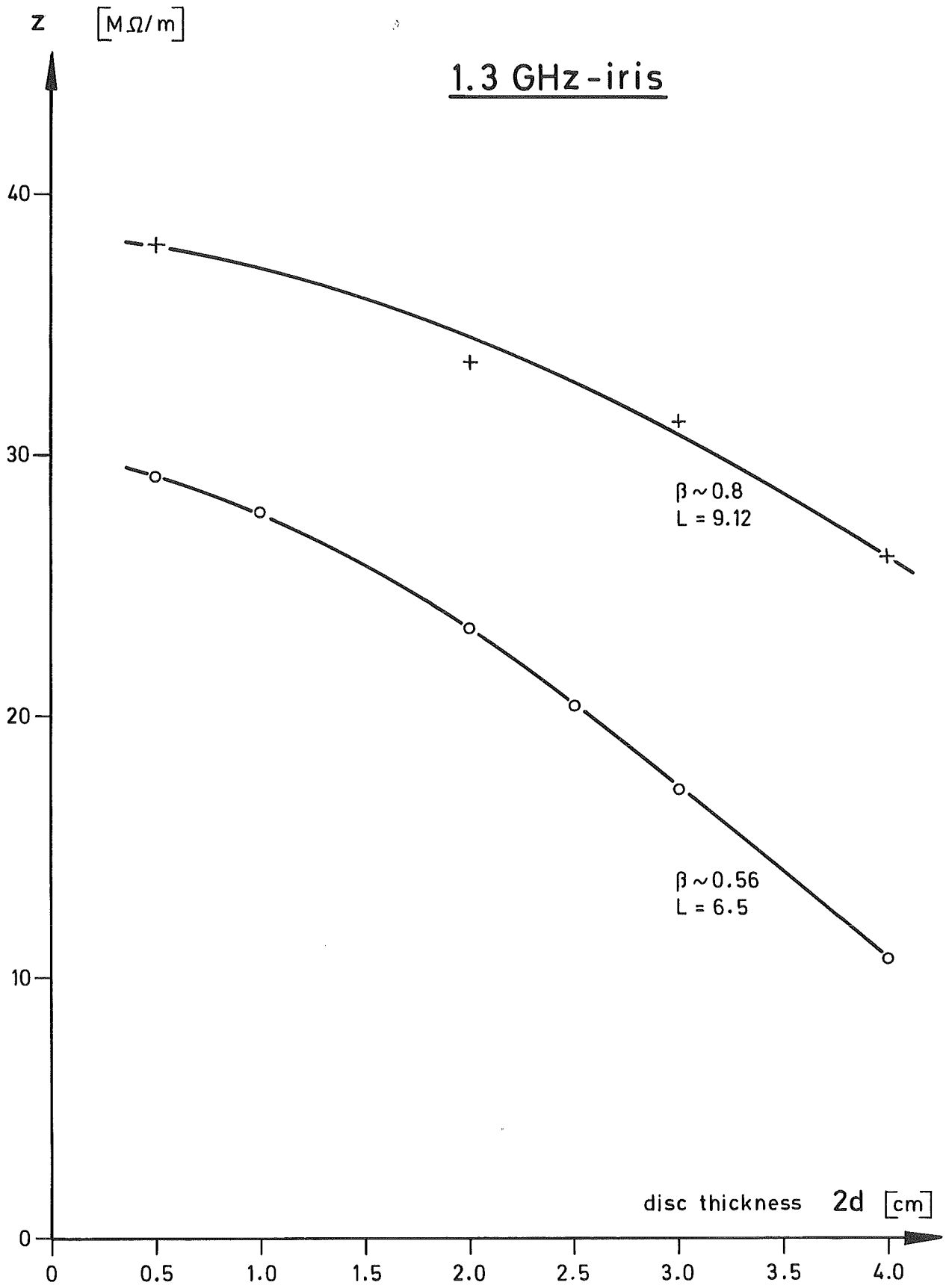


fig. 8b

1.3 GHz - iris

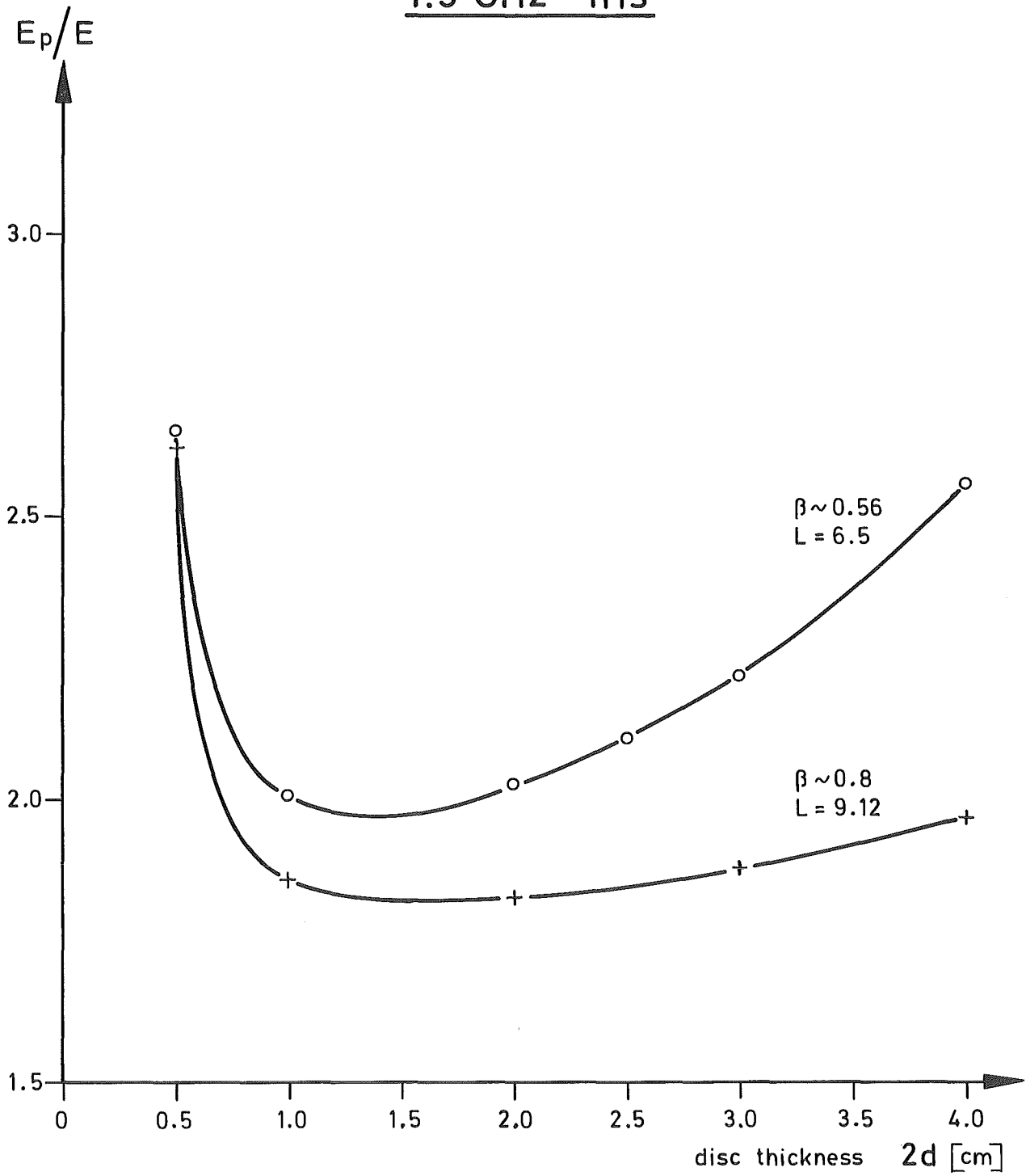


fig. 8c

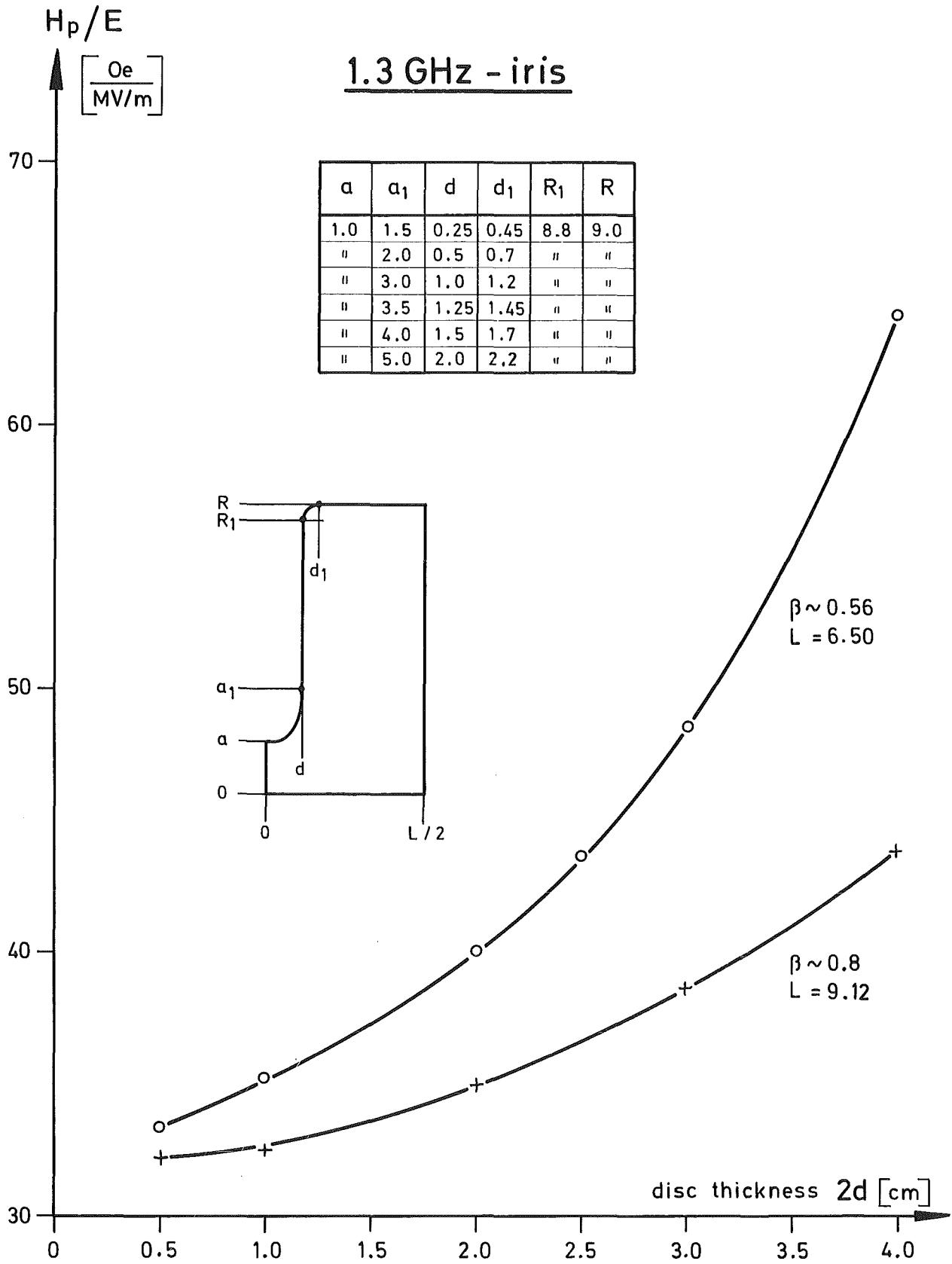


fig. 9a

1.3GHz reentrant-iris

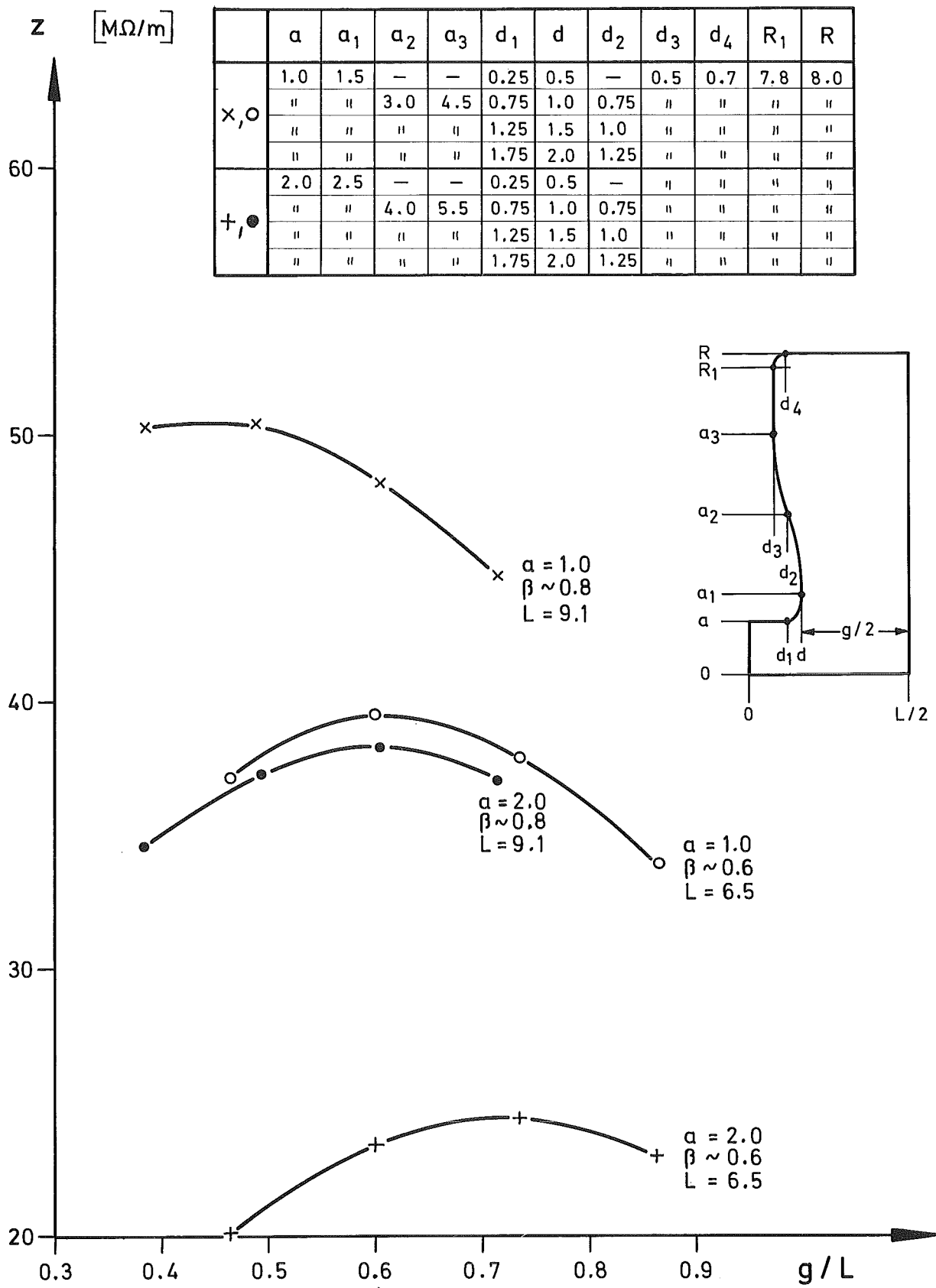


fig. 9b

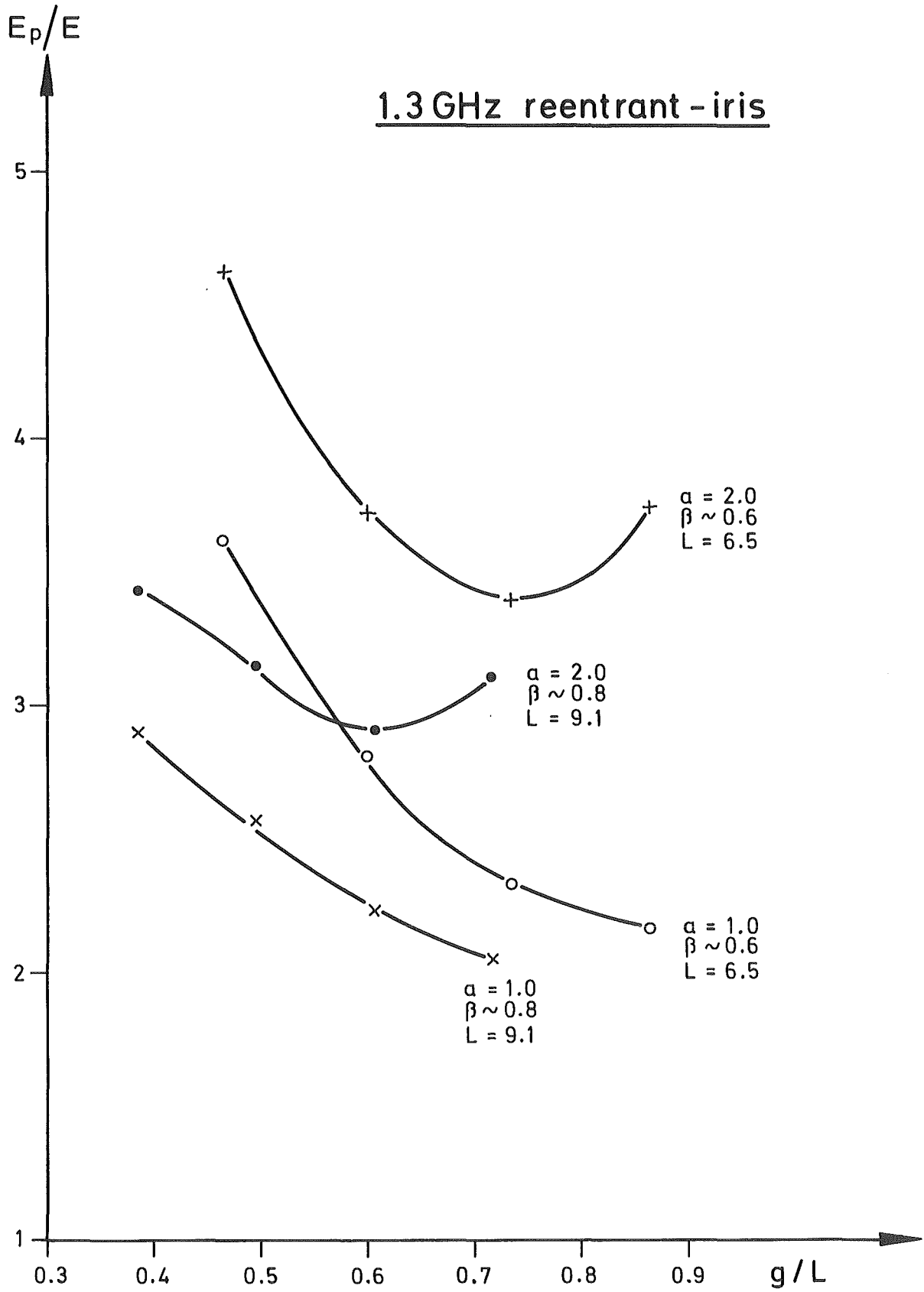


fig. 9c

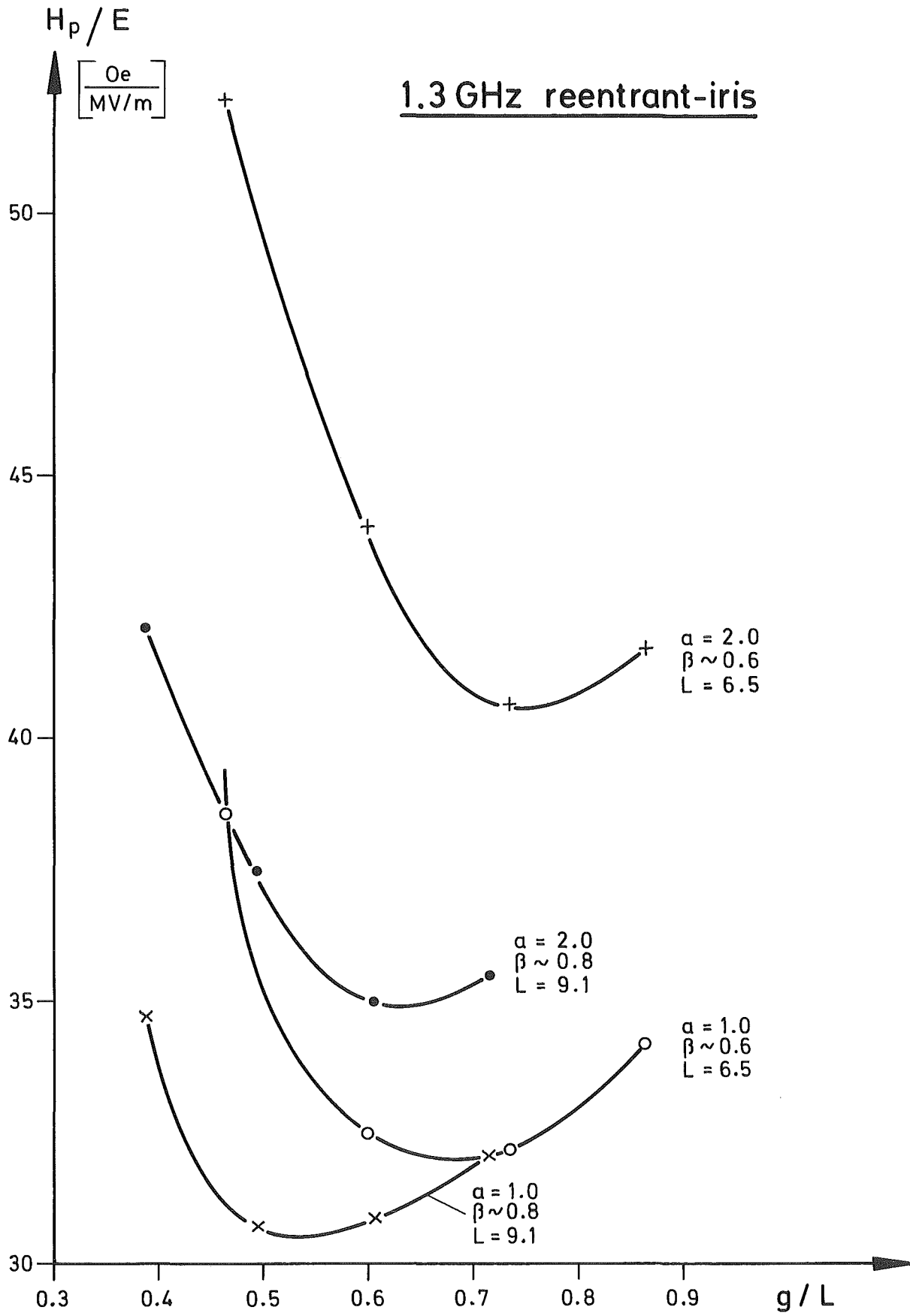


fig. 10a

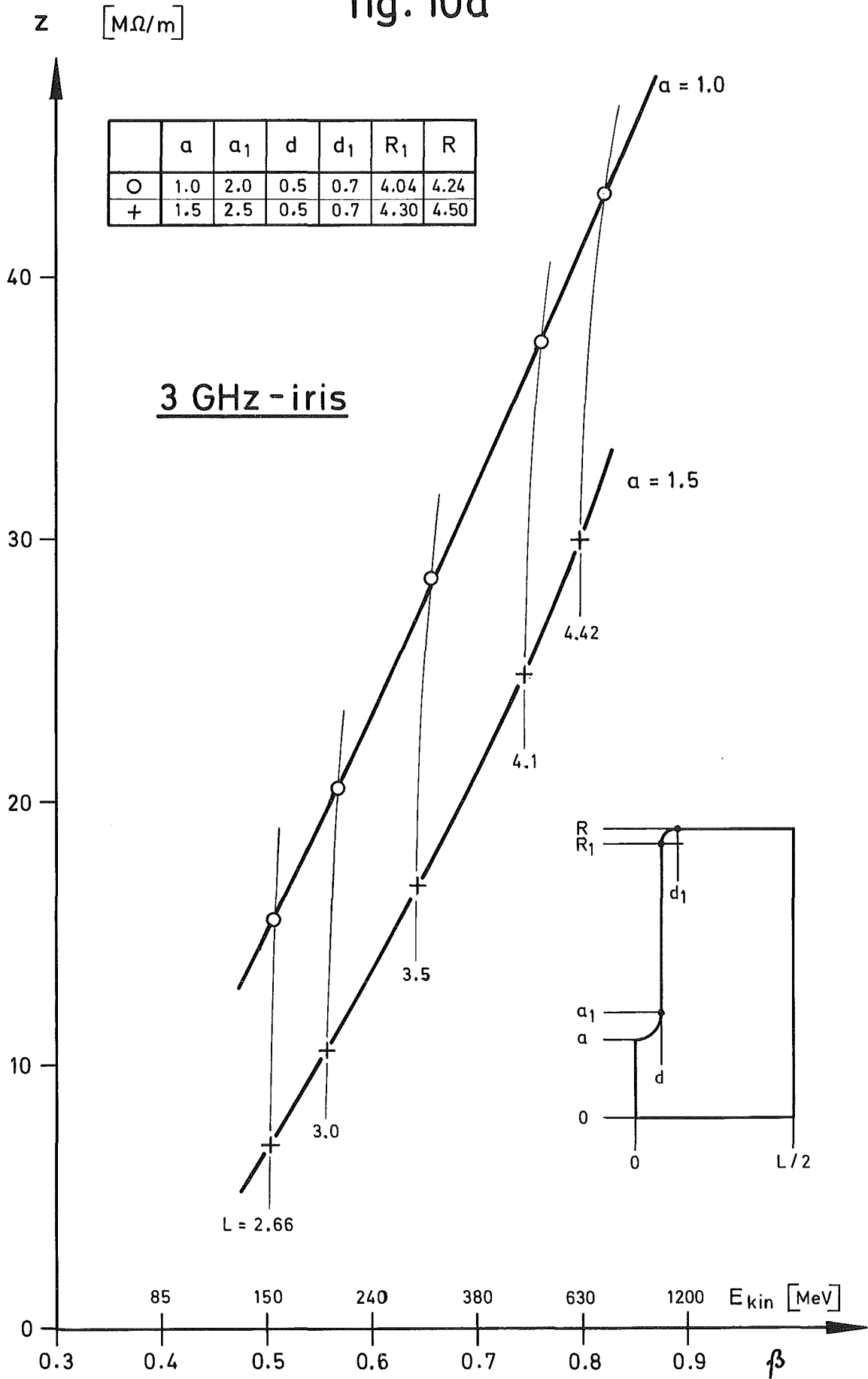


fig. 10b

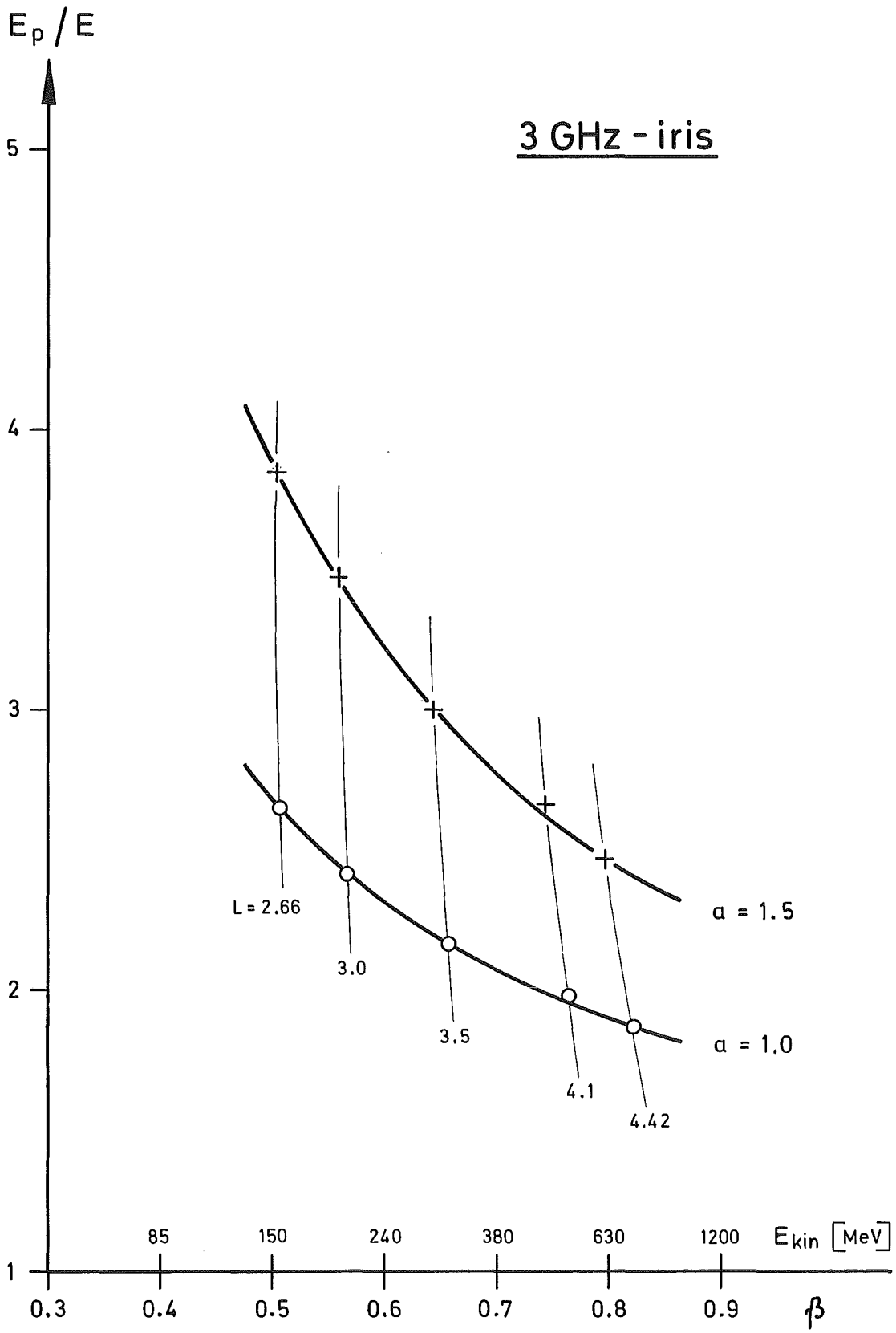


fig. 10c

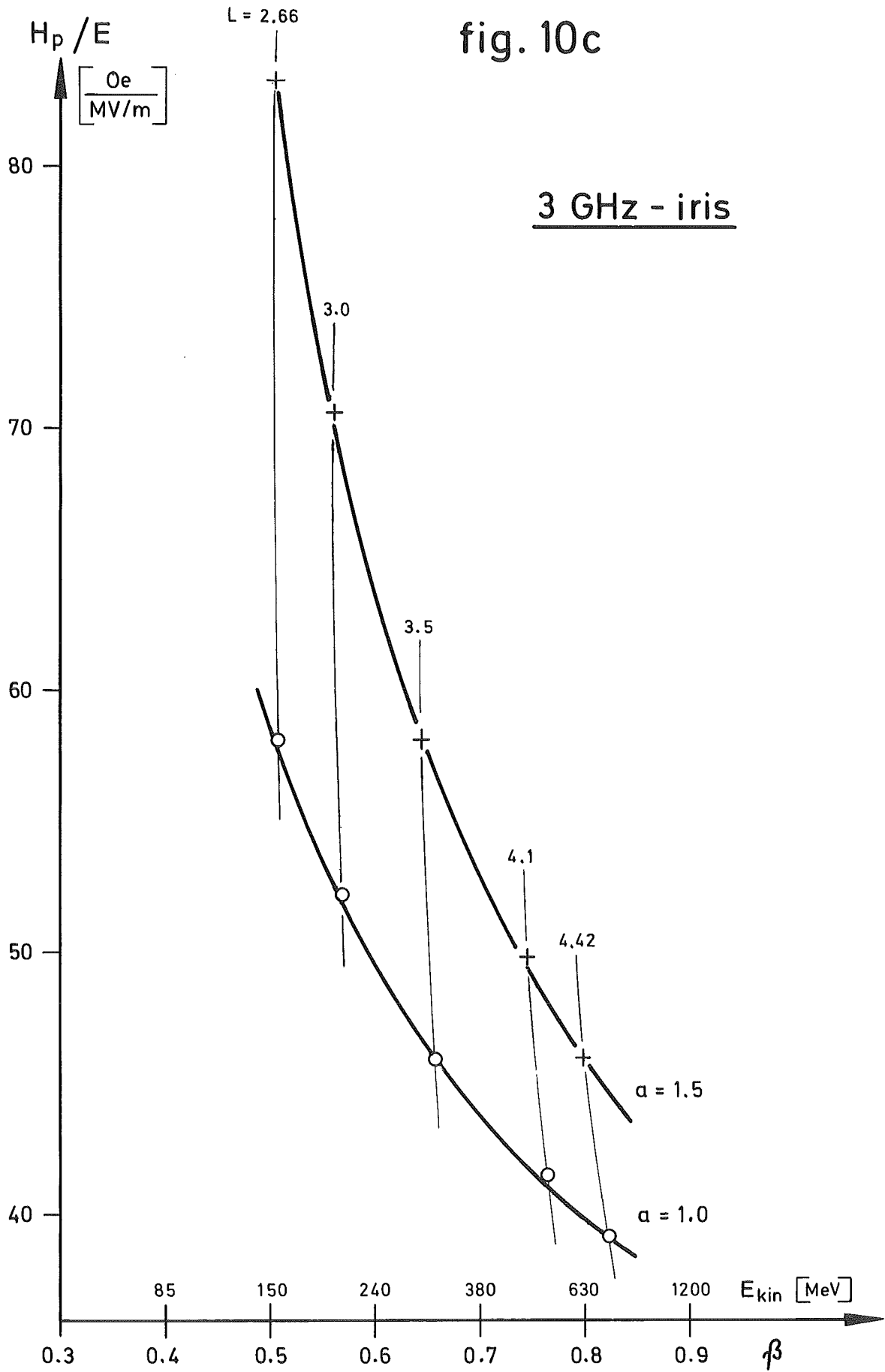


fig. 11a

3 GHz - iris ($\beta = 0.67$)

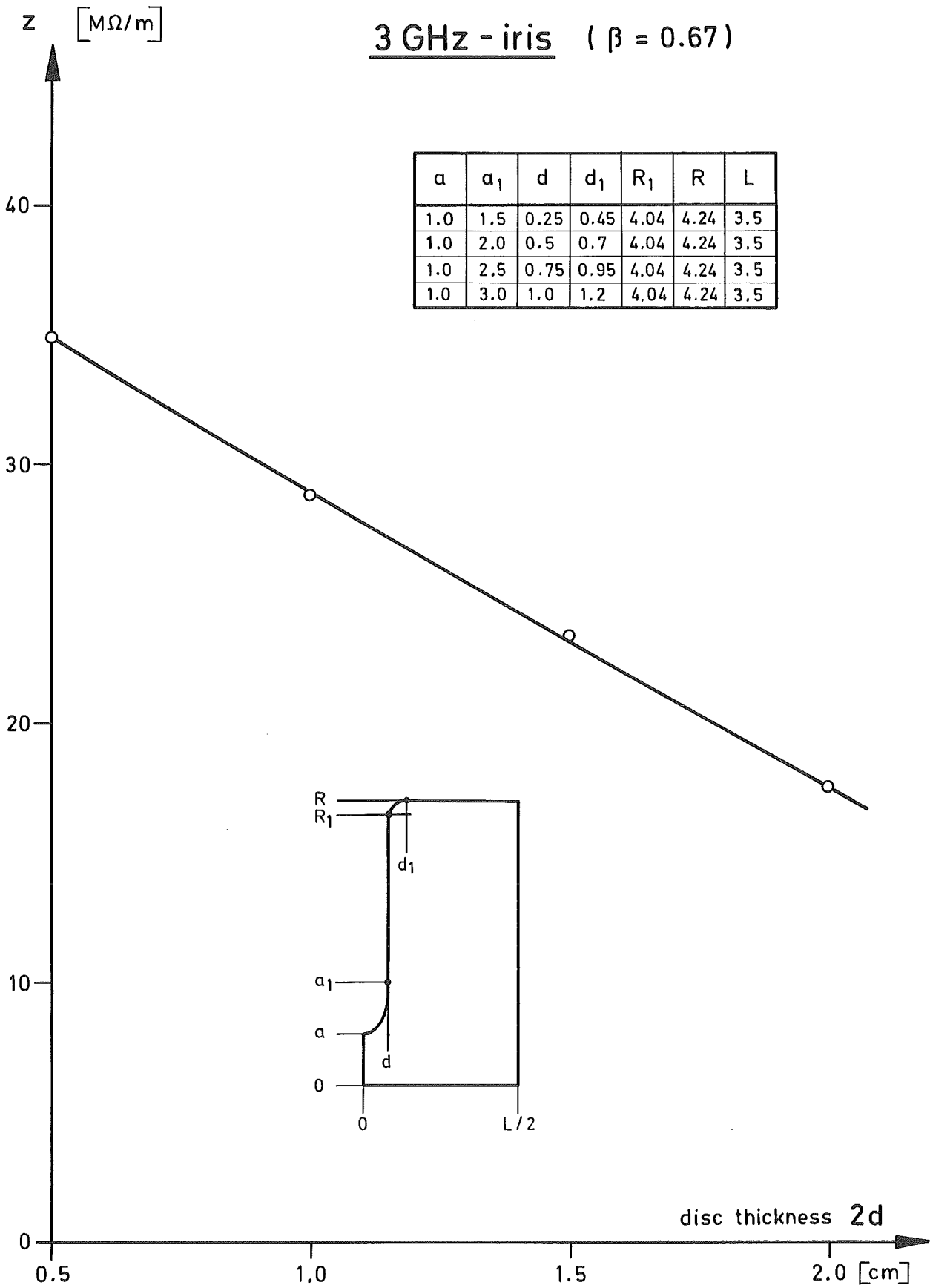


fig. 11b

3 GHz - iris ($\beta = 0.67$)

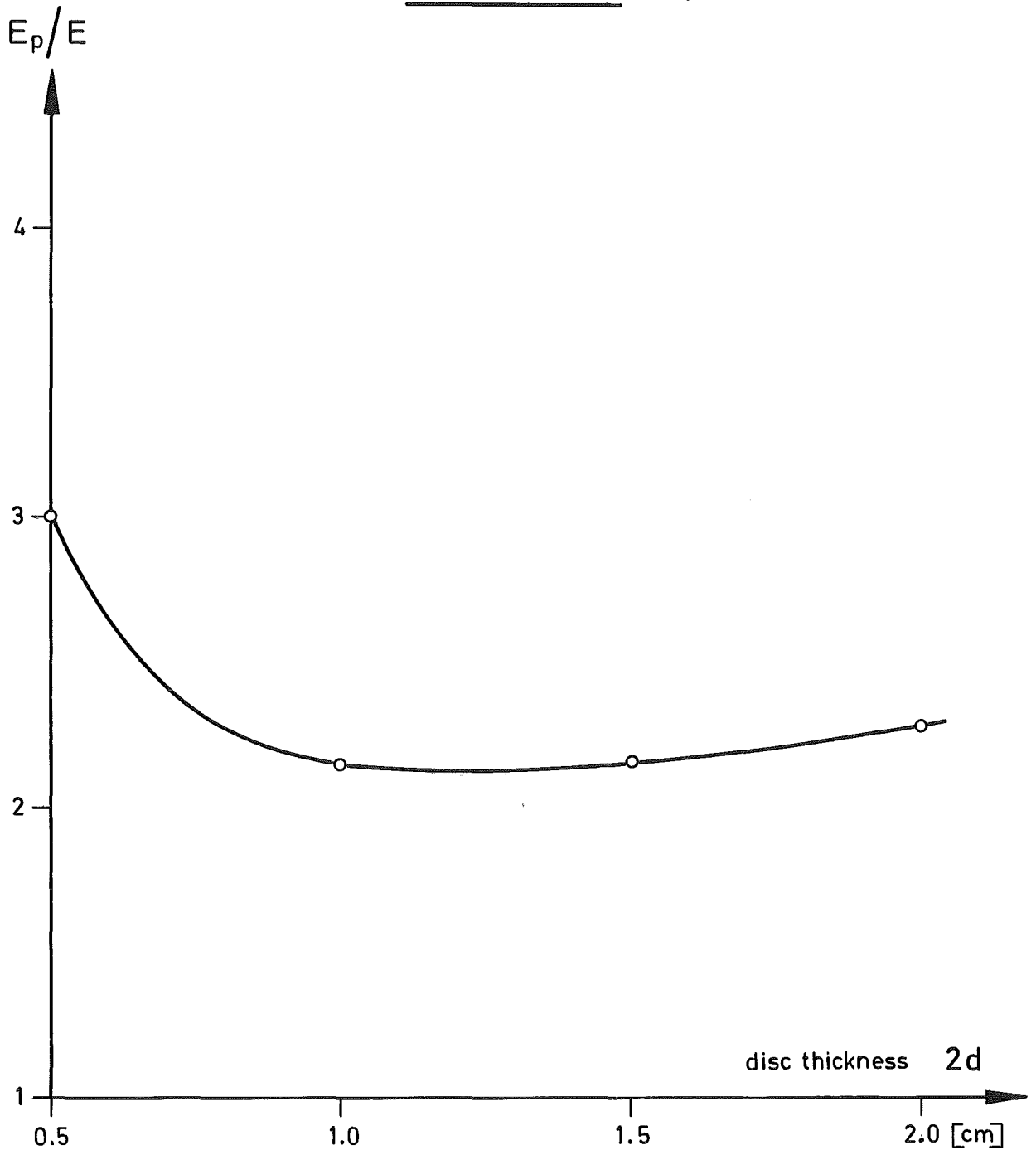


fig. 11c

3 GHz - iris ($\beta = 0.67$)

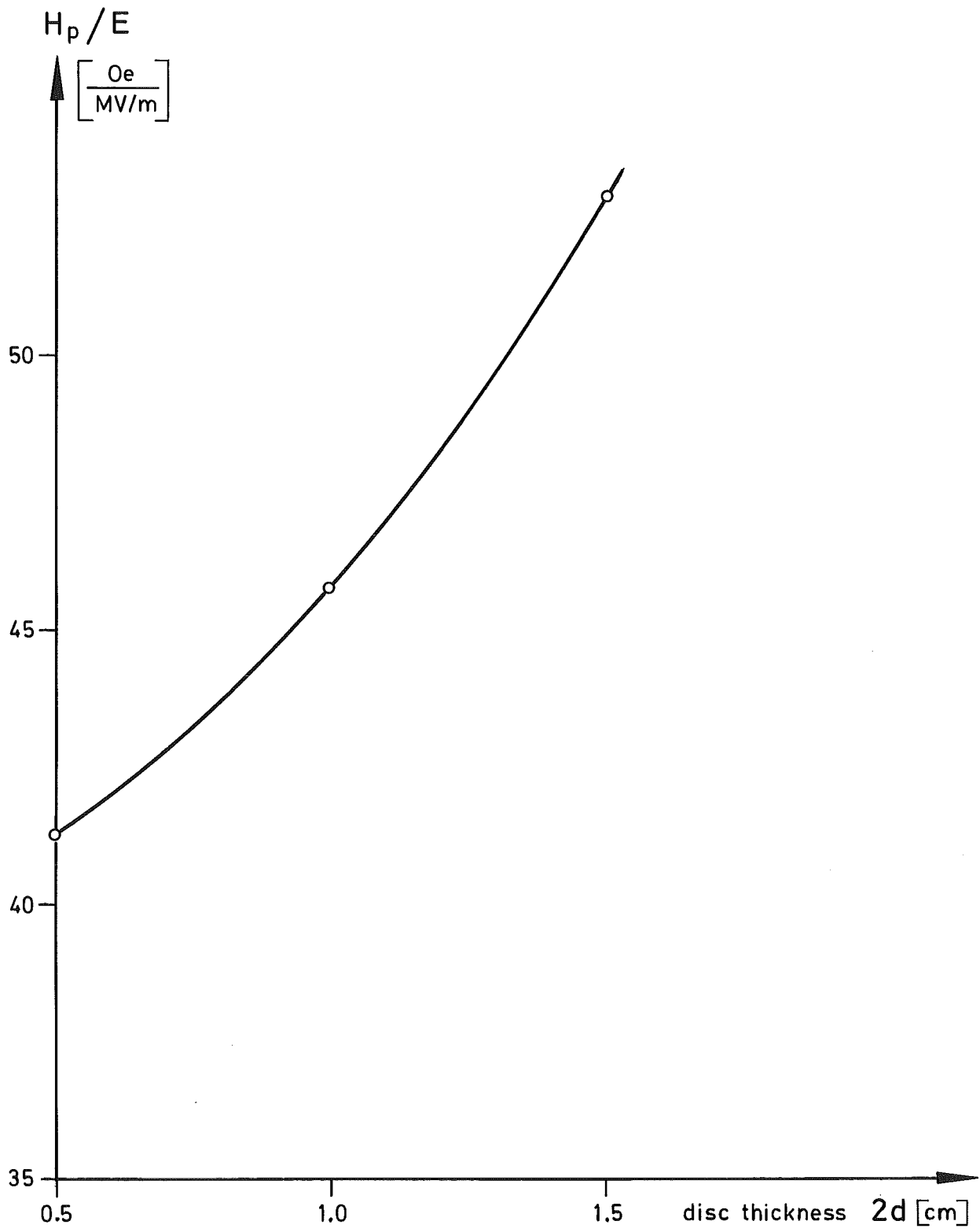


fig. 12a

number of cells per module N	module length NL in m
1	0.128
2	0.257
4	0.514
6	0.770
8	1.027
10	1.284
13	1.669
26	3.338

$E_{eff} = 4 \text{ MV/m}$

transit-time-factor

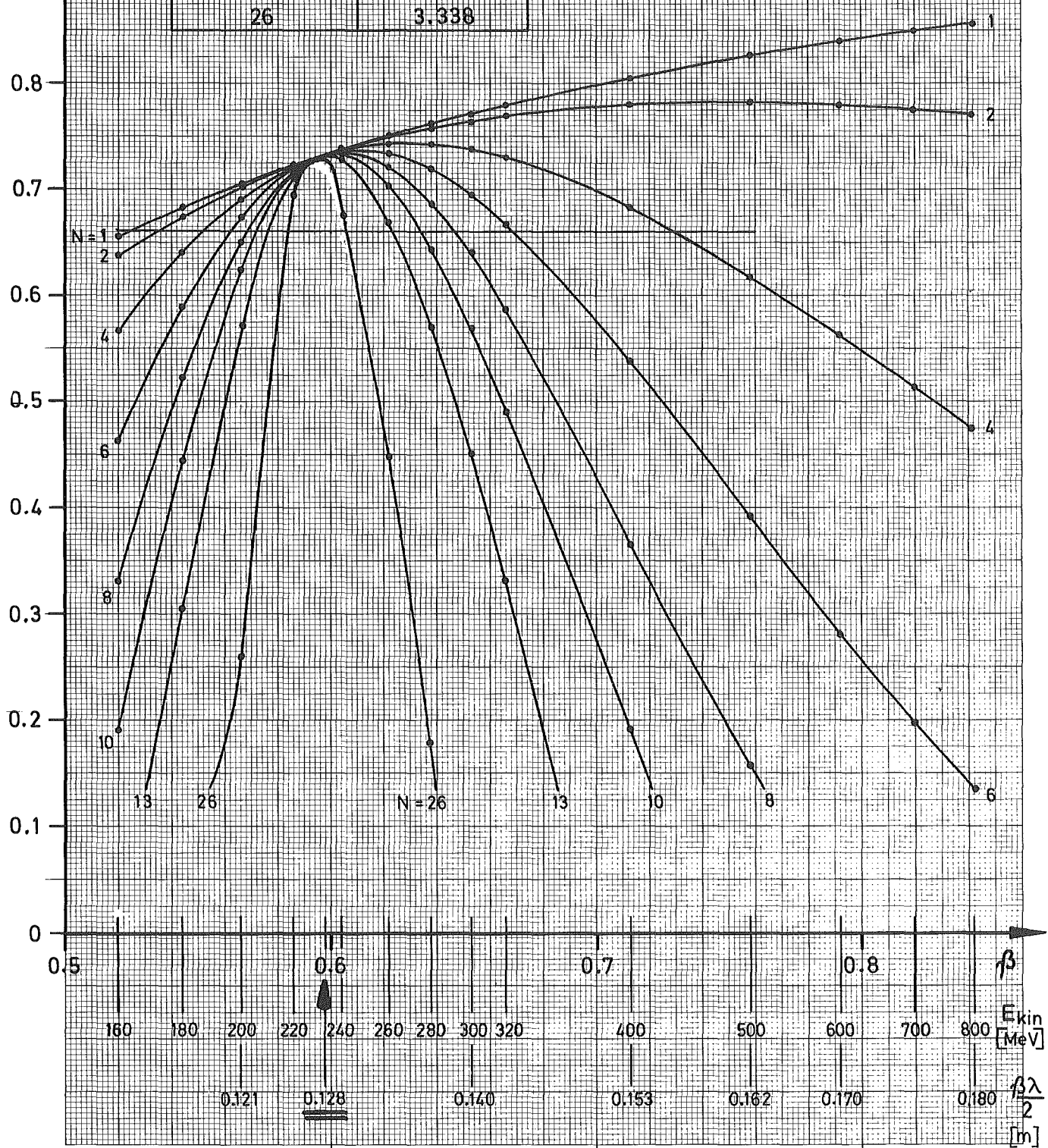


fig. 12 b

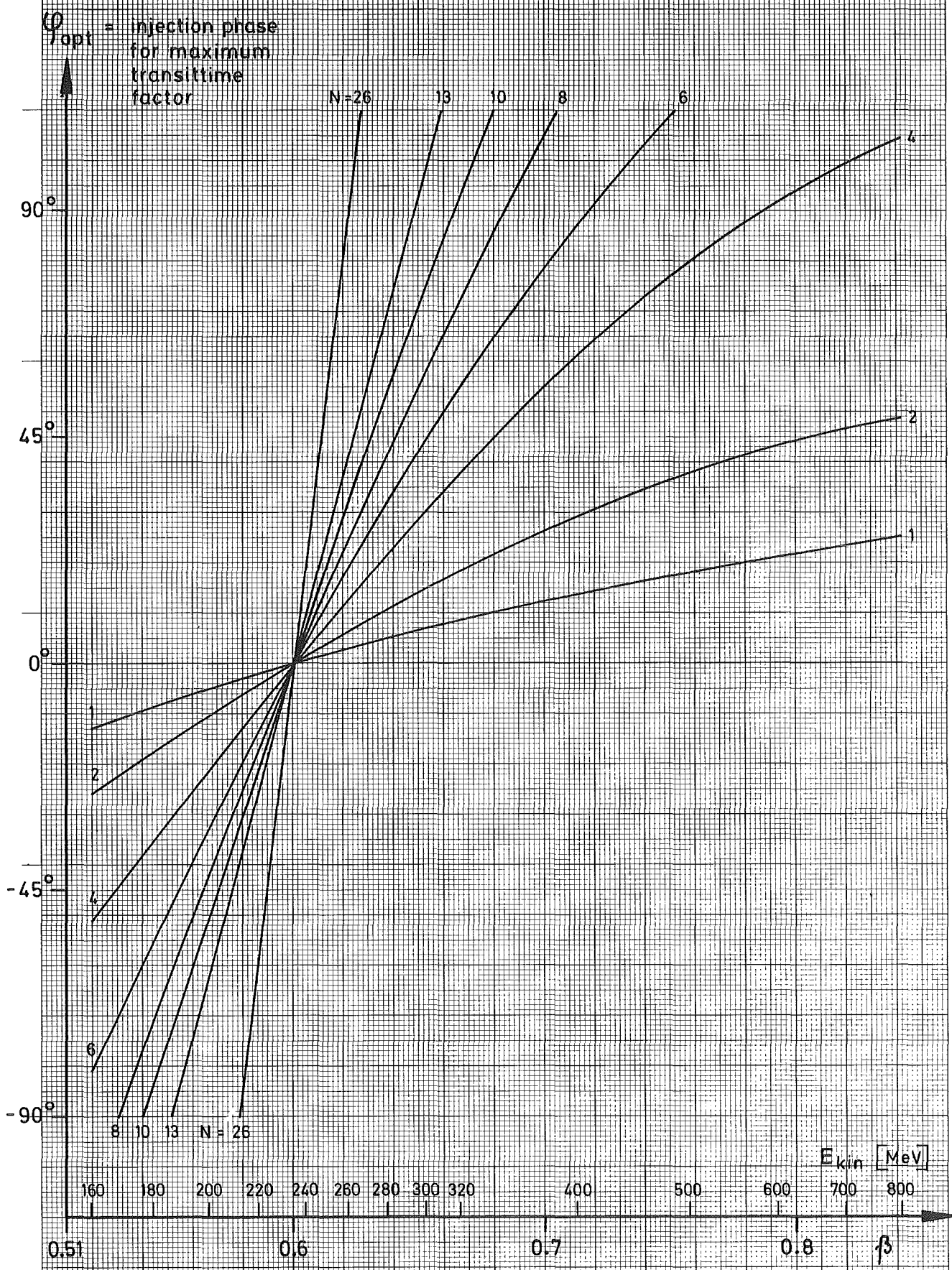


fig. 12c

number of cells per module N	module length NL in m
1	0.153
2	0.306
4	0.612
6	0.918
8	1.224
10	1.530
13	1.989
26	3.978

$E_{eff} = 4 \text{ MV/m}$

transit time factor

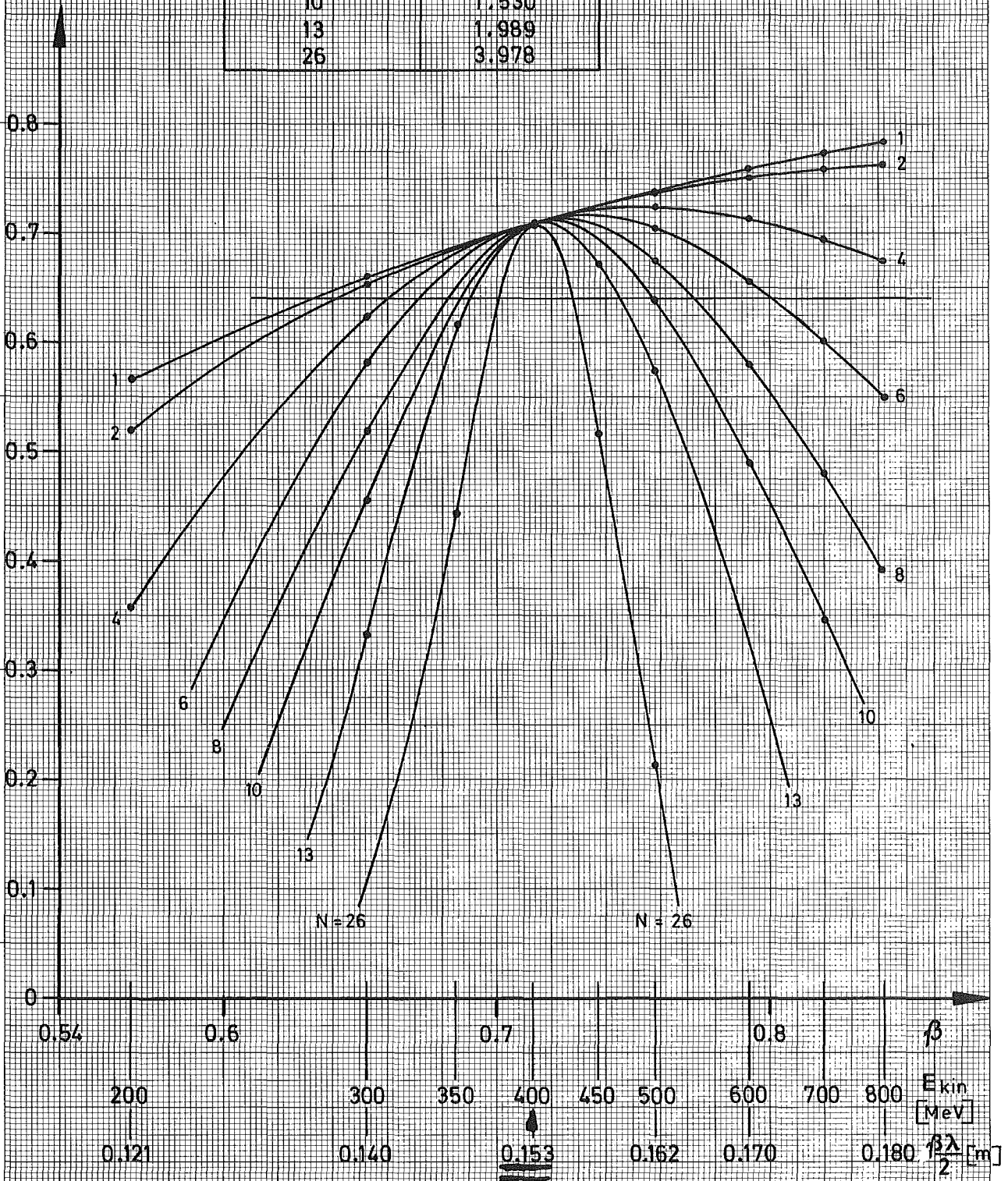


fig. 12d

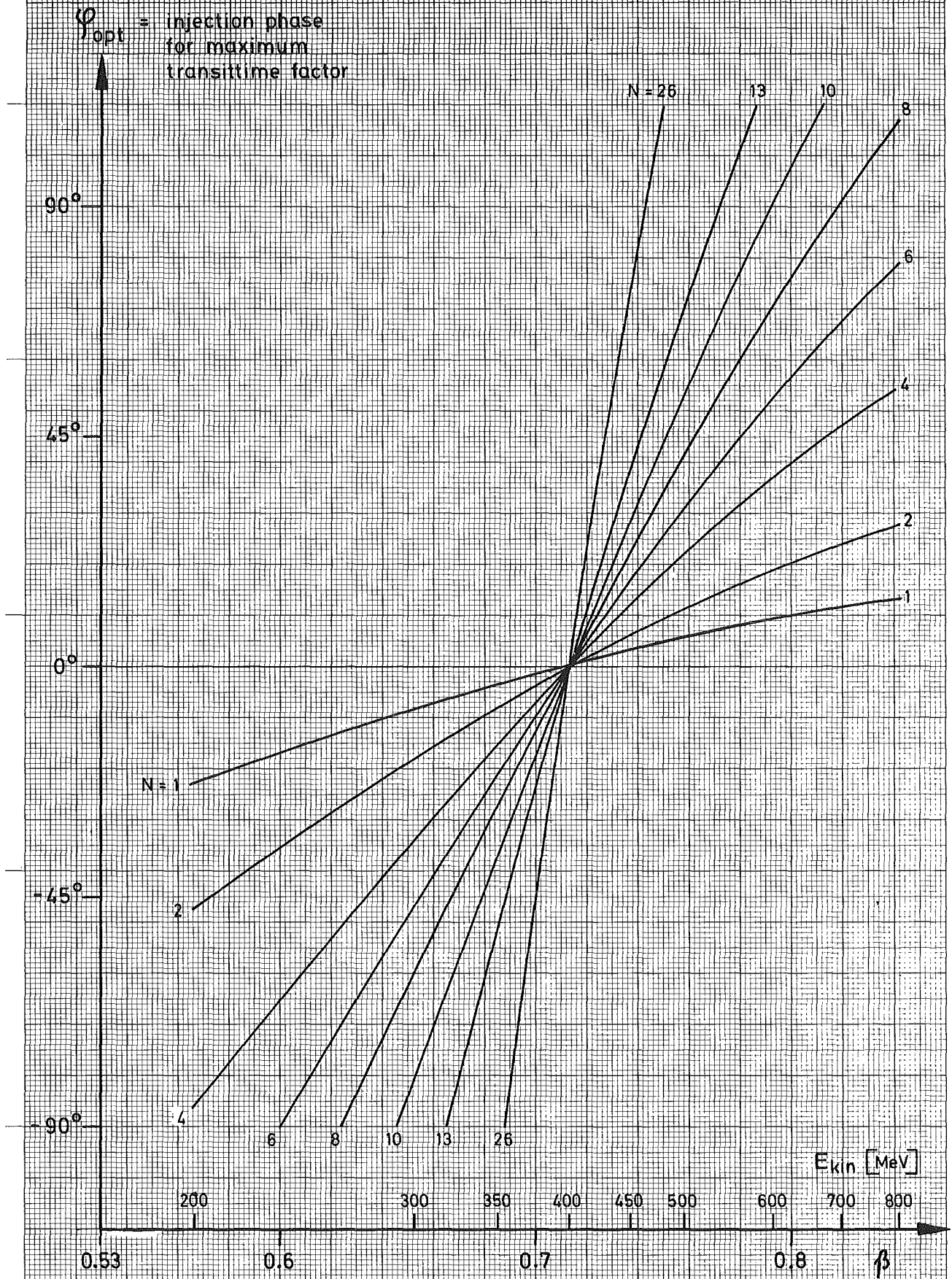


fig. 13a

1.3 GHz - iris

number of cells per module N	module length NL in m
14	1.050
29	2.175
58	4.350

$E_{eff} = 4 \text{ MV/m}$

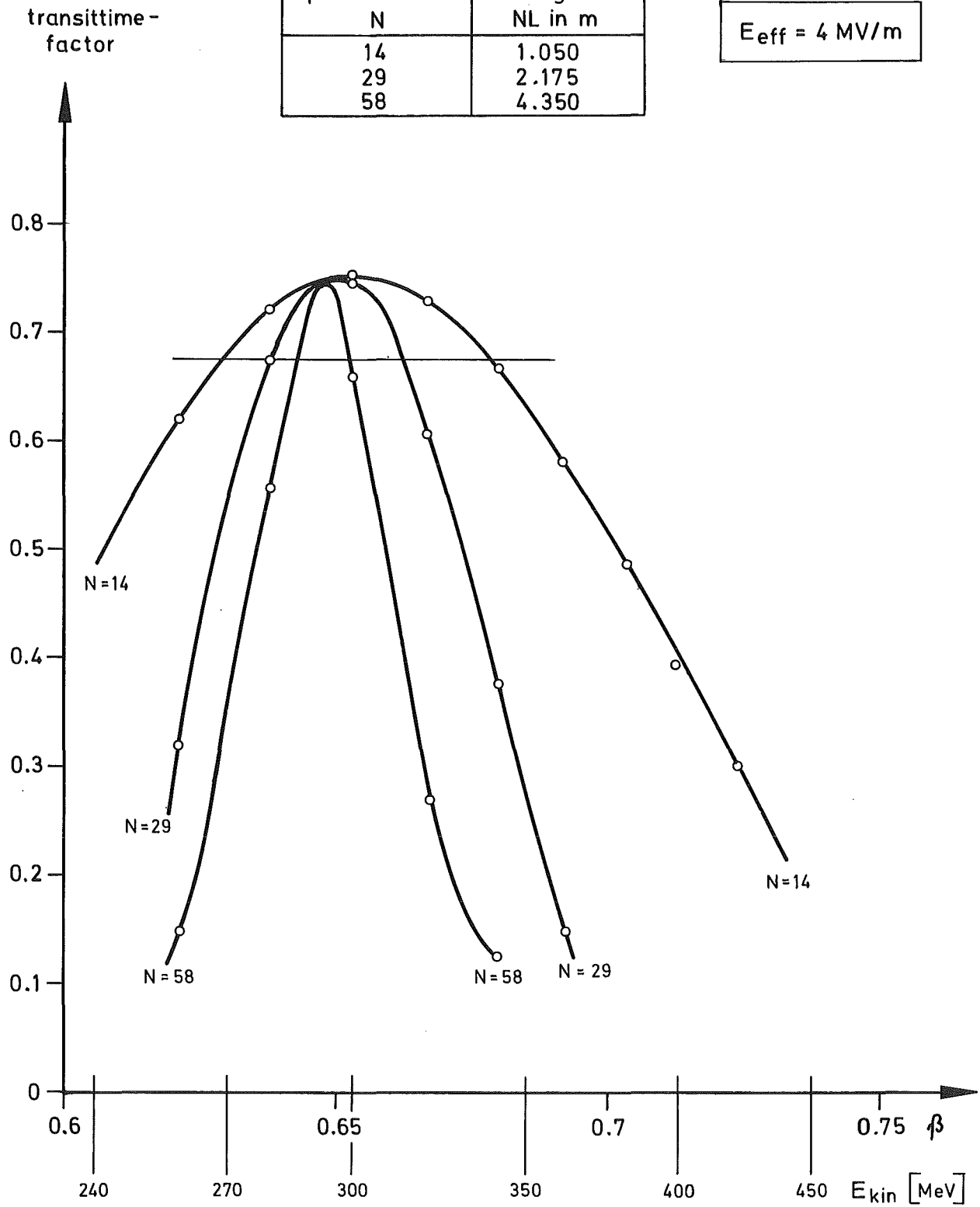
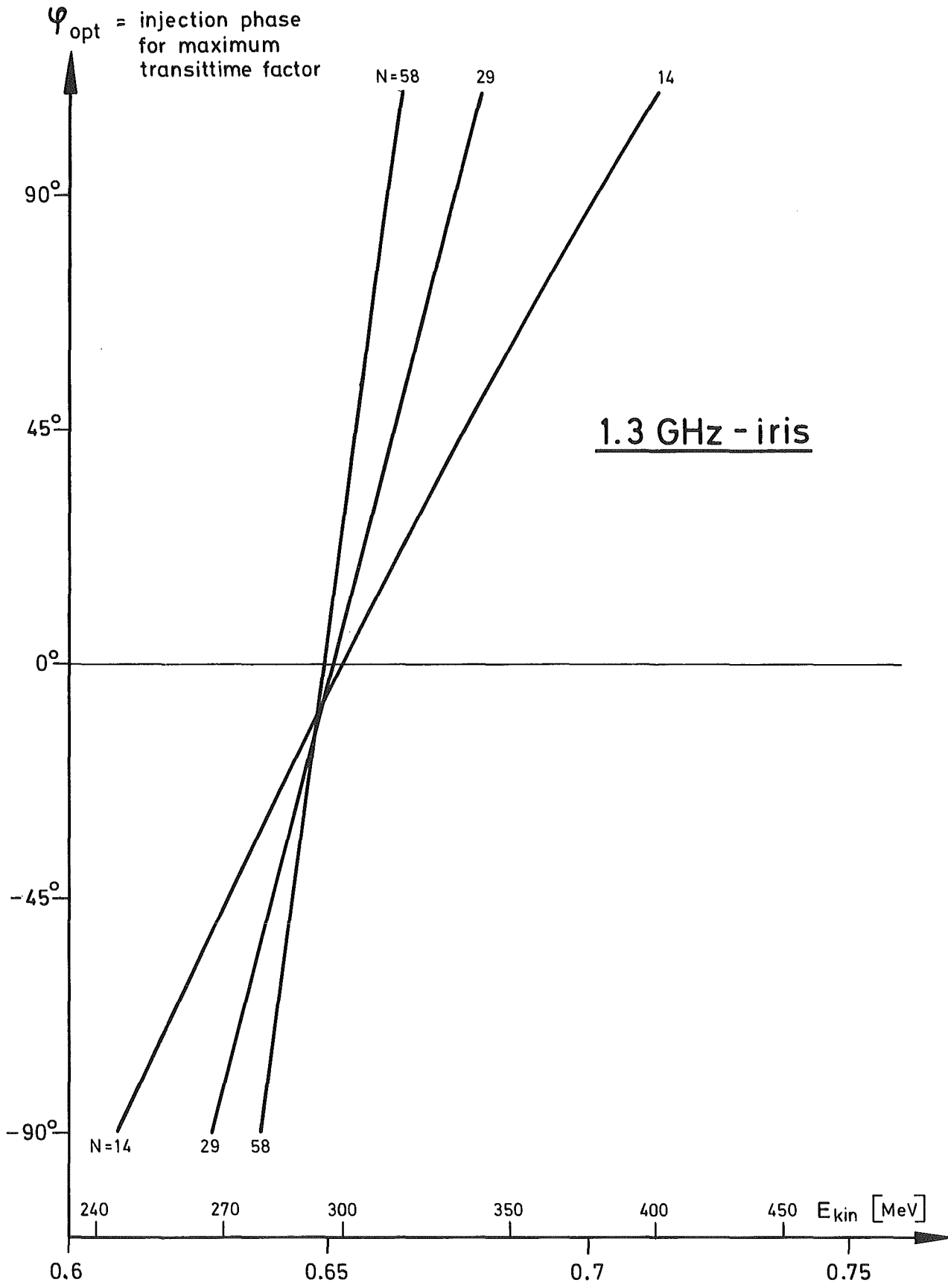


fig. 13b



3 GHz - iris

fig. 14a

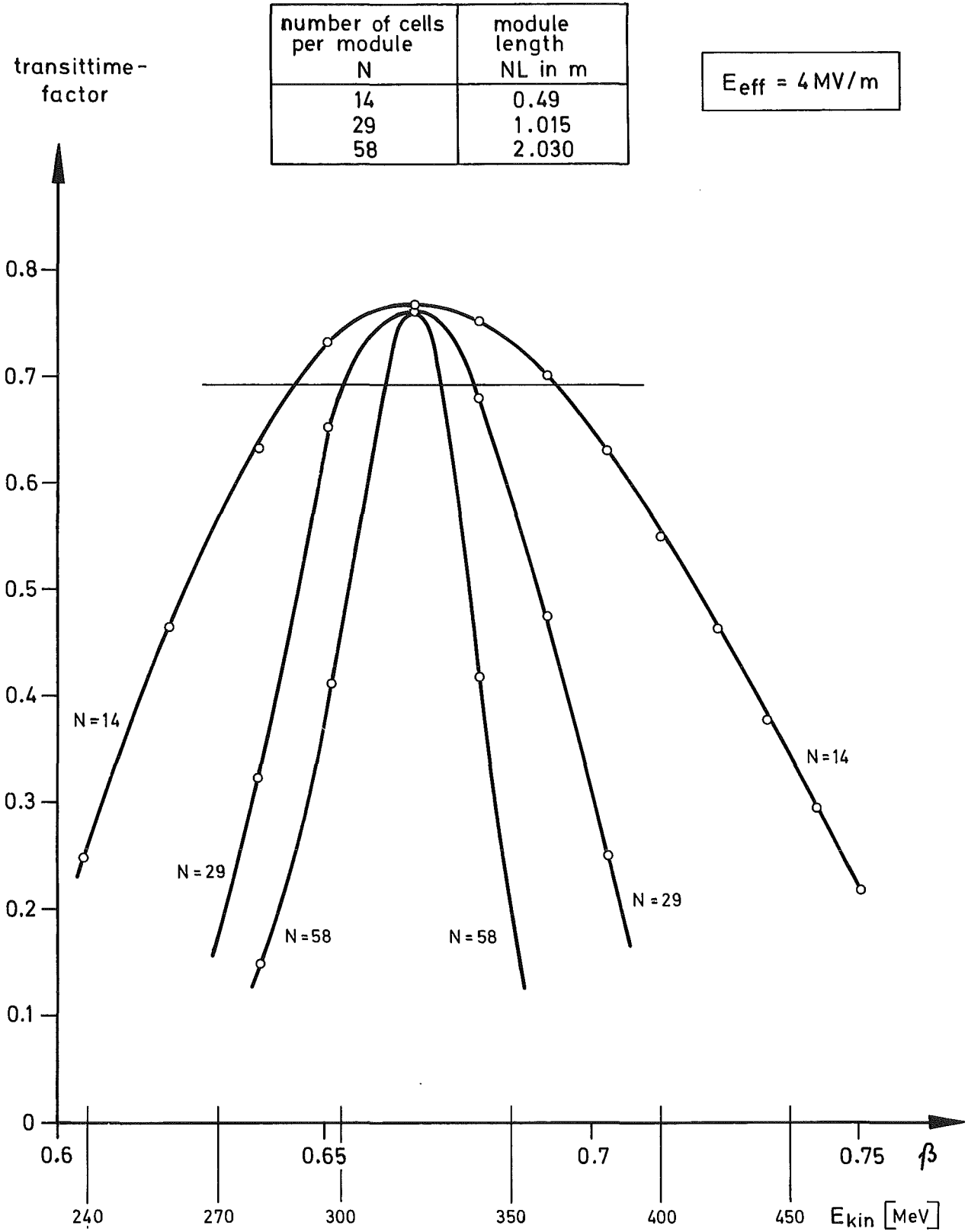
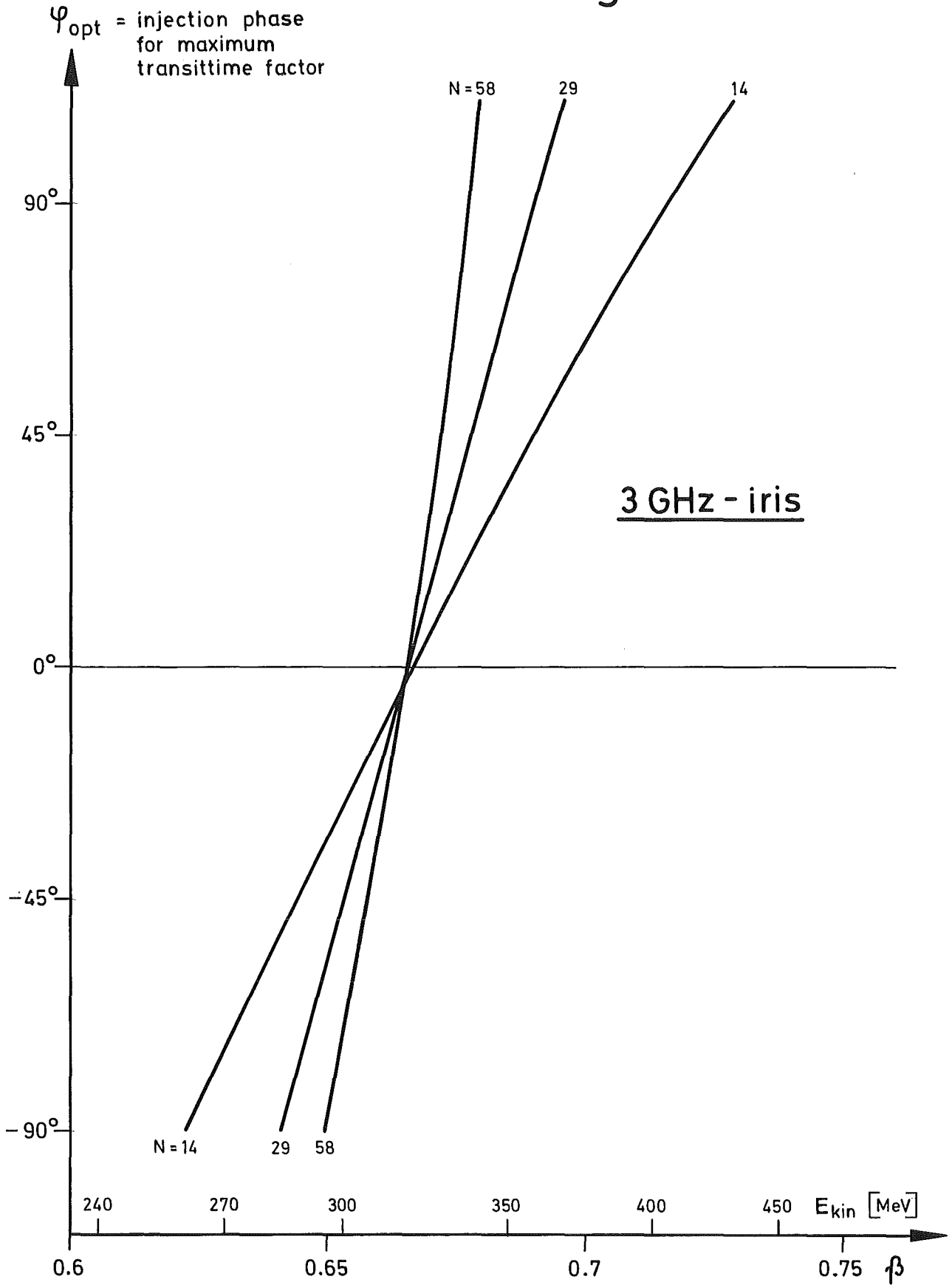
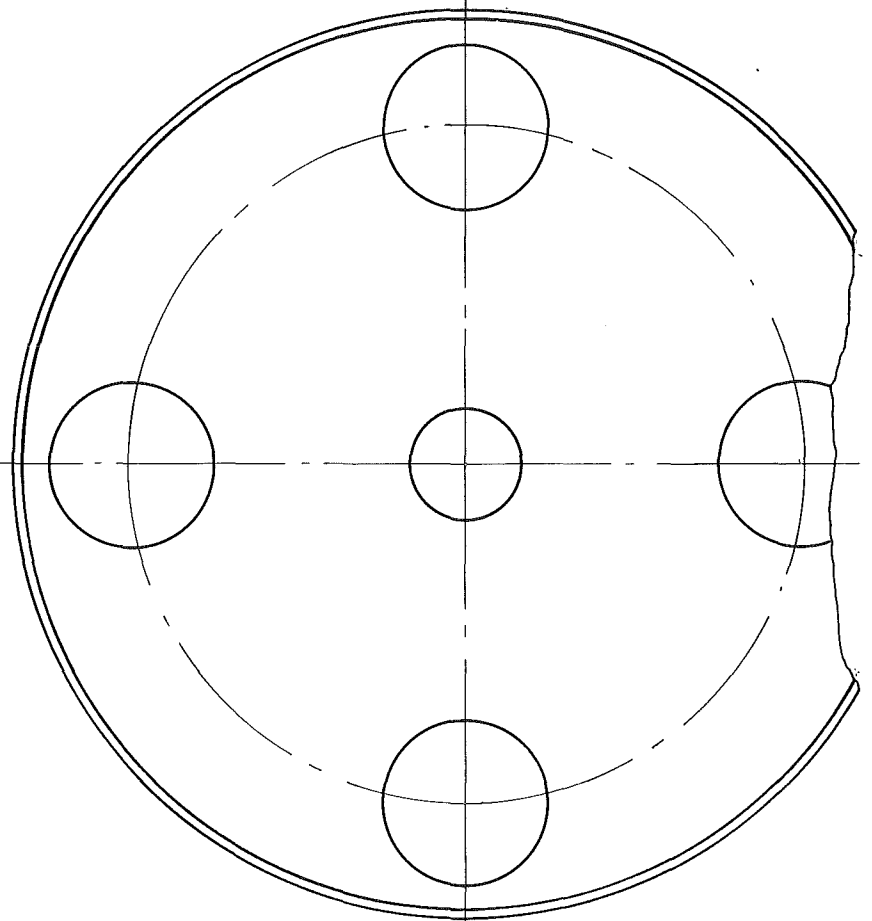
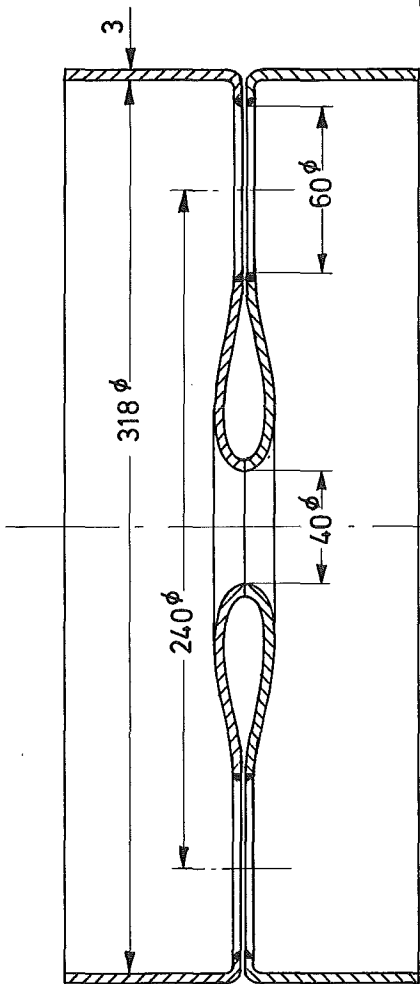
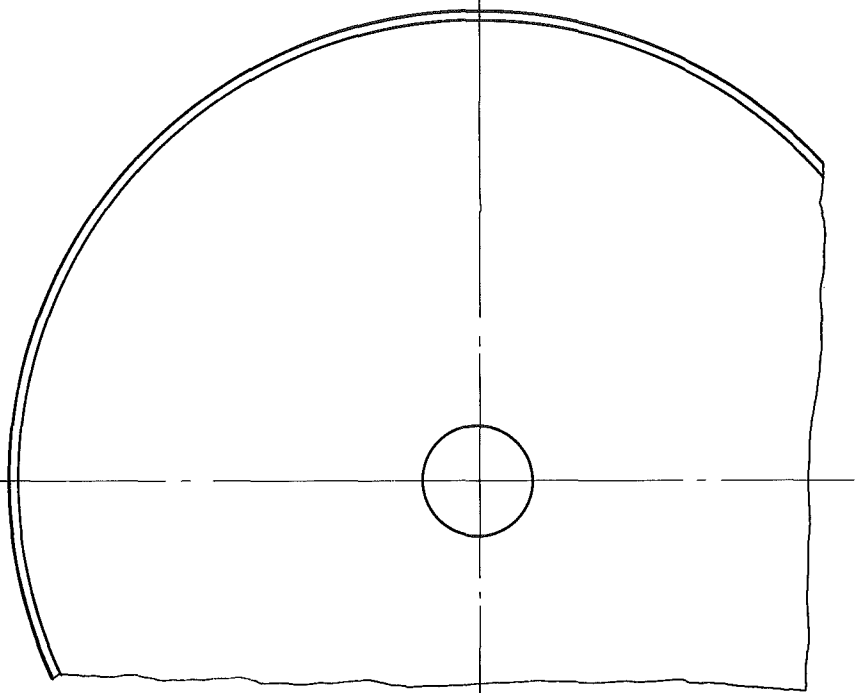
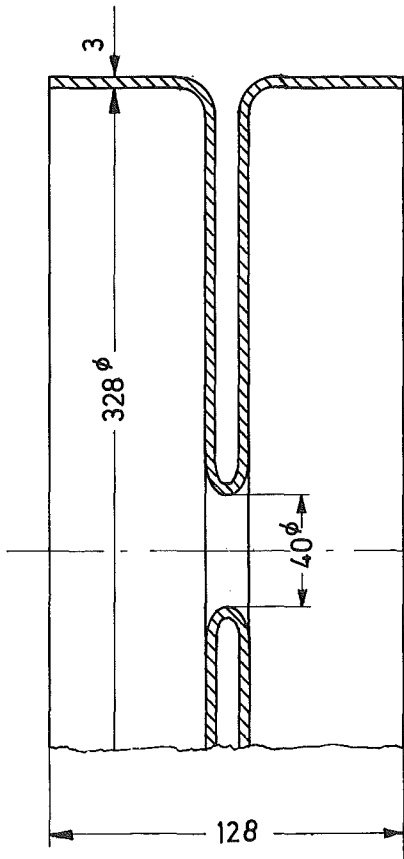


fig. 14b



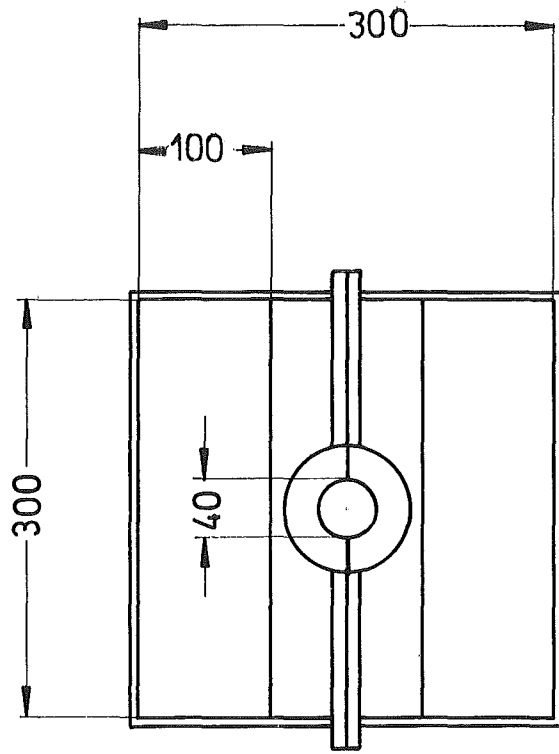
700 MHz - iris

fig.15



700 MHz - slotted iris

fig.16



700MHz -muffin tin structure

